20. PETROLOGY OF THE BASALTIC ROCKS DRILLED ON LEG 33 OF THE DEEP SEA DRILLING PROJECT

Everett D. Jackson, Keith E. Bargar, Brent P. Fabbi, and Chris Heropoulos,
U.S. Geological Survey, Menlo Park, California

ABSTRACT

Six flow units of basalt were penetrated at the base of Hole 315A, located near Fanning Island in the Line Islands chain; intercalated sedimentary rocks, if present, were not recovered. Ten flow units of basalt were penetrated in Hole 317A, located on the high Manihiki Plateau; four of these flow units are intercalated with thin beds of baked volcaniclastic siltstone. Basement was not reached in Hole 316, near Christmas Island in the Line Islands chain, nor in Hole 318, between Ahe and Arutua atolls in the Tuamotu Islands chain, but centimeter-sized pebbles of volcanic rocks were recovered from breccia beds at both these sites. The basaltic rocks in Hole 315A are highly altered, chiefly to montmorillonite group minerals and calcite, but not to the extent that their textures, original mineralogy, and major- and minor-element abundances could not be established. The flow units show textural differences, but their composition is similar to basalts of the oceanic island type, intermediate between Hawaiian tholeiite and alkalic basalt. The pebbles of Hole 316 may also be of this type. These basalts are much less alkalic than the amphibole-bearing basalts drilled in the more northerly Line Islands on Leg 17, which appear to resemble Hawaiian post-erosional basanites and nephelinites. It would appear from existing analyses that the Line Islands are composed of basaltic rocks that are very similar to those of the Hawaiian chain.

Basalts drilled in Hole 317A differ in character from those of Hole 315A. They are less altered, and their textures, mineralogy, and major and minor element compositions unquestionably show them to be basalts of the oceanic ridge tholeiite type. They resemble basalts drilled beneath the Ontong-Java Plateau during Leg 30. Basalts from both areas are similar to rocks forming at present-day spreading centers, and do not support the contention that these plateaus are subsided microcontinents. The basalts are, however, exceedingly vesicular, and must have been erupted at water depths of less than 400 meters, or perhaps even subaerially. This implies that the Manihiki Plateau has subsided between 3000 and 3500 meters during the last 110 to 120 m.y.

Basaltic pebbles from the northwestern end of the Tuamotu chain are also of the oceanic island type. Age data down the chain are scanty, and it is not possible at present to say whether this part of the Tuamotu chain is of the progressively propagating type.

INTRODUCTION

Of the four deep holes drilled on Leg 33, all bottomed in or passed through thick sections of volcaniclastic sediments. Hole 315A penetrated about 110 meters of this material before basalt flows were reached; Hole 316 penetrated more than 250 meters of this material and was abandoned before reaching basement; in Hole 317A considerable amounts of volcanogenic debris are interbedded with calcareous material more than 260 meters above the contact with the uppermost basalt flow; in Hole 318 nearly 200 meters of predominantly volcaniclastic sediments were penetrated at the bottom of the hole before drilling was terminated. The petrology of these volcaniclastic silts and sands is described in other sections of this report (Kelts and McKenzie, this volume; Jenkyns, this volume). One centimeter-sized basalt fragment was recovered from Hole 316, and two fragments of similar size were recovered from Hole 318; none of these samples was large enough for work other than that permitted by thin section and X-ray techniques, and descriptions of these three fragments are discussed separately in a later section of this paper. The main body of this report deals with the geologic setting, petrography, mineralogy, and chemical composition of the basaltic flows recovered from Hole 315A in the Line Islands and from Hole 317A beneath the Manihiki Plateau.

GEOLOGIC SETTING AND STRATIGRAPHY OF FLOW UNITS

Hole 315A

Hole 315A is located 93 km northeast of Fanning Island, and both bathymetry and reflection profiles suggested that basement here would consist of lava flows associated with the Fanning edifice rather than flat-lying oceanic crust. The generally elevated nature of the basement at this site and its smooth slope away from Fanning Island were our principal criteria in choosing the location. The volcaniclastic debris (see Kelts and McKenzie, this volume) is compositionally similar to the mildly alkalic basalts penetrated in Hole 315A, suggesting that the debris was derived from the Fanning edifice. The age of the basalts based on extrapolated accumulation rates beneath the lowest identifiable fossils is ~85 m.y. (see Part I of this volume), and that age has been generally confirmed by K/Ar ages of 91.2 ±2.7 m.y. reported by Lanphere and Dalrymple (this volume).

Hole 315A entered basalt at a depth of 996.3 meters below the mudline in the lower 20 cm of Core 30A (Figure 1). A total of 38 meters of basalt were penetrated, and 7.6 meters recovered. Although recovery was poor, the lack of correlation between drilling rate and recovery led us to believe that no sedimentary material is present below Core 30A (see Table1).

Six flow units were tentatively identified aboard ship (Figure 2), and subsequent petrologic study has shown no reason to revise this stratigraphy. The basalt at the base of Core 30A (Flow unit 1A) appears identical to that of Core 31A, and it would seem that the lower part of Core 31A was not recovered, in spite of the slow drilling rate. Core 32A began and ended in flow units not seen in either Core 31A or Core 33A, and the loss could have been at either end or both. Core 32A contains the only complete flow unit with both altered glass contacts intact (Flow Unit 3); it is 1.5 meters thick. Core 33A contains basalt that appeared identical with that at the top of Core 34A; it seems likely, therefore, that the upper part of Core 33A was unrecovered, and the lower part of Core 34A was lost. If correctly assembled, the thicknesses or minimum thicknesses of flow units are as shown in Table 1.

TABLE 1
Drilling Summary of the Deepest Cores of Hole 315A

Core	Drilled Interval (m)	Drilling Rate (m/hr)	Recovery (%)	Flow Unit Thickness (m) (see Figure 1)
25A-30A	57.0	4.0-15.0	28.4-54.7	1A ⩾ 0.2
31A	9.5	42.0	5.3	1B ⩾ 1.0
32A	9.5	26.0	52.6	2 ⩾ 1.75 3 1.55 4 ⩾ 1.85
33A	9.5	15.0	7.4	5A ⩾ 1.3
34A	9.5	9.5	12.6	5B ⩾ 0.2 6 ⩾ 1.7

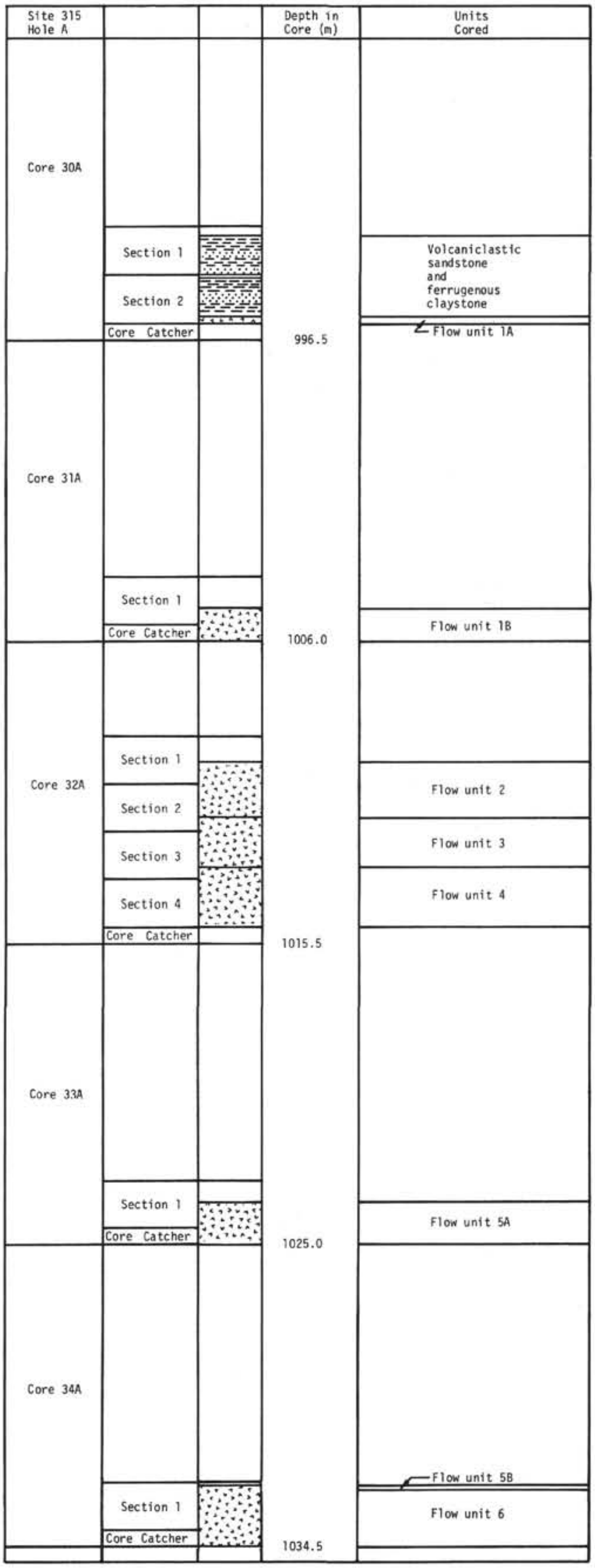

Figure 1. *Recovery of cored intervals from the deepest part of Hole 315A.*

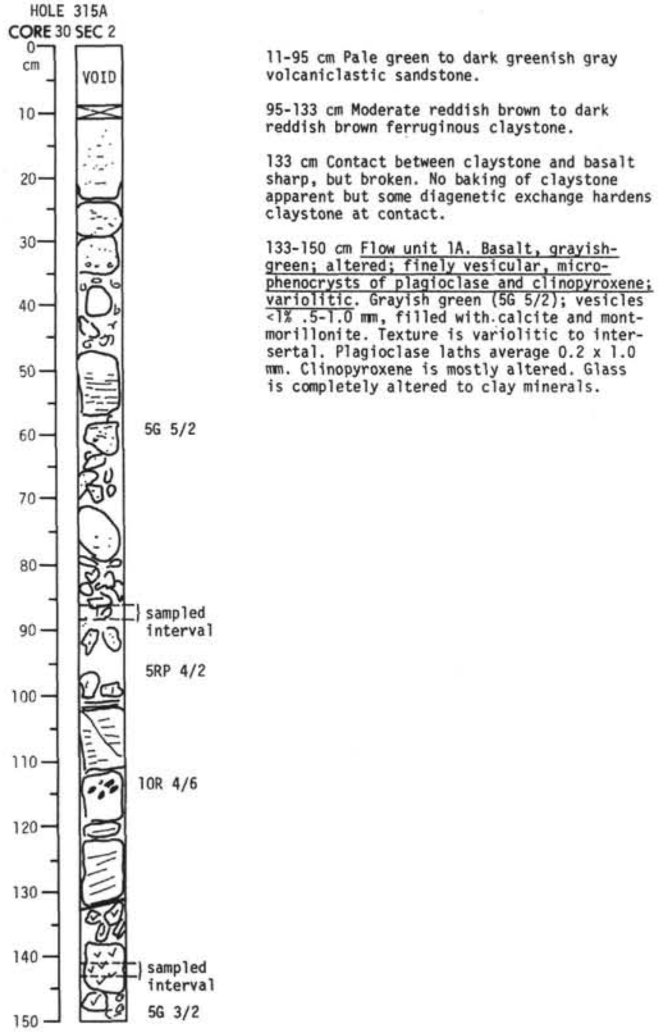

Figure 2. *Visual core description of basaltic rocks and associated sedimentary rocks of Hole 315A. Sampled intervals below sections are core-catcher samples from the deepest part of Hole 317A.*

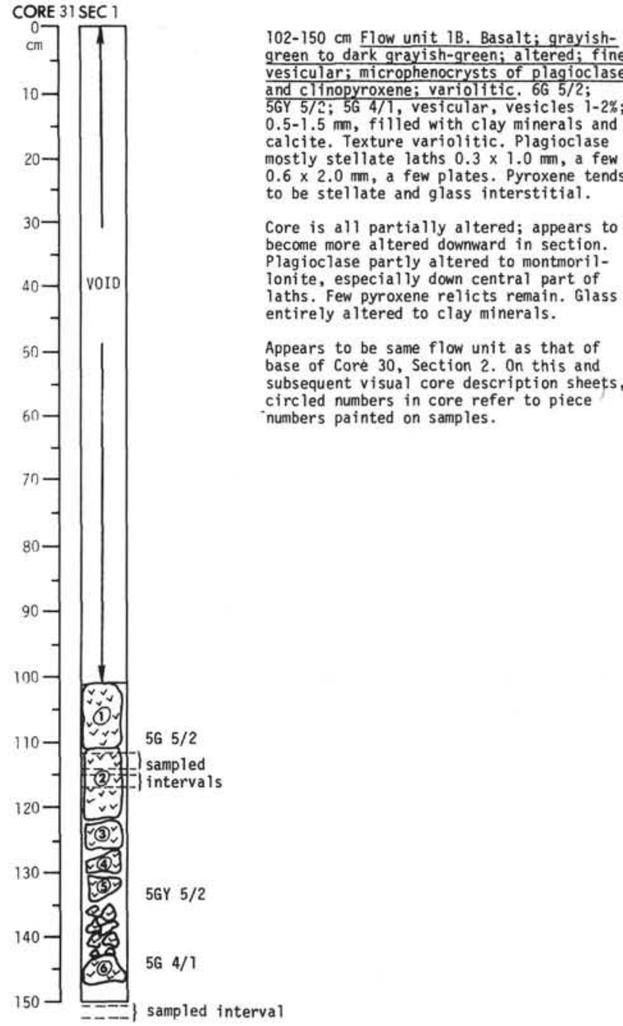

Figure 2. *(Continued).*

Hole 317A

Hole 317A was drilled near the center of the Manihiki Plateau, about midway between the Danger-Nassau, Manihiki-Rakahanga island groups, and Suvarov island, all low corraline islands that bound the plateau. The geologic setting of the Manihiki Plateau has recently been described by Winterer et al. (1974) and Jenkyns (this volume). The petrology of basalts dredged from more northerly parts of the plateau is given by Clague (this volume).

Basalt was penetrated in Hole 317A at a depth of 910 meters in the lower 4.6 meters of Core 31A (Figure 3). A total of 28.5 meters of penetration below Core 31A revealed a section that consists largely of basalt but contains several intercalated beds of baked volcaniclastic siltstone (Figure 4). In the total core recovered below the first contact with basalt, three such sedimentary units were noted, two in Core 31A and one in Core 33A. Recovery in general was good, and there appeared to be some correlation between drilling rate and recovery in this hole (see Table 2). Drilling rates in basalt in both Holes 315A and 317A were faster than we had anticipated; rates in 317A basalt were, in general, faster than those in 315A, which contains more altered basalt.

Ten flow units were identified aboard ship (Figure 4), and subsequent petrologic studies have shown no reason to change this stratigraphy. Magnetic studies (Cockerham and Jarrard, this volume) show that the entire core is normally magnetized. The missing part of the section of Core 31A probably represents volcaniclastic sediments above and between flow units (see Figure 4). Core 32A was full, and the basalt at its top appears identical with that at the base of Core 31A. The basalt at the top of Core 33A appears identical to that at the base of Core 32A and probably belongs at the top of the core. Some section is surely missing at the base of the volcaniclastic sandstone (Figures 3 and 4), and this probably accounts for much of the missing interval in Core 33A. The flow unit at the top of Core 34A appears identical with that at the base of Core 33A, and the missing interval in that core is most likely near its base. If correctly assembled, the thicknesses or minimum thicknesses of flow units are as shown in Table 2.

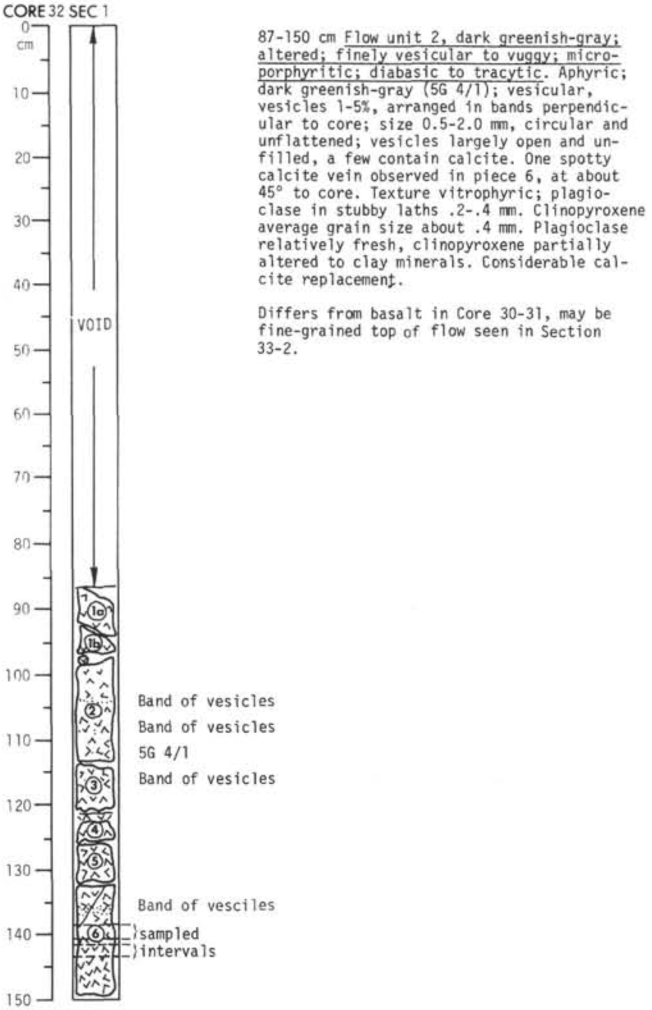

Figure 2. *(Continued).*

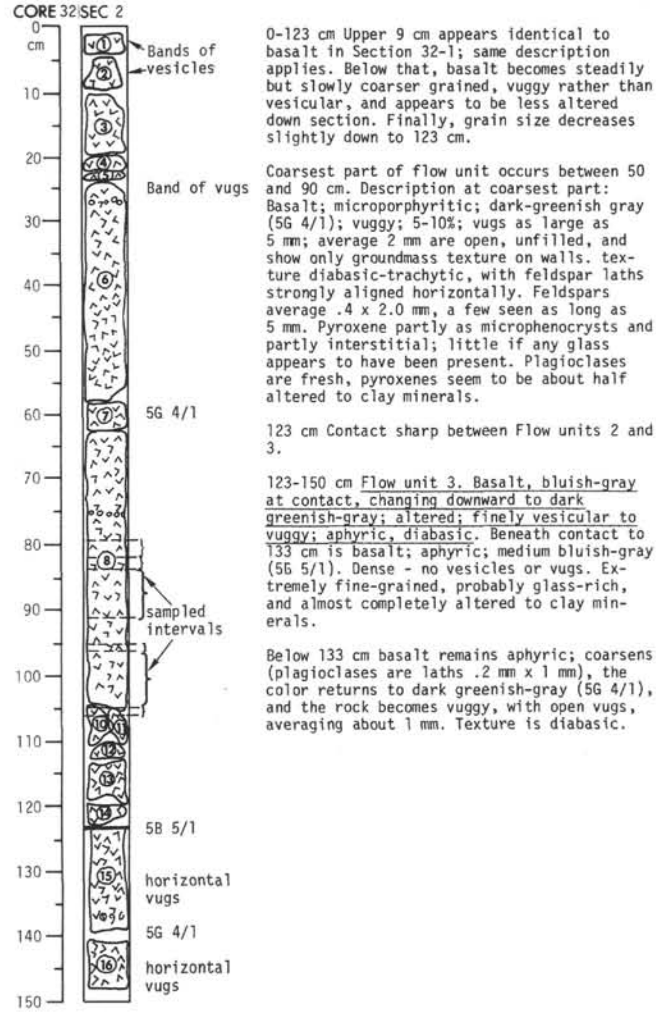

Figure 2. *(Continued).*

X-RAY DIFFRACTION DATA AND PETROGRAPHY OF HOLES 315A AND 317A

Introduction

Samples from the six flow units of Hole 315A and the ten flow units of Hole 317A were rather limited in number. In most cases, two core plugs of 2.5 cm outside diameter (each plug weighing about 40 g) were made available from each flow unit. For each hole, however, one quarter core of the freshest flow unit was cut for wet-chemical analyses and for plagioclase separations for K/Ar analyses (see Figures 2 and 4 for sampled intervals, and Lanphere and Dalrymple, this volume, for results).

X-ray diffraction studies, petrographic examination, and chemical analyses for both major and minor elements show only small internal differences between the basalts of either site. However, the basalts from the two sites are vastly different in character from each other. Basalts from Hole 315A are salite-bearing transitional basalts with relatively high K_2O contents, and most nearly resemble rocks transitional between Hawaiian tholeiites and pre-erosional Hawaiian alkalic basalts. They have a chemical affinity to the hawaiites and mugearites reported by Bass et al. (1973) from Site 165, although they are much less strongly alkalic. Basalts from Hole 317A, on the other hand, are oceanic ridge tholeiites with very low K_2O values that contain low calcium pyroxenes as well as augite and are similar to basalts from Site 289 beneath the Ontong-Java Plateau (Stoeser, in press).

X-ray Procedures

Whole-rock samples and vesicle fillings were analyzed by standard X-ray procedures on a Norelco diffractometer with unfiltered CuKα radiation. One basalt sample was selected from each hole, and its mineral constituents were separated by bromoform (Schoen and Lee, 1964) and magnetic (Hess, 1959) methods. The separated minerals were than X-rayed, and the resulting diffractograms were used as standards for subsequent mineral identifications. Anorthite content of the two separated plagioclases was determined by the method of Jackson (1961) (Tables 3 and 4, at end of chapter).

Several clay vesicle fillings and whole-rock samples that contained abundant clay were glycolated (Bradley, 1945) and X-rayed again. In every case, a comparison of the two diffractograms indicated that all were expanding

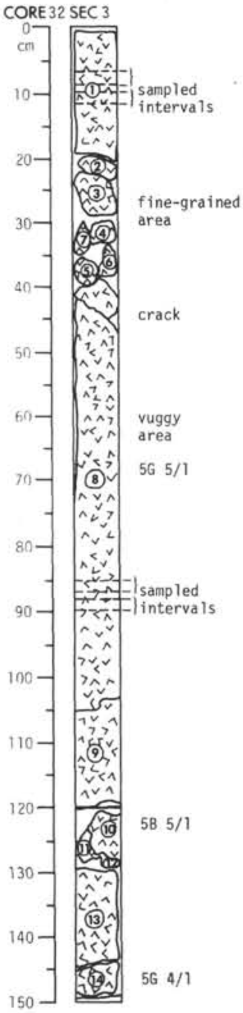

0-121 cm Upper 6 cm appears identical to that described at base of Core 32, Section 2. From 6-18 cm, basalt gradually coarsens and becomes vuggy, with vugs averaging 1 mm and reaching as large as 3 mm. From 18-45 cm basalt becomes fine-grained and loses vugs. From 45-107 cm, the basalt is slightly coarser-grained and vuggy; the vugs reaching maximum development between 45-75 cm. Between 107-121 cm, the basalt gradually becomes slightly finer-grained.

Coarsest part of flow unit (45-107 cm) is basalt; aphyric; medium greenish-gray (5G 5/1); vuggy (10-15%); vugs flattened, average 2 mm, reach 3 x 5 mm, unfilled, no crystal lining. Texture is diabasic with feldspar laths locally alined horizontally. Feldspar average .3 x 4.0 mm, but in some cases reach .3 x 15 mm. Pyroxene interstitial; little if any glass present. Plagioclase fairly fresh; clinopyroxenes seem to be considerably altered.

121 cm Contact between Flow units 3 and 4.

121-150 cm Flow unit 4. Basalt, bluish-gray at contact, changing downwards to dark greenish-gray; altered, finely vesicular to vuggy; aphyric, diabasic to intersertal. From 121-121 cm, basalt aphyric, medium bluish-gray (5B 5/1), nearly aphanitic, contains a few 0.5 mm round vesicles, but dense, probably contains altered glass. Grades downward to coarser, somewhat vuggy basalt much like that at the top of the section. Color changes to dark greenish-gray (5G 4/1). Both plagioclase and clinopyroxene appear to be considerably altered.

Figure 2. *(Continued).*

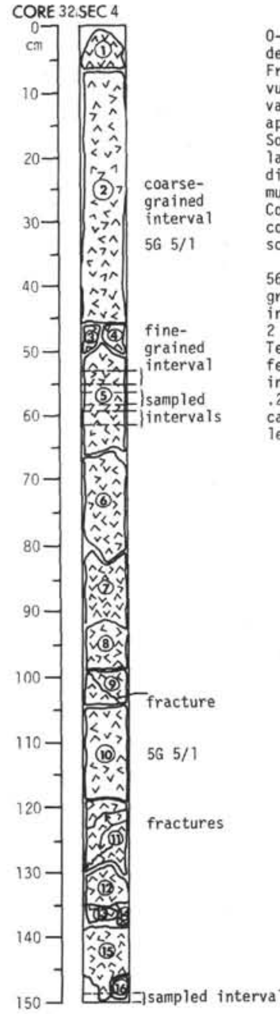

0-56 cm Upper 6 cm appears identical to that described at the base of Core 32, Section 3. From 6-49 cm, basalt is somewhat coarser and vuggy, much like that described in the interval 45-107 cm in Core 32 Section 3, but apparently contained more intersertal glass. Some are even vuggier, however, and feldspar laths lie at angles up to 15° from perpendicular to section. From 47-56 cm basalt is much like that described from 18-45 cm in Core 32 Section 3. From 56-150 cm, basalt coarsens somewhat to medium-grained, described below.

56-120 cm Basalt; aphyric; medium greenish-gray (5G 5/1). Locally vuggy, 0-10%, averaging about 5%; vugs average 1.5 mm, reaching 2 x 4 mm, locally flattened, no linings. Texture diabasic, locally variolitic, feldspar alignment much less pronounced than in interval 6-49 cm above. Feldspars average .2 x .8 mm, a few crystals as long as 2.0 mm can be found. Pyroxenes interstitial, at least partially altered.

Figure 2. *(Continued).*

clays of the montmorillonite (smectite) group. Most whole-rock diffractograms showed (001) *d*-values to range generally from 14.5 to 15.5Å, suggesting that Ca is the exchangeable cation. Only one vesicle filling from each hole had a ~12.5Å *d* spacing, suggesting Na to be the exchangeable ion (Grim, 1968). Several clay samples had (001) *d*-values falling between 12.5 and 14.5Å. Generally these intermediate *d*-values were associated with green vesicle fillings noted in Tables 3 and 4, and, in some cases, with green clay alteration in the groundmass of the basalts. However, the association is less than perfect, inasmuch as some of the green vesicle fillings have *d*-values occurring in the 14.5 to 15.5Å range. In one sample (315A-32-4, 53-55 cm) partial electron microprobe analyses were made for green vesicle-filling clay and brown clay that had replaced intersertal groundmass. In the green clay, K_2O averaged 0.05%, Na_2O, 1.43%, and CaO, 1.06%. In the brown clay, K_2O averaged 0.08%, Na_2O, 1.13%, and CaO, 1.39%. In general, we suspect that the green clays are enriched in Na_2O and the brown clays are enriched in CaO.

Six of the green clay samples were saturated with Li following the method of Green-Kelly (1953). The results of these analyses suggest that the clays fall near the beidellite end of the montmorillonite-beidellite series. However, we were unable to separate pure brown clay minerals for Li saturation, and we are unable to say whether or not these fall closer to end-member montmorillonite. Hereafter, we simply refer to all clay minerals as montmorillonite, in the sense that it is a group name for expanding clays. The color is noted, where appropriate, to indicate the exchangeable cation.

X-ray Mineralogy, Hole 315A

X-ray mineral identifications and estimates of approximate order of abundance were made for nine samples from the sedimentary section (Core 22A to Core 30A) above the basalts of Hole 315A. Core 22A contains, in order of decreasing abundance, calcite, plagioclase, montmorillonite, magnetite, anatase, and clinoptilolite.[1] Two samples from Core 23A consist of the some minerals in about the same abundance as observed for Core 22A, except that anatase is absent. In Core 25A, the one sample that was X-rayed consists of

[1]Clinoptilolite was distinguished from heulandite by the method of Mumpton (1960) and Murata and Whitely (1973).

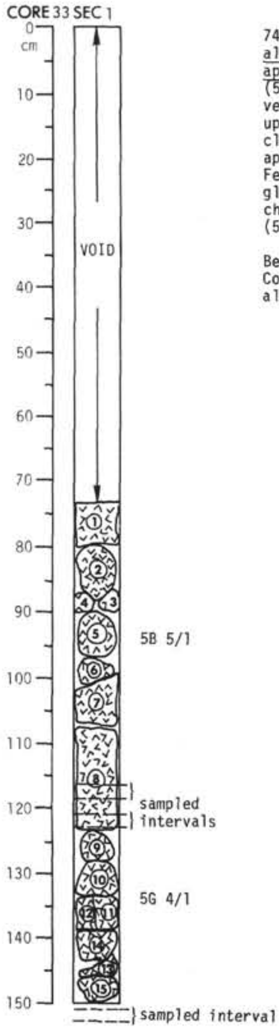

74-150 Flow unit 5A. Basalt, bluish-gray, altered, finely vesicular; aphyric, aphanitic. Aphyric; medium bluish-gray (5B 5/1); vesicular, 1-5%, averaging 3%, vesicles average .5 mm in diameter range up to 1.5 mm, all filled with calcite and clay minerals. Very fine-grained to aphanitic. Texture diabasic to intersertal. Feldspar appears partly fresh; pyroxenes and glass appear to be badly altered. Color changes downward to dark greenish-gray (5G 4/1).

Bears little resemblance to flow units of Core 32. This appears to be a different unit altogether.

Figure 2. *(Continued).*

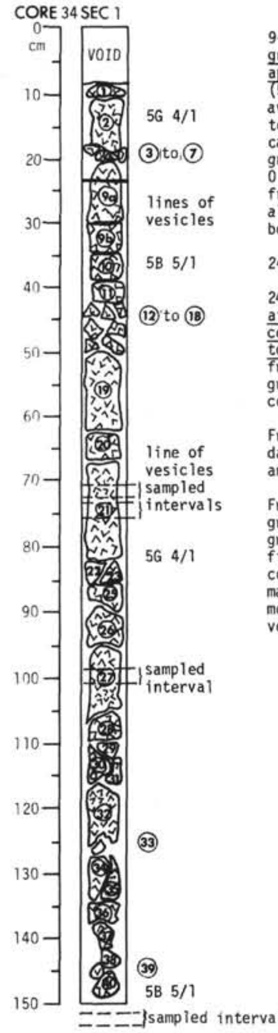

9-24 cm Flow unit 5B. Basalt; dark greenish-gray; altered; finely vesicular; aphyric; aphanitic. Aphyric, dark greenish-gray (5G 4/1); vesicular, 0-10% average 5%; average size 1.0 mm, but some flattened up to 2.0 x 3.0 mm. All vesicles filled with calcite and/or clay minerals. Very fine-grained, diabasic texture. Feldspar averages 0.1 x 0.4 mm in laths. Feldspar appears fresh, pyroxenes and glass appear badly altered. Material from 9-24 cm appears to be the same as Core 33 Section 4 (bottom).

24 cm Contact between Flow units 5B and 6.

24-150 cm Flow unit 6. Basalt, bluish-gray at top and base, dark greenish-gray in central part; altered; intersertal-diabasic to vitrophyric; aphyric; aphanitic. Material from 24-34 cm is aphanitic, medium bluish-gray (5B 5/1). Suspect a new flow unit is coming in here. Contact completely sharp.

From 34-130 cm unit changes in color to dark greenish-gray; becomes somewhat coarser and appears to contain more calcite.

From 130-150 cm, the unit becomes finer-grained, changes in color to medium bluish-gray and becomes aphanitic. Feldspars very fine and fresh, groundmass appears to be completely altered glass. Bottom of core may represent the base of flow unit. Becomes more coarsely vesicular downward with vesicles up to 10 mm.

Figure 2. *(Continued).*

nearly the same minerals as were found in Core 22A, but plagioclase is subordinate to montmorillonite and clinoptilolite, magnetite is absent, and a small amount of quartz is present. Core 25A was the lowest core of the sedimentary section in which calcite was observed. Core 28A contains plagioclase and montmorillonite as the dominant minerals, and clinoptilolite and anatase as subordinate components; pyroxene is of intermediate abundance and was identified only in this core. The two samples analyzed from Core 29A were very different; one contains only montmorillonite and plagioclase, and the other, quartz and celadonite. Finally, two sedimentary samples from Core 30A contain montmorillonite, K-feldspar, and possibly a small amount of anatase.

Three basalt samples were analyzed from Flow Unit 1A (Core 30A). These consist predominantly of montmorillonite and plagioclase with lesser amounts of calcite, pyroxene, magnetite, and a trace of anatase, in approximate order of decreasing abundance. X-ray analyses of three whole-rock samples and three vesicle fillings from Flow Unit 1B (Core 31A) indicate that the principal minerals are again montmorillonite and plagioclase with small amounts of magnetite and pyroxene, although identification of the latter mineral is somewhat questionable in two of the samples. Traces of anatase, pyrite, and ilmenite were tentatively identified in two of the samples. Vesicle fillings are composed predominantly of montmorillonite and calcite, although small amounts of pyrite also occur. The dominant minerals of Flow Unit 2 (Core 32A) occur in about the same abundances as those in Core 31A; however, anatase was not detected, and ilmenite was identified in only two of the five whole-rock samples. Vesicle-filling mineral associations are the same as those of Core 31A. In Flow Unit 3 (Core 32A) montmorillonite, plagioclase, pyroxene, and magnetite are the four predominant minerals in the whole-rock X-ray diffractograms. Vesicle fillings are predominantly composed of montmorillonite, with some pyrite and, possibly, a trace of calcite. In addition, one vesicle filling appears to contain a minor amount of marcasite (Sample 315A-32-3, 85-87 cm). Flow Unit 4 (Core 32A) has the same whole-rock mineral assemblage as Flow Unit 3. Tentative identification of ilmenite from two samples and of anatase from one sample were the only trace minerals suggested by the whole-rock X-ray analyses. Vesicle fillings of the flow unit have the same montmorillonite-calcite-pyrite mineral association found in vesicles of the flow units

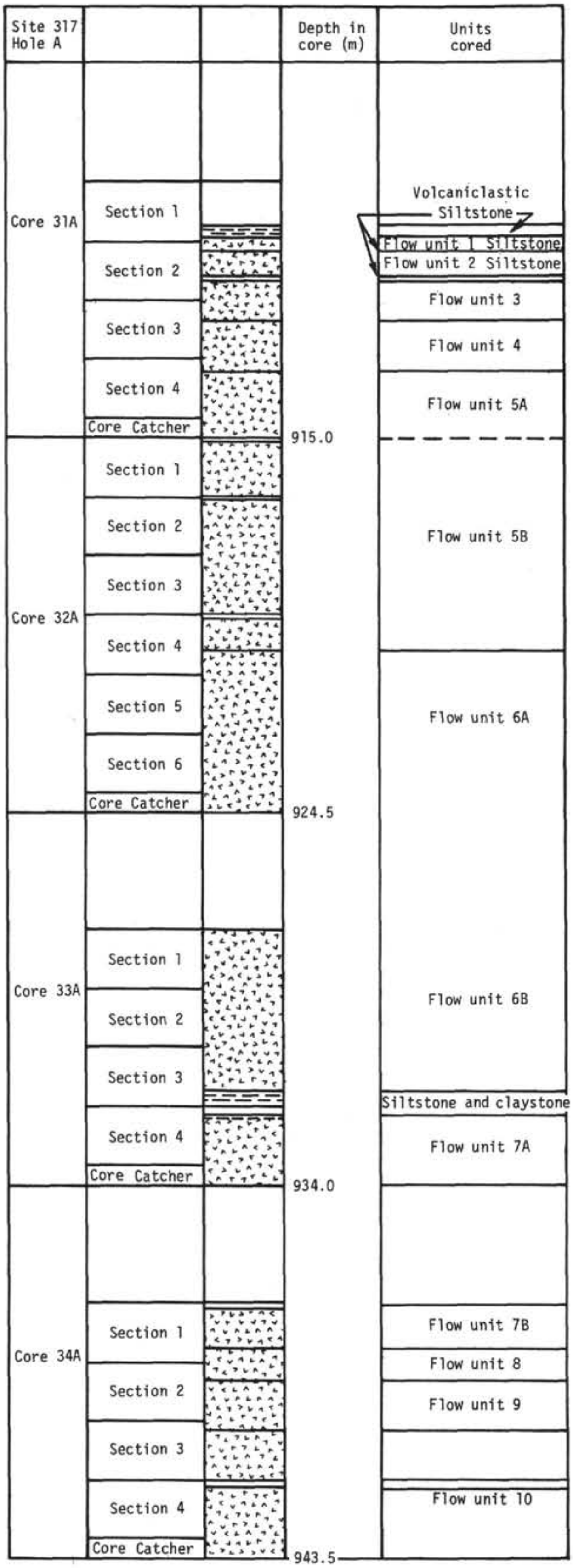

Figure 3. *Recovery of cored intervals from the deepest part of Hole 317A.*

above. Whole-rock analyses of Flow Unit 5A (Core 33A) indicate that (in order of abundance) montmorillonite, plagioclase, magnetite, and ilmenite are present, but pyroxene could definitely be identified from only one sample where it is slightly more abundant than magnetite and ilmenite. Vesicle fillings are mainly composed of calcite; however, pyrite was identified from one vesicle. Finally, Flow Unit 6 (Core 34A) contains montmorillonite, plagioclase, pyroxene, magnetite, and ilmenite (whole-rock analyses), and montmorillonite and calcite are present as vesicle fillings. In addition, a heavy mineral separation performed on one of the samples (315A-34-1, 99-101 cm) revealed the presence of a small amount of anatase in the heavier fraction of this sample.

The absence or masking of pyroxene in the X-ray analyses of rocks where it is a visible constituent is an artifact of the low intensity of the main pyroxene peaks compared to those of montmorillonite, plagioclase, and calcite. Even X-ray diffraction patterns of pyroxene separates did not show strong peaks.

X-ray Mineralogy, Hole 317A

For Hole 317A, several X-ray analyses were made of sediment samples above the basalt flows, as well as of the sediments intercalated between basalt flows in Core 33A. Two samples from Core 29A contain only montmorillonite and analcime. In Core 30A, montmorillonite and analcime are the dominant minerals in the five samples analyzed; however, one sediment sample from the core catcher contains only montmorillonite and plagioclase. Small amounts of hematite and K-feldspar were also noted in several of the samples analyzed. One sample from Core 31A contains only montmorillonite, while a second sample from the same core has montmorillonite, heulandite[2], celadonite, plagioclase, and quartz in approximate order of decreasing abundance. The volcaniclastic sediment between basalt flows in the upper part of the sedimentary section of Core 33A consists of plagioclase and pyroxene as the dominant minerals, with smaller amounts of heulandite, celadonite, montmorillonite, quartz, and pyrite. The lower part of this section contains, in approximate order of decreasing abundance, montmorillonite, quartz, calcite, plagioclase, pyroxene, pyrite, and magnetite.

X-ray analyses of the basalt in Core 31A (Flow Units 1 through 5A) indicate that the entire core is uniformly composed of montmorillonite, plagioclase, and pyroxene with traces of magnetite. Vesicle fillings commonly consist of either montmorillonite or calcite, although quartz was found in one vesicle (317A-34-1, 80-82 cm). Flow units 5B and 6A in Core 32A contain the same minerals in order of abundance as the whole-rock and vesicle-filling analyses of Core 31A; however, no quartz vesicle fillings were noted. About half of the analyses of Core 33A (Flow Units 6B and 7A) show plagioclase as the predominant mineral, while the other half show montmorillonite as the major constituent. The abundance of pyroxene is about the same as in Cores 31A

[2]Distinguished from clinoptilolite by the method of Mumpton (1960) and Murata and Whitely (1973).

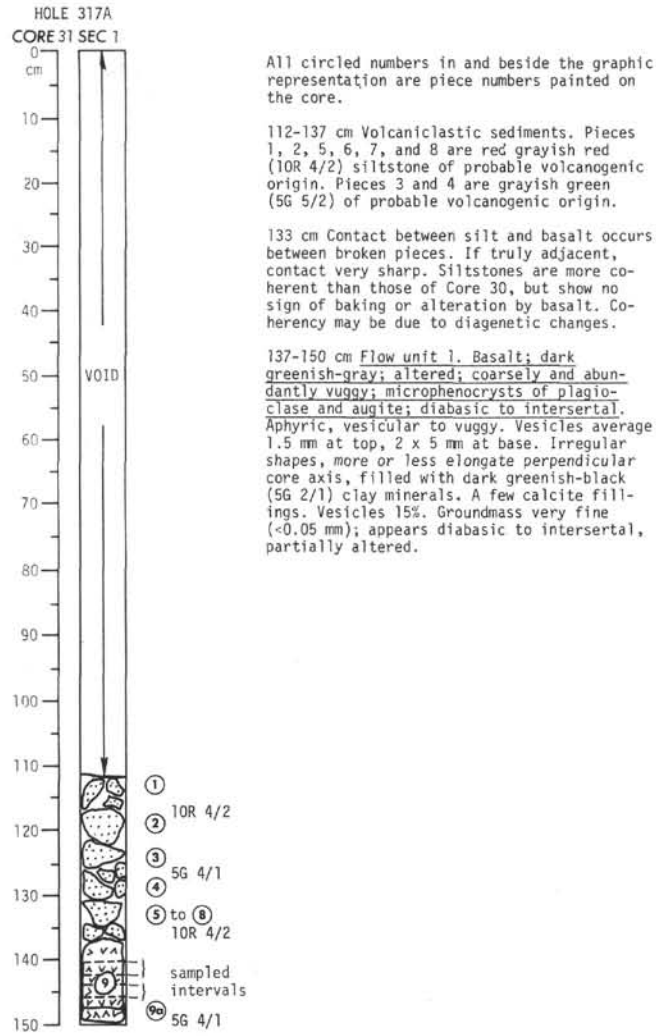

Figure 4. *Visual core description of basaltic rocks and associated sedimentary rocks of Hole 317A. Sampled intervals below sections are core-catcher samples.*

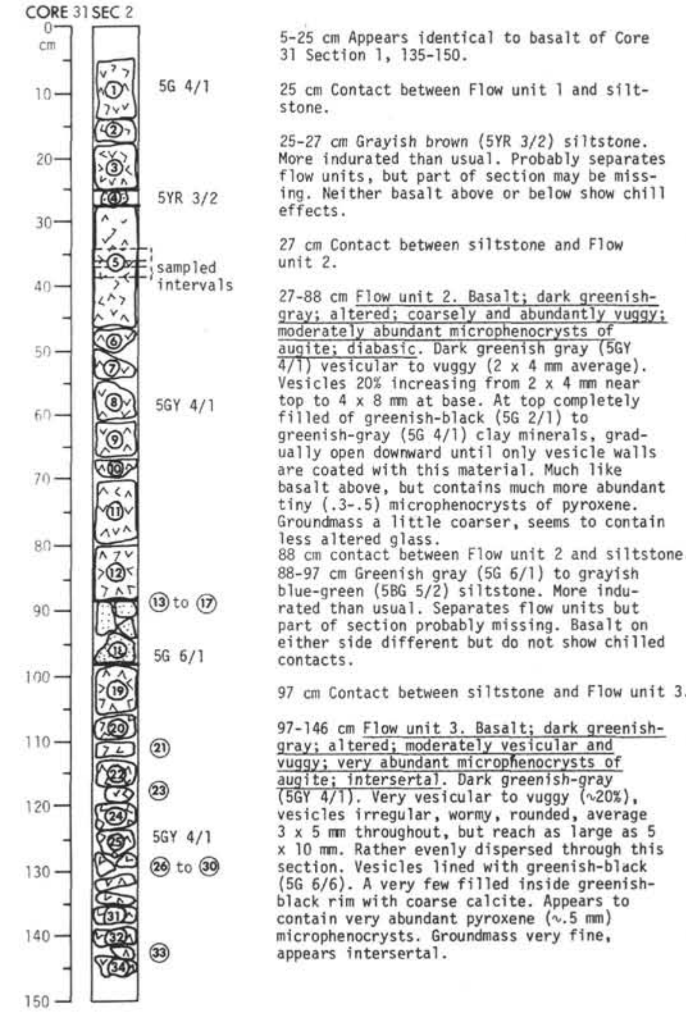

Figure 4. *(Continued).*

and 32A, but magnetite could be identified in only two samples. Vesicle fillings are the same as those of Core 32A. In Core 34A (Flow Units 7B, 9, and 10), montmorillonite is the dominant mineral, followed by plagioclase and pyroxene. Magnetite was identified in three samples and heulandite in one sample (317A-34-3, 115-117 cm). In addition to montmorillonite and calcite vesicle fillings, celadonite fills some of the vesicles in the interval 34-2, 84-86 cm to 34-4, 62-64 cm and is also present in three of the whole-rock analyses from this interval. Again, pyroxene appeared to the suppressed in the diffraction patterns, and, for most samples was visible optically in greater abundance than was indicated by X-ray analysis.

Petrography, Hole 315A

Petrographic data for the sampled basalts of Hole 315A are given in Table 3. Modes of the rocks are given as percentages of phenocrysts and microphenocrysts, percentages of vesicles, and percentages of groundmass. No attempt was made to point count minerals and alteration products of the groundmass, although the extent of alteration is described for each sample. As described in Figure 2 and Table 3, all flow units are similar but texturally distinct. Flow Unit 1 contains less than 1% iddingsite, presumed to have formerly been olivine; otherwise all flow units are barren of olivine. Flow Units 1 and 2 contain rather abundant microphenocrysts of plagioclase and augite,[3] except near their chilled margins, and while Flow Units 3 to 6 are described as aphyric, plagioclase and augite of about the same composition are only slightly smaller than 0.5 mm. All flow units are vesicular, and the vesicles are small, ranging from 0.1 to 2.0 mm in size, but averaging about 0.5 mm in most flow units. Vesicles are also moderately sparse, ranging from 1.5 to 9.0%, and averaging only about 5% of the rocks. The amount of former groundmass glass ranges from abundant to sparse, but all flow units contain some. All flow units contain magnetite and ilmenite, separately in some flow units and as complex intergrowths in others. No sample examined contained

[3]Strictly speaking, the "augite" of this section and of Table 3 is salite.

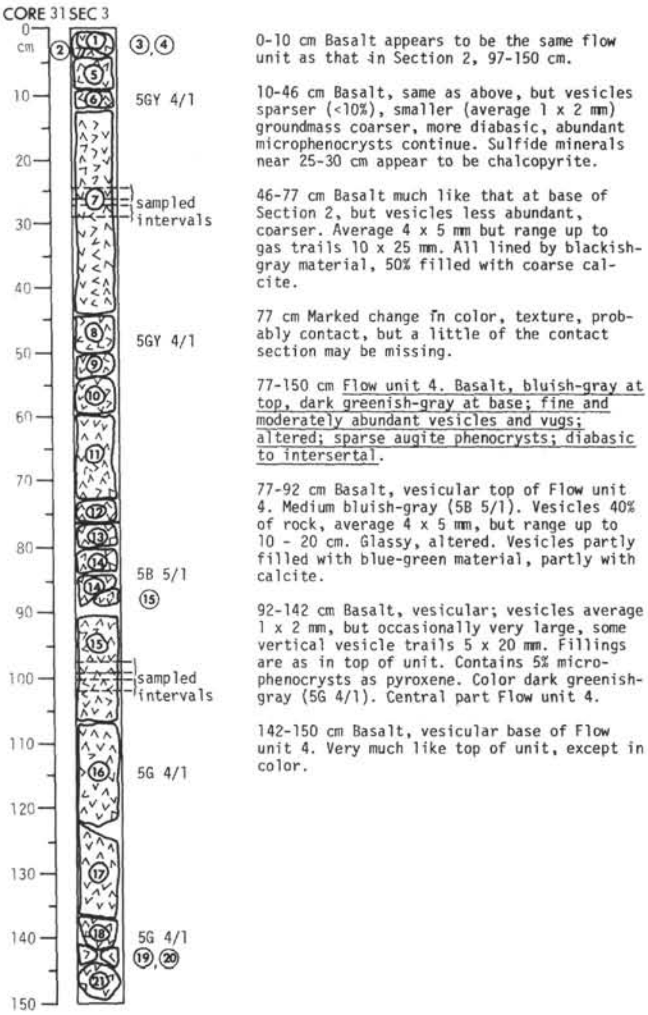

Figure 4. *(Continued).*

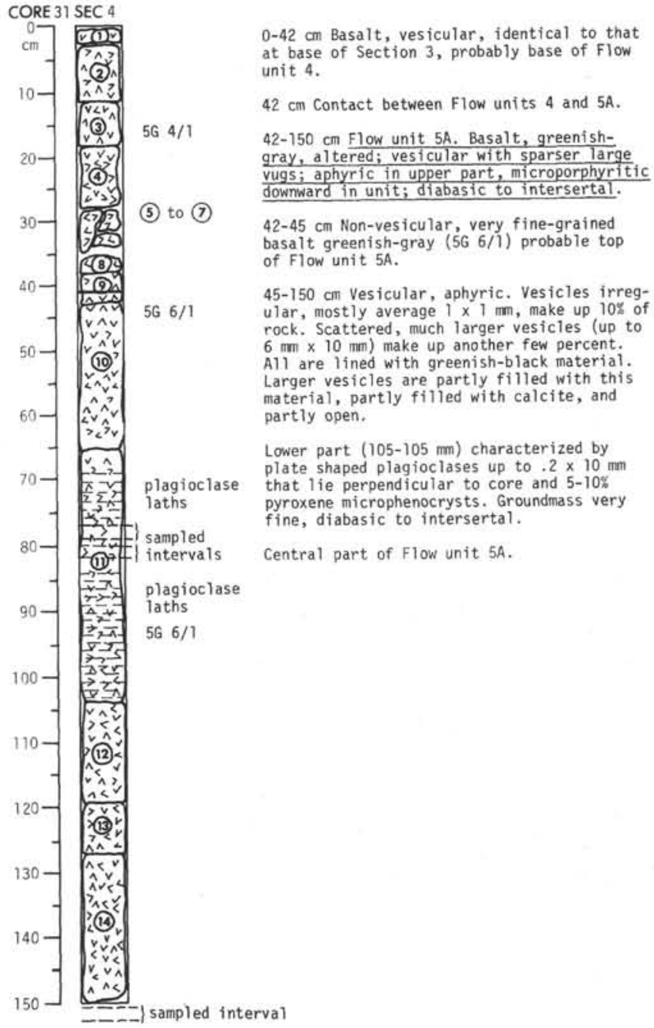

Figure 4. *(Continued).*

chromite. Chalcopyrite, believed to be primary, is very sparsely present, and although pyrrhotite was looked for, it was not seen. All the basalts are altered, but the extent of alteration is quite variable. All intersertal material believed to have formerly been glass is altered to brown montmorillonite, except in the case of Flow Unit 1 where some green montmorillonite replaces either glass or brown montmorillonite. All vesicles are partially to completely filled with alteration products. Almost without exception, brown montmorillonite lines vesicle walls, whereas the centers of the vesicles, where filled, consist of green montmorillonite, and less commonly, calcite or pyrite. A few pyrite and brown montmorillonite veins were observed, and, in a few samples, ilmenite is partially altered to anatase. For each rock thin-sectioned, a second uncovered section was routinely stained with potassium cobaltinitrite (Laniz et al., 1964) for potassium feldspar, but none was found, nor was any present in the X-ray diffraction patterns (Table 3). A third section of each sample was routinely stained for nepheline (Shand, 1939), but again none was observed, and chemical data below suggest that none was present prior to alteration. No celadonite or clinoptilolite were found either optically or by X-ray diffraction.

Although the rocks are described as moderately to heavily altered, few of the primary minerals—augite, plagioclase, magnetite, or ilmenite—are altered in most rocks examined. Alteration was confined principally to in situ alteration of original glass to montmorillonite, and to the vesicle-filling minerals described above. The textures of the rocks are therefore quite well preserved (Plate 1).

The preservation of textures has permitted the rather detailed descriptions given in Table 3. Minor textural variations at the sampled intervals confirm the identification of the flow units of Figure 2.

Petrography, Hole 317A

Petrographic data for Hole 317A are given in Table 4. Modes for phenocrysts, vesicles, and groundmass are given as in Table 3. As described in Figure 4 and Table 4, all 10 flow units are similar but texturally distinct. No sample examined contains olivine. If olivine were ever present in these rocks, it must have occurred as microlites in the altered groundmass of those rocks that contained original glass. Flow Units 1-5 contain small amounts of microphenocrysts of plagioclase, augite, and a pyroxene with low birefringence and a 2V of about

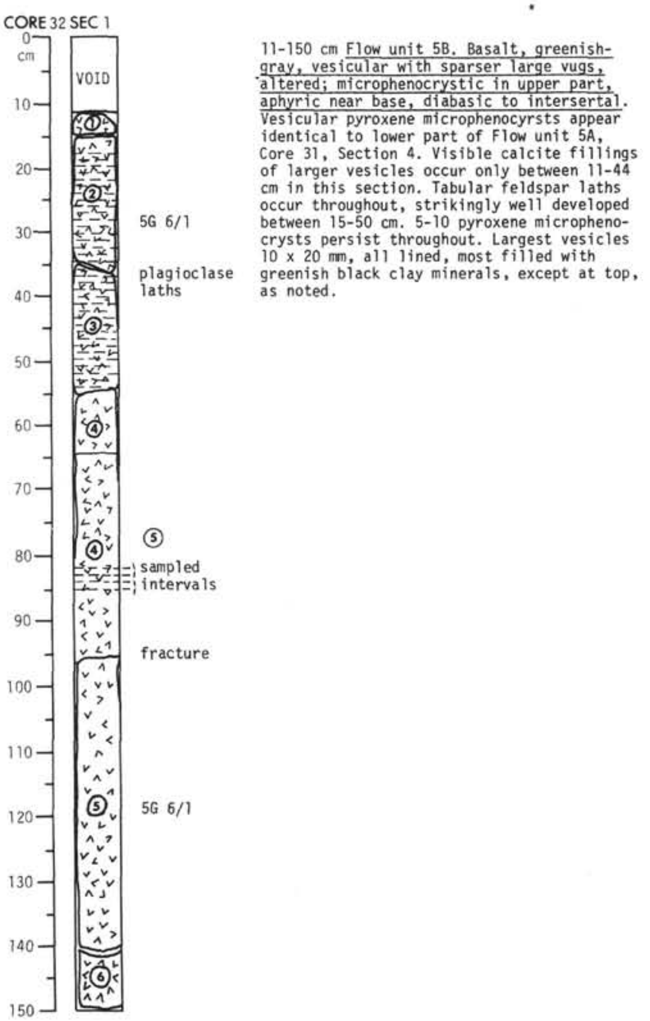

Figure 4. *(Continued).*

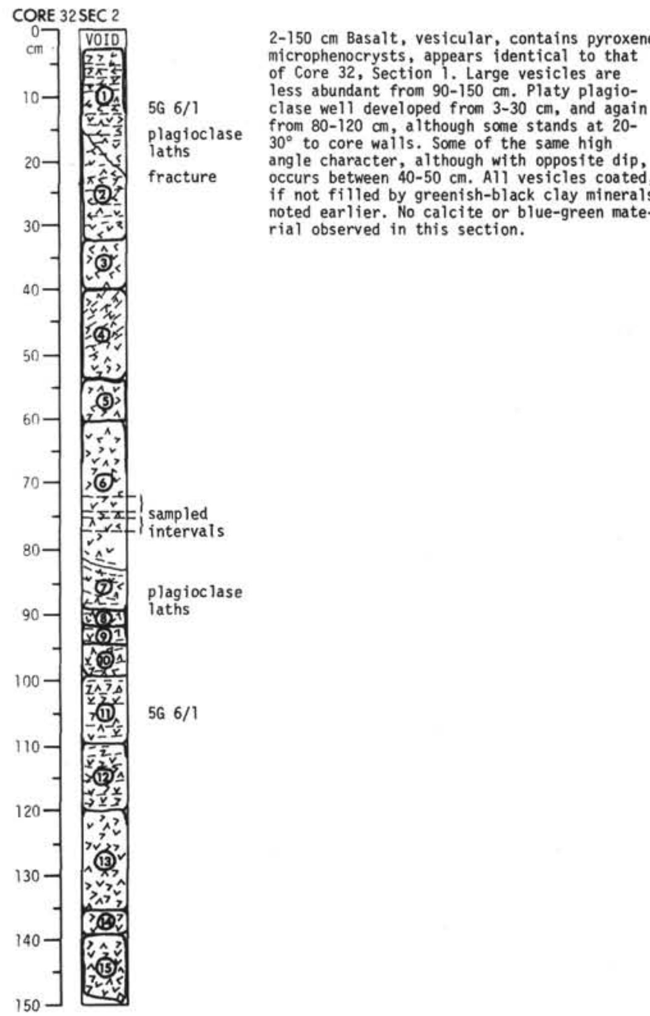

Figure 4. *(Continued).*

20°. This is referred to a Ca-poor augite in Table 4, although subsequent probe analyses suggest it is best described as low-calcium augite and ferroaugite. Flow Units 9 and 10 contain small (1.5 mm) glomeroporphyritic clots of plagioclase and pyroxene that are not uncommon in tholeiitic basalts (Dalrymple et al., 1974). The remainder of the flows are technically aphyric, although both pyroxenes and plagioclase are commonly only slightly less than 0.5 mm in grain size. Most of the flow units have diabasic to intersertal textures, although Flow Unit 7 is perhaps better described as intergranular-intersertal, and Flow Unit 10 is a vitrophyre. All flow units contain both augite and a low-calcium pyroxene. All flow units are vesicular, and the vesicles or vugs are extremely large (some are as large as 20 mm, and in most flow units they average 5.0-6.0 mm). Vesicles are also extremely abundant ranging from 5% to 30% of the rocks, and averaging about 10%. The amount of altered groundmass glass ranges from abundant to sparse, but all flow units contain some. All units contain small amounts of magnetite and ilmenite, in some cases as discrete grains and in some cases as complex intergrowths. No chromite was observed in any sample. Chalcopyrite blebs are more common than in the basalts of Hole 315A, and, in most cases, they are intergrown with pyrrhotite. All the basalts of Hole 317A are altered, but as a whole, they are a good deal fresher than those of Hole 315A in spite of their greater age. All original glass is altered to brown montmorillonite, except in Flow Units 9 and 10, where small amounts of celadonite occur. All vesicles are partially filled with alteration products. Almost without exception, brown montmorillonite coats the outer vesicle walls, and the inner parts of the vesicle walls, if filled, are occupied by green montmorillonite, or, far less commonly, calcite, very minor amounts of quartz, and in one vesicle of Flow Unit 10, celadonite and heulandite. No pyrite was observed either optically or in X-ray diffraction patterns. As with the basalts of Hole 315A, stained sections and X-ray data revealed no trace of potassium feldspar or nepheline.

Although the basalts of Hole 317A are described as somewhat to heavily altered, the extent of alteration is largely a function of the amount of original glass present and the extent to which vesicles are filled. The textures of the rocks are perfectly preserved (Plate 2).

The megascopic identification of flow units of Figure 4 is confirmed by minor variations in groundmass tex-

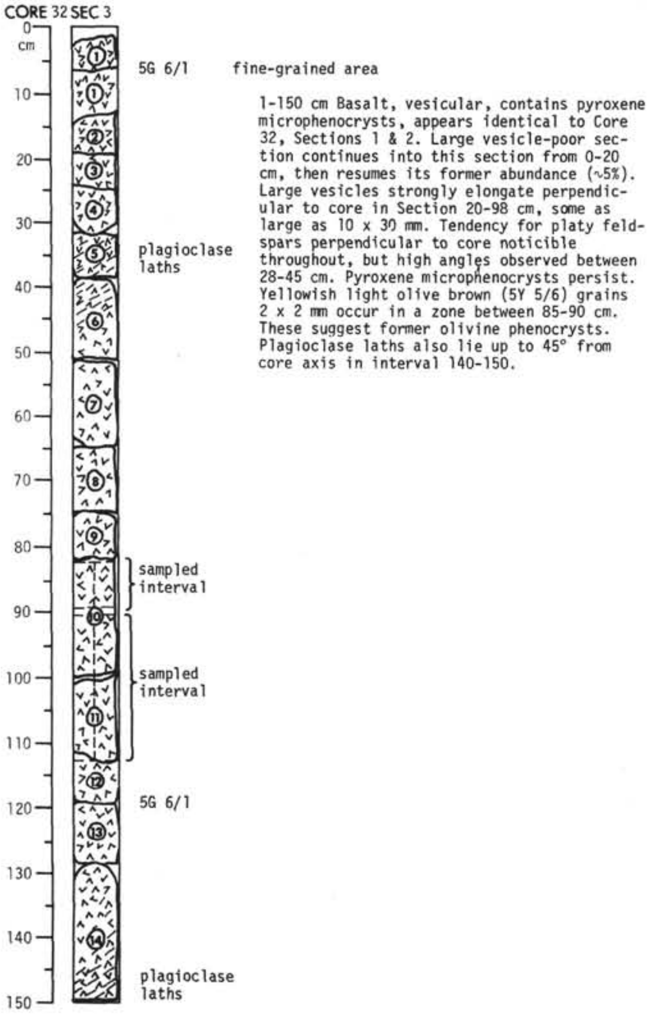

Figure 4. *(Continued*

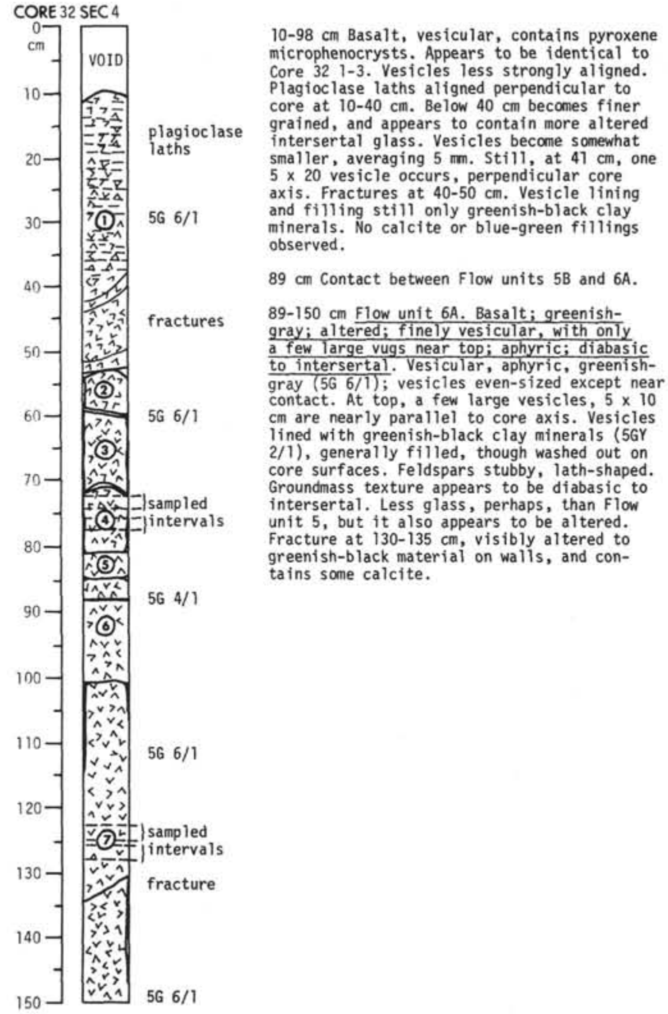

Figure 4. *(Continued).*

tures and by variations in chemical composition noted below. The textures and mineralogy of these rocks appear identical to those of oceanic ridge basalts recovered from DSDP Legs 6, 7, 16, 17, 18, 19, 30, and 32 in the Pacific Basin, except for vesicle size. Moberly and Heath (1971) reported amygdules in the basalt at Site 61 that range in size from 5 to 20 mm, but, for the most part, basalts with abyssal characteristics are dense (Stoeser, in press) to finely vesicular (Bass et al., 1973). The size and abundance of vesicles and vugs in the 317A basalts seem highly unusual (Plate 3). Moore (1965) showed that vesicles in the pillowed rims of Hawaiian tholeiites decrease in both size and abundance with increasing water depth. Aumento (1971) was unable to find any such variation in dredged abyssal basalts from the Atlantic. This discrepancy may stem from the fact that Moore (1965) confined his study to pillow skins, whereas Aumento (1971) studied pillow interiors as well. Nevertheless, Aumento showed that of hundreds of Atlantic basalts collected at water depths between 1000 and 3500 meters, none contain circular vesicles with average sizes larger than 3 mm, although he omitted "larger, lensoid vesicles of dubious origin" (op. cit., p. 1316) from his study. Earlier, more detailed descriptions of these "larger, lensoid vesicles" (Aumento, 1968) show them to be large tabular vugs in rocks that also contain smaller vesicles. All in all, these larger cavities bear little resemblance to the coarse and abundant vesicles of the basalts of Hole 317A. Moore and Schilling (1973), again measuring only the outer 1-cm rind of pillows at progressively shallower water depths up the Reykjanes Ridge, show a striking correlation between volume percent vesicles and water depth. At water depths of 1000 meters, their samples contain about 5% vesicles; at 700 meters 10%; at 500 meters, 20%; and at 200 meters, 30%. Only two samples of 78 contain 30% vesicles at water depths greater than 400 meters. Although these data may not be directly comparable to those for the basalts of Hole 317A, it seems reasonable to conclude that they were erupted in relatively shallow water, or that they contained unusually large amounts of volatile constituents. Vesicles in the basalts of Hole 315A, on the other hand, are of a size and volume appropriate to water depths of 1000-3000 meters.

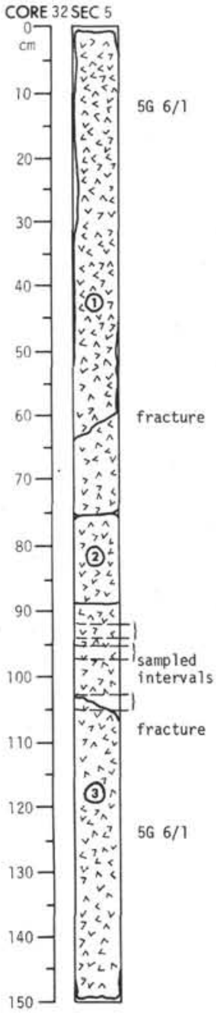

Figure 4. *(Continued).*

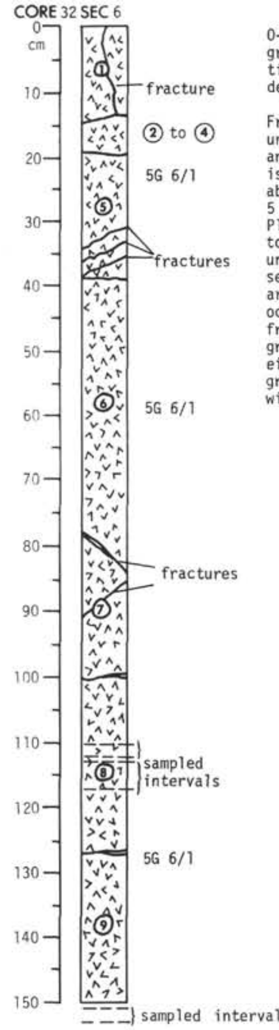

Figure 4. *(Continued).*

CHEMICAL COMPOSITION OF THE BASALTS FROM HOLES 315A AND 317A

Major Elements

One sample from Hole 315A (32-2, 96-105 cm) and one sample from Hole 317A (32-3, 100-111.5 cm) were analyzed for major elements by conventional wet chemical methods (Peck, 1964; see Tables 5 and 6). Thirty other analyses for major elements shown in Tables 5 and 6 were obtained by a combination of analytical techniques. X-ray fluorescence techniques were employed for the determination of SiO_2, Al_2O_3, Fe_2O_3, MgO, CaO, K_2O, TiO_2, P_2O_5, and MnO (Fabbi, 1972); Cl (Fabbi and Espos, 1972a); BaO and SrO (Fabbi, 1971); total S as S (Fabbi and Moore, 1970); and Rb_2O (Fabbi and Espos, 1972b). Classical chemical techniques were used to determined H_2O^+, H_2O^-, and FeO. Na_2O was determined by flame photometry because loss of detector resolution during X-ray fluorescence (XRF) analysis affected the determination of Na_2O. Comparative Na_2O values (Table 7) illustrate differences in accuracy resulting from loss of detector resolution, accuracy obtained with a stable high-resolution detector (Fabbi, 1973), and flame photometric results. There is generally good agreement for the Na_2O values that are within the limits of precision of the two techniques (XRF ±7% and flame photometer ±2%) and the associated sampling errors. Errors caused by the low-resolution detector increase with higher concentrations of Na_2O.

Two duplicate analyses determined by both wet-chemical methods and X-ray fluorescence were made for each hole (Samples 315A-32-2, 96-105 cm and 317A-32-3, 100-111.5 cm). Results in Tables 5 and 6 show the analyses to be within precision limits of the XRF method, except for differences in H_2O^+ and H_2O^-, although the total water in the samples is nearly identical. In general, the duplicate analyses differ by less than 0.3% for major constituents, and 0.03% for less abundant constituents.

It is clear from the major-element data that the basalts are considerably altered. The total water content of basalts from Hole 315A ranges from 5.98% to 7.88% and averages 6.85%. More than half of the iron in these samples is oxidized. The basalts of Hole 317A are

CORE 33 SEC 1

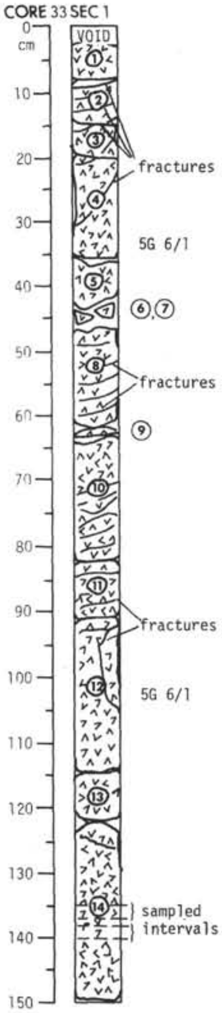

2-150 cm Flow unit 6B. Basalt; greenish-gray; altered; finely vesicular; aphyric; diabasic intersertal. Vesicular, aphyric, greenish-gray (5G 6/1). Appears identical to Core 32, Section 6, but more fractured, veined, and altered in the upper part, perhaps fresher in the lower part. The core is especially badly fractured in the interval 7-30 cm, 48-80 cm, and 90-105 cm. All veins and incipient fractures are altered, and, frequently the basalt between them is colored greenish-black. Texture and size of vesicles continue fine toward the lower end. All vesicles are filled with greenish-black clay minerals. A little calcite was observed near some fractures and broken ends.

Figure 4. *(Continued).*

CORE 33 SEC 2

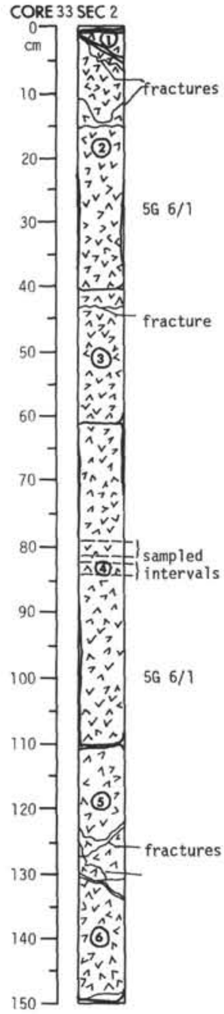

1-150 cm Basalt, vesicular, aphyric, greenish-gray (5G 6/1). Almost identical to Core 32, Section 5, perhaps has finer vesicles and is finer grained than Core 32, Section 6, Core 33, Section 1, although almost surely part of the same flow unit. Small fractures 1-15 cm, 42 cm, 122-135 cm, some alteration but not nearly so marked as in Core 33, Section 1.

Figure 4. *(Continued).*

somewhat fresher; total water content ranges from 2.69% to 7.00% and averages 4.00%; less than half the iron is oxidized.

Minor Elements

Complete spectrographic analysis was performed on 30 basalt samples utilizing the semiquantitative six-step method (Myers et al., 1960). The data supplemented our information in regard to the petrologic studies using major- and minor-element correlations. Good agreement was observed in most minor elements when compared with values obtained by X-ray fluorescence.

Cr, Nb, Ni, Zr, Y, and V (Tables 8 and 9) were also quantitatively determined by the powder D-C arc technique (Bastron et al., 1960). Interlaboratory synthetic standards and chemically analyzed rock standards were used to draw our analytical curves and to read off our concentration values. Because of the basic nature of the samples, analytical curves generated by the W-1 (diabase) and BDR (Columbia River Basalt) standard rock dilutions were favored over the curves obtained by the use of synthetic interlaboratory standards. Therefore, by using standards of chemical composition similar to that of the samples, matrix effects were minimized that otherwise might have adversely affected the overall accuracy of our analysis.

A direct comparison of the values obtained by both methods indicates that good agreement exists among all elements analyzed, with zirconium (Zr) having the poorest agreement because of its refractory nature in the arc. An overall accuracy of ±15% for all elements was maintained. Ce, Co, Cr, Cs, Eu, Fe, Gd, Hf, Sc, Ta, Tb, Th, Yb, Zn, and Zr were determined by fluorimetric analysis (Flanagan et al., in press) and U by radioactivation techniques (Tables 10 and 11). It is apparent from inspection of Tables 5, 6, 8, 9, 10, and 11 that although the minor-element contents of basalts in Holes 315A and 317A show little internal variation, abundances of most elements in the rocks from the two holes are significantly different. For example. Ba, Sr, Nb, P, Ti, V, Y, and Zr and much lower in basalts of Hole 317A than in those of 315A, whereas Cr, Ni, and Sc are higher.

Mineral Analyses

Plagioclase and pyroxene analyses for three selected flow units of Holes 315A and 317A are given in Table 12. Compositions of plagioclase microphenocrysts in Hole 315A are nearly constant with An values of 61-62;

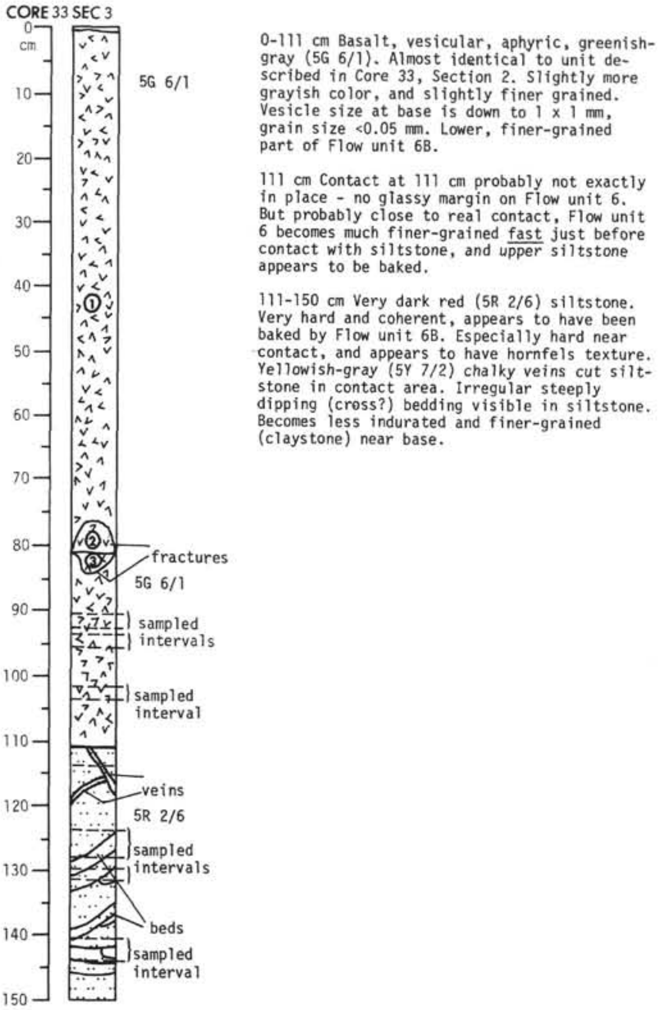

Figure 4. *(Continued).*

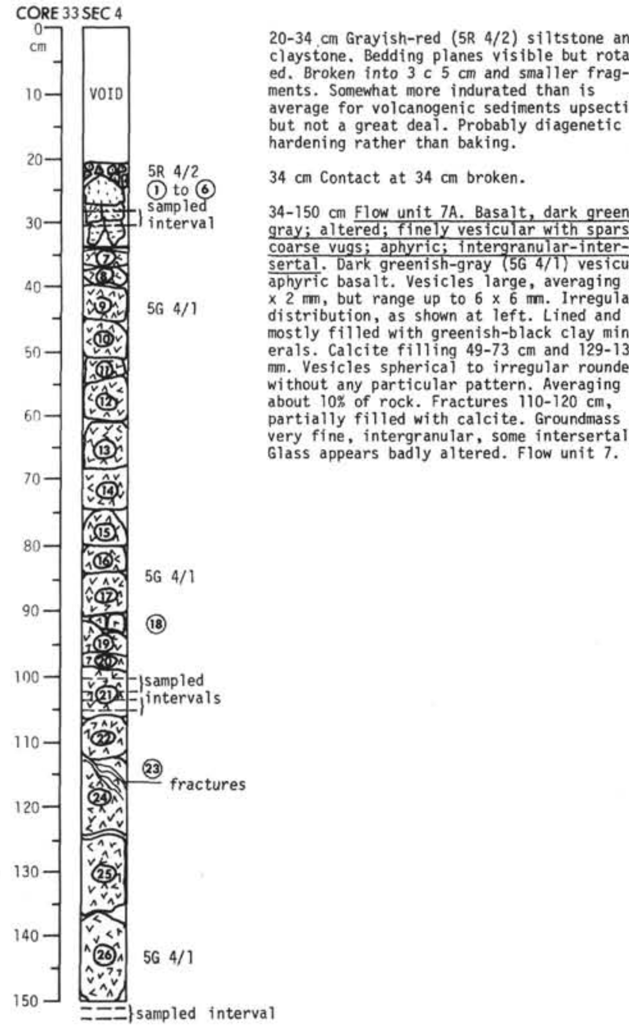

Figure 4. *(Continued).*

one groundmass plagioclase analyzed also has a composition of An_{61}. Three groundmass plagioclases from Hole 317A have a range in composition of An_{58-69}. These values are lower than those given by the X-ray method (see Tables 3 and 4), but energy-dispersive methods were used for determining microprobe values of CaO and K_2O in the plagioclases, and K_2O values, while significant with respect to one another, may be uniformly high. In fact, separated plagioclase whose K_2O content was determined by isotope dilution for 315A-32-2, 83.5-91 cm and 317A-32-3, 84-85 cm and 86-88 cm give values 0.16%-0.18% and 0.09%-0.10%, respectively (Lanphere and Dalyrymple, this volume). In addition, the IV coordinated ions in all the plagioclases are low, probably reflecting the presence of Fe_2O_3, which was not determined (see Beeson, 1973).

All of the analyzed pyroxenes of Hole 315A are salites; the two microphenocryst averages are almost identical with $Ca_{49-50}Mg_{32}Fe_{18-19}$, whereas the groundmass pyroxene proved to be somewhat richer in Fe and poorer in Ca (Table 12). The pyroxenes of Hole 317A are more variable, but easily separable from those of Hole 315A by their lower Ca content and greater range of Mg and Fe contents (see Figure 5). It is apparent that two pyroxenes are present in each flow unit of Hole 317A analyzed. It is also apparent that the augites of Flow Unit 2, whether present as microphenocrysts or groundmass minerals, have a rather restricted range composition of $Ca_{38-40}Mg_{50-54}Fe_{8-10}$, whereas one groundmass pyroxene with low birefringence and small (20°) 2V is a calcium-poor augite with ratios of $Ca_{32.5}Mg_{53}Fe_{14.5}$. In Flow Unit 5B, both microphenocrysts analyzed are characterized by low birefringence and low 2V and proved to be calcium-poor ferroaugites, whereas the one groundmass augite analyzed contains more Ca and much less Fe. In Flow Unit 7B, where three groundmass pyroxenes were analyzed, two are augites with compositions of $Ca_{37-39}Mg_{47-52}Fe_{10-14}$, whereas the other one was a low birefringence and low 2V pyroxene with a composition of $Ca_{25}Mg_{54}Fe_{21}$. The wide range and unusual composition of the pyroxenes in Hole 317A and their differences in different flow units merit further study.

Dry Reduced Analyses and Norms

The dry reduced chemical analyses of the basalts of Hole 315A are given in Table 13. These analyses show

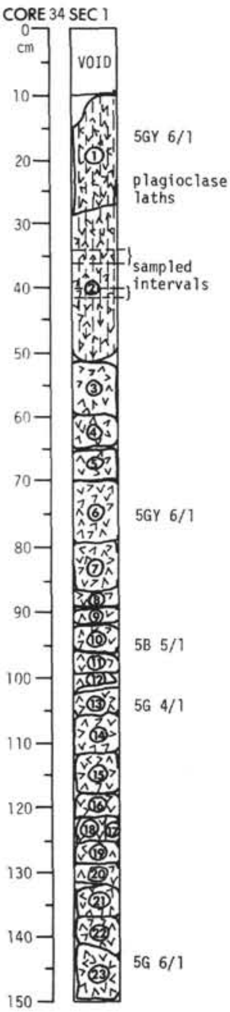

10-90 cm Flow unit 7B. Basalt; greenish-gray; finely vesicular with sparse coarse vugs in upper part; aphyric; intergranular-intersertal. Basalt, greenish-gray (5GY 6/1) vesicular aphyric basalt. Probably lower part of Flow unit 7A. Vesicles large in upper part -- up to 5-10 mm - some in obliqur trails 50 mm long. Gradually changes downward to irregular shaped vesicles averaging 1 mm in diameter. Mostly filled with greenish-black clay minerals, but calcite is also fairly abundant. Unit characterized by vertical feldspar laths -- as large as .5 mm x 4.0 mm in upper part, average size in lower .1 x 3.0 mm grading downward in size. Some of these are in vertical variolitic sheaves. Glass not abundant if present.

90 cm Contact at 90 cm between Flow units 7B and 8 altered.

90-150 cm Flow unit 8, dark greenish-gray; altered; vesicular to coarsely vuggy; plagioclase phenocrysts and glomeroporphyritic clots of pyroxene and plagioclase; diabasic-intersertal.

90-110 cm Medium bluish-gray (5B 5/1) fine-grained, heavily altered.

110-150 cm Dark greenish-gray (5G 4/1) vesicular, with plagioclase phenocrysts and glomeroporphyritic clots of pyroxene and plagioclase. Vesicles very abundant in this, the upper part of flow unit. Size range 1 x 1 mm to 10 x 15 mm, averaging 2 x 3 mm. Vesicles make up 30% of rock from 118-143 cm. Plagioclase phenocrysts are small, blocky, 1 mm x 1 mm. Clots larger - 2 x 2 mm. Phenocrysts make up ∿5% of vesicular rock, clots perhaps 10%. Vesicles lined and filled partly by greenish-black clay minerals, and partly by microcrystalline pale blue-green (5BG 7/2) clay minerals. Coarse calcite fills vesicles in lower part of vesicular section. Lowest unit (142-150 cm) is finer grained, aphyric, and has fewer vesicles.

Figure 4. *(Continued).*

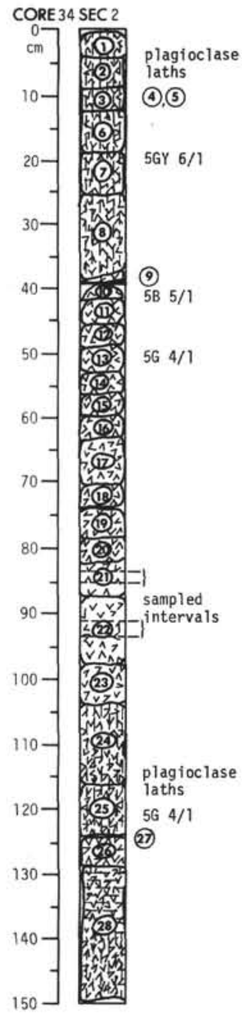

0-39 cm Basalt, greenish-gray (5GY 6/1), vesicular, aphyric, vertical feldspar laths. Appears identical to flow unit at base of Section 1, but contains vertical feldspar laths like those in the lower part of Flow unit 7.

39 cm Contact at 39 cm between Flow units 8 and 9 altered.

39-150 cm Flow unit 9. Basalt greenish-gray; altered; vesicular to very coarsely vuggy; local plagioclase phenocrysts and abundant glomeroporphyritic clots of pyroxene and plagioclase; intersertal-diabasic.

39-44 cm Medium bluish-gray, fine-grained, heavily altered.

44-150 cm Greenish-gray (5G 4/1) vesicular, plagioclase phenocrysts and glomeroporphyritic clots. Vesicles very large in central part -- up to 15 x 15 x 20 mm. Much like upper and middle part of Flow unit 8 down to 110 cm. Then becomes gradually finer, like lower part of Flow unit 8. Light blue-green vesicle filling material concentrated near upper contact; calcite in central part.

Figure 4. *(Continued).*

no quartz or nepheline in their norms, and their total-alkali to SiO_2 ratios place them above Macdonald's (1968) line separating alkalic basalts from tholeiites. We consider this line more appropriate for oceanic rocks than Irvine and Baragar's (1971) line. Nevertheless, the norms of these rocks contain from 2.43% to 9.06% normative diopside, from 4.43% to 16.65% normative hypersthene, and from 15.03% to 22.35% normative olivine, where neither olivine nor low-calcium pyroxene was observed in the rocks. Furthermore, normative An values are, in general, less than 50, whereas feldspar in the rocks has values in the range An_{59} to An_{68}. In addition, En-Fs ratios are lower than observed in mineral analyses of the pyroxenes (see above). It is possible that in the process of alteration, both SiO_2 and CaO may have been selectively removed, and Na_2O and MgO added to the rocks. Their total chemical composition, which will be disucssed further below, is similar to oceanic island, not oceanic ridge lavas, although the problem of whether they are somewhat altered oceanic island tholeiites, mildly alkalic basalts, or transitional between the two remains in some doubt.

The dry reduced analyses from Hole 317A (Table 14) differ considerably from those of Hole 315A, and their norms are in better accord with their observed mineralogy. Five of the analyses have 0.05%-0.6% normative quartz; none has normative nepheline. Their normative diopside contents range from 15.2% to 27.2%, their normative hypersthene contents range from 18.2% to 27.7%, and their normative olivine contents range from 0 (in five samples) to 11.1%. Furthermore, normative An contents are much more nearly compatible with those observed in the rocks. These rocks contain no modal olivine, and Ca-rich pyroxene generally exceeds Ca-poor pyroxene. It would appear that the dry reduced analyses of basalts of Hole 317A more closely approximate their original compositions even though, in some cases, SiO_2 and CaO may have been lost during alteration, and some Na_2O and MgO may have been added.

As a test of this possibility, we plotted Na_2O, MgO, CaO, and SiO_2 against total water content in rocks of both holes in Figure 6. Normally, oxides on this diagram should show increases proportional to their relative abundance in the rocks. This figure failed to confirm that dry reduced Na_2O was much affected by degree of alteration as evidenced by total water content, unless Na_2O was added at water levels less than 2.5%. Figure 6 does show clearly, however, that dry reduced

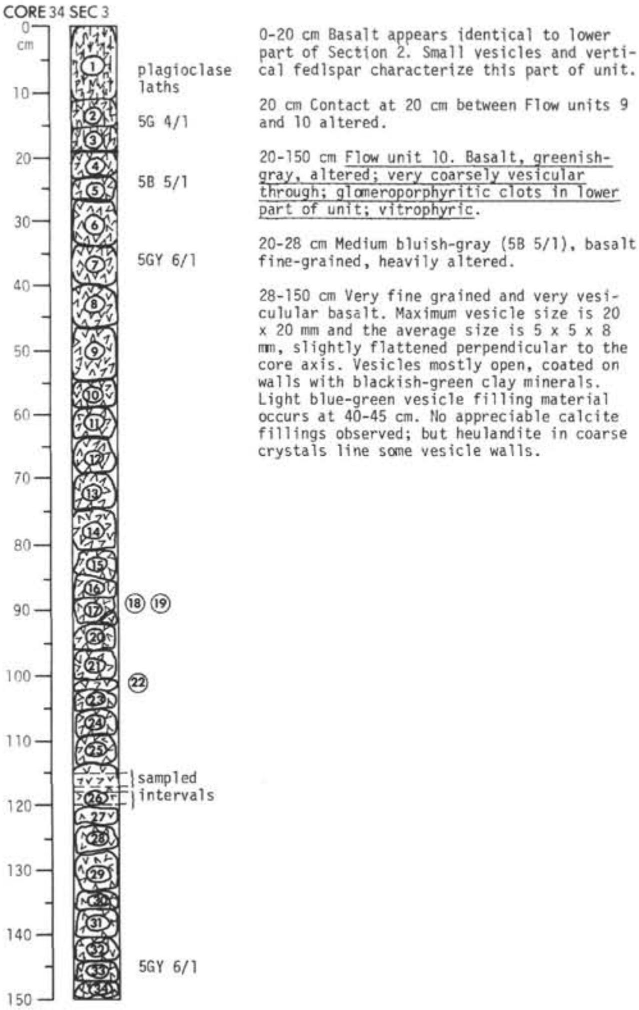

Figure 4. *(Continued).*

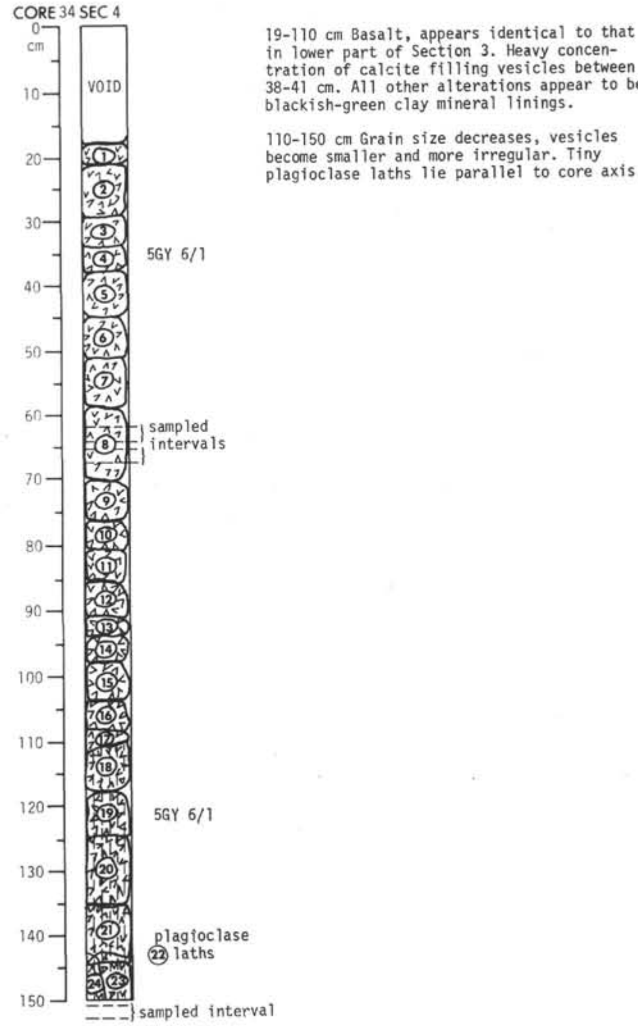

Figure 4. *(Continued).*

CaO and SiO_2 decrease somewhat irregularly, with increasing water content of the basalts of both holes. Dry reduced MgO increases, as it should, but more than its relative abundance in the basalts would suggest that it should.

The range and average values of both major and minor elements of basalts from both holes are compared in Table 15. Differences between both ranges and averages show that the basalts from the two holes differ from one another for nearly every oxide or element, except for CaO, Co, Cs, and Rb. Considering that the dry-reduced whole-rock analyses are fairly representative of the fresh basalts that once resided at Sites 315 and 317, that the minor-element contents for the most part are representative of original contents in the basalts, and that the mineral analyses are representative of the basalts at both sites, then it is clear that the chemical compositions of the basalts of 317A are much like those of other oceanic ridge tholeiites drilled in the Pacific. It seems equally clear that the chemical composition of the basalts from Hole 315A are not of that type, but are more nearly comparable to basalts of oceanic islands.

COMPARISONS WITH COMPOSITIONALLY RELATED BASALTS

Mineral Compositions

Plagioclase compositions in the basalts of Hole 315A range from $An_{58.9}$ to $An_{68.6}$, whereas those of the basalts of Hole 317A range from $An_{58.0}$ to $An_{73.5}$, and average to higher An values. Such ranges of An values have been reported for oceanic island tholeiites and alkalic basalts (Keil et al., 1972) for oceanic ridge tholeiites (Ridley et al., 1974; Stoeser, in press), and although oceanic ridge basalts generally contain more An-rich feldspar, the reported values give little clue as to basaltic type.

Fodor et al. (1975) show salite to be the common pyroxene of Hawaiian alkalic basalts, whereas high-calcium pyroxenes of the Hawaiian tholeiitic suite have Ca contents of 40 more percent or less. On this criterion the Hole 315A pyroxenes are similar to those of alkalic basalts of the oceanic island type. Both Hawaiian tholeiites and oceanic ridge tholeiites commonly contain two pyroxenes, but the Hawaiian ones range between

TABLE 2
Drilling Summary of the Deepest Cores of Hole 317A

Core	Drilled Interval (m)	Drilling Rate (m/hr)	Recovery (%)	Flow Unit Thickness (m) (see Figure 3)
25A-30A	57.0	3.2-5.5	63.2-100.0	
31A	9.5	11.1	50.5	1 0.3 2 0.65 3 1.25 4 1.15 5A ⩾ 1.6
32A	9.5	19.0	91.6	5B ⩾ 5.3 6A ⩾ 5.1
33A	9.5	15.0	61.1	6B ⩾ 4.1 7A ⩾ 1.7
34A	9.5	14.3	58.9	7B ⩾ 0.8 8 1.0 9 1.3 10 ⩾ 3.3

augite and pigeonite, whereas pyroxenes of oceanic ridge tholeiites more commonly range toward calcium-poor augites and calcium-poor ferroaugites (Fodor et al., 1975; Ridley et al., 1974; Stoeser, in press). Clearly, the pyroxenes of Hole 317A are of the oceanic ridge tholeiite type.

Minor Elements

A number of authors have considered that certain stable (refractory) minor elements preserve their primary concentrations and ratios even in highly altered volcanic rocks, and that these elements are of greater assistance than major elements in identifying basaltic suites in their partially altered parents (Ishikawa, 1968; Kay et al., 1970; Hart and Nalwalk, 1970; Hart, 1971; Schilling, 1971; Matthews, 1971; Pearce and Cann, 1973; Bass et al., 1973; Stoeser, in press; Marshall, in press). One such discriminant plot is that of P_2O_5 against TiO_2 in weight percent (Figure 7). The fields of Figure 7 are from Bass et al., (1973), but we have plotted Macdonald and Katsura's (1964) average alkalic basalts and tholeiites on the diagram for comparison, and these fall quite satisfactorily into Bass et al.'s (1973) fields. Basalts of Hole 317A fall in the lower left corner of the diagram, well into the oceanic ridge tholeiite (ocean ridge basalt) field, and compare well with Stoeser's (in press) values from the Ontong-Java Plateau. The ratios for the basalts of Hole 315A, on the other hand, straddle the field between Hawaiian tholeiites and true alkalic basalts; the Hole 315A rocks are clearly of the oceanic island type, but are much less strongly alkalic than Bass et al.'s (1973) rocks from Site 165, which contain between 6% and 15% normative nepheline and approximately twice as much K_2O as post-erosional basalts of the Honolulu Volcanic series (Jackson and Wright, 1970). These rocks were called hawaiites and mugearites by Bass et al. (1973), but as Natland (this volume) points out, they are better called potassic basanites and nephelinites.

On a Zr-Nb plot, the basalts of Hole 317A are below the limit of detectability of Nb, but nonetheless, fall safely within the oceanic ridge tholeiite field (Figure 8). Very little is known about the quantitative ratios of Nb and Zr in Hawaiian basalts, but such data as are available are given in Figure 8. Unpublished semiquantitative spectrographic data suggest that Hawaiian tholeiites generally have Nb values detectable at >10 ppm and Zr values ranging from 70 to 150 ppm, whereas alkalic basalts have Nb values that range from 10 to 40 ppm, and Zr values that range from 70 to 250 ppm. The Hole 315A basalts thus appear to fall in the field for Hawaiian alkalic basalt rather than tholeiite ratios.

On a plot of Zr against Sr (Figure 9), the basalts of Hole 317A again fall within the established oceanic ridge tholeiite (ocean ridge basalt) field, along with Stoeser's Ontong-Java samples. Again the basalts of Hole 315A are ambiguous. Their Zr values are those of Hawaiian alkalic basalts; their Sr values those of Hawaiian tholeiites. Unless the rocks have lost Sr, or, less likely gained Zr, they plot in a presently unique field.

Pearce and Cann (1973) have devised several diagrams for the minor-element distinction of basaltic subtypes. They generally divide basaltic rocks into four categories, "ocean floor basalts" for which term we use oceanic ridge tholeiites; "low potassium tholeiites" by which they mean tholeiites of island arcs; "within plate basalts" in which they combine both continental and oceanic island type tholeiites and alkalic basalts; and "calc-alkali basalts" by which they mean andesitic rocks of island arcs. One of their discriminant plots is Ti against Zr (Figure 10). Ti-Zr ratios of the Hole 317A basalts fall in their fields B and C. Stoeser's (in press) Ontong-Java samples fall outside their field B. Ti-Zr ratios of the Hole 315A basalts and Bass et al.'s (1973) rocks fall outside any field in the diagram. Another of Pearce and Cann's (1973) plots which purports to discriminate tholeiite from alkalic rocks involves the ratio Y/Nb (Figure 11). The basalts from Hole 317A cannot be unequivocally plotted because Nb was reported as not detected at 15 ppm; but could well plot into the tholeiitic field. The basalts from Hole 315A, however, are plainly transitional on this diagram. Pearce and Cann's (1973) discriminant diagram that involves ratios of Ti, Y and Zr (Figure 12) does not separate the rather different basalts of Holes 315A and 317A.

Our data plotted on Ishikawa's (1968) diagrams (Figures 13a and 13b) also shows little discrimination, although the 315A basalts tend to favor alkalic rather than tholeiitic Hawaiian trends. There appears to be considerable scatter among oceanic ridge tholeiites, including the basalts of Hole 317A.

Schillings's (1966) chrondrite-normalized rare-earth patterns for average Hawaiian tholeiite and average Hawaiian alkalic basalt show the characteristic mild enrichment of light rare-earth elements typical of these rocks. The Hole 315A basalts show the same type of enrichment, but to a lesser extent (Figure 14a). Figure 14b shows the same comparison between the basalts of Hole 317A and other oceanic ridge tholeiites. Both have characteristic flat patterns with a slight depletion of light rare-earth elements.

Shih (1974) has suggested that enrichment or depletion in light rare-earth elements can be used to distinguish between basaltic suites, and that the chondrite-normalized Ce/Yb ratio is a reliable indicator of rare-

TABLE 5
Chemical Analyses of Basalts from Hole 315A

Flow Unit	1B	2				3		4	5a	6
Lab. No. Sample (Interval in cm)	M121852W[a] 31-1, 115.5-117.5	M121853W[a] 32-1, 141.5-143.5	M121854W[a] 32-2, 82.5-83.5	M121860W[a] 32-2, 96-105	D103734[b] 32-2, 96-105	M121855W[a] 32-3, 9.5-11.5	M121856W[a] 32-3, 87.5-89.5	M121857W[a] 32-4, 59-61	M121858W[a] 33-1, 116.5-118.5	M121859W[a] 34-1. 73.5-75.5
SiO_2	44.69	45.95	45.23	44.51	44.67	45.51	44.94	45.61	44.75	44.41
Al_2O_3	15.22	14.66	14.46	14.27	14.49	14.45	15.57	15.06	14.79	14.38
Fe_2O_3	7.72	6.68	8.56	7.07	5.88	6.86	6.52	5.92	6.88	7.48
FeO[c]	4.17	6.12	4.34	6.29	7.03	6.00	5.46	6.72	6.24	5.58
MgO	7.11	6.97	6.52	6.73	7.13	7.09	7.31	7.57	7.57	7.06
CaO	6.95	6.01	6.77	7.00	6.66	6.61	7.00	7.46	5.98	5.65
Na_2O[c]	3.15	3.33	3.40	3.35	3.41	3.24	3.07	2.84	3.27	3.23
K_2O	0.31	0.40	0.48	0.42	0.46	0.45	0.35	0.26	0.46	0 50
H_2O+[d]	1.78	1.66	1.36	3.00	1.86	2.77	3.23	3.56	3.28	3.21
H_2O-[c]	5.26	4.92	4.99	3.44	4.12	3.71	3.78	3.20	4.58	4.67
TiO_2	2.29	2.55	2.91	2.92	2.93	2.77	2.22	2.27	2.53	2.85
P_2O_5	0.30	0.31	0.32	0.30	0.33	0.31	0.25	0.30	0.30	0.32
MnO	0.46	0.34	0.33	0.40	0.40	0.39	0.33	0.24	0.25	0.36
CO_2[d]	0.25	<0.05	<0.05	0.22	0.45	<0.05	0.09	0.09	0.20	0.05
Cl	0.005	0.005	0.005	0.060	n.d.	0.005	<0.005	<0.005	0.010	0.005
BaO	0.0111	0.0143	0.0145	0.0139	n.d.	0.0103	0.0108	0.0106	0.0161	0.0156
SrO	0.0325	0.0280	0.0290	0.0280	n.d.	0.0280	0.0295	0.0285	0.0295	0.0320
S	0.111	0.052	0.032	0.153	0.20	0.167	0.139	0.103	0.116	0.058
Rb_2O	<0.0013	<0.0013	<0.0013	<0.0013	n.d.	<0.0013	<0.0013	<0.0013	<0.0013	<0.0013
SO_3	n.d.[g]	n.d.	n.d.	n.d.	.00	n.d.	n.d.	n.d.	n.d.	n.d.
Cr_2O_3[e]	n.d.	n.d.	n.d.	n.d.	<0.03	n.d.	n.d.	n.d.	n.d.	n.d.
NiO[f]	n.d.	n.d.	n.d.	n.d.	0.008	n.d.	n.d.	n.d.	n.d.	n.d.
Subtotal	–	–	–	–	100.06	–	–	–	–	–
Less Zero	–	–	–	–	.10	–	–	–	–	–
Total	99.81	100.00	99.75	100.17	99.96	100.37	100.30	101.24	101.26	99.86

[a]X-ray fluorescence: A.N. Elsheimer and L. Espos, Analysts; B.P. Fabbi, Project Leader.
[b]Conventional rock analysis; Elaine L. Brandt, Analyst; D.R. Norton, Project Leader.
[c]Lois B. Schlocker, Analyst; F.O. Simon, Project Leader.
[d]Marcelyn Cremer, Analyst; F.O. Simon, Project Leader.
[e]Colorimetric determination, G.D. Shipley, Analyst; Claude Huffman Jr., Project Leader.
[f]Atomic absorption, G.D. Shipley, Analyst; Claude Huffman Jr., Project Leader.
[g]n.d. not determined, [in X-ray fluorescence analyses.]

earth fractionation. The basalts of Hole 317A have Ce/Yb ratios ranging from 0.5 to 1.2, and average 0.8. These presumably are in the range of Shih's (1974) "ocean ridge basalts." The basalts of Hole 315A, on the other hand, have Ce/Yb ratios ranging from 2.0 to 2.6, and average 2.3. These values are intermediate between oceanic ridge tholeiites and Shih's (1974) "more alkaline" basalts from near Horizon Guyot, for which he gives values for Ce/Yb of 4 to 8.

Data for minor elements in both Hawaiian basalts and oceanic ridge tholeiites are at best scattered in the literature, and in part unpublished. We have compiled from existing data the ranges of concentrations and averages of selected minor elements in Hawaiian tholeiites, Hawaiian pre-erosional alkalic basalts, and oceanic ridge basalts (Tables 16a and 16b). It is apparent that a good deal of overlap occurs in minor-element concentrations of Hawaiian tholeiites and alkalic basalts (Table 15a). Five elements, Co, Cu, Sc, Ti, and Y, as determined from the sources now available to us, are sufficiently overlapping as to be of little use in distinguishing the two types of basalt. However, the basalts of Hole 315A have Ba, Sr, and V values that are more similar to those typical of Hawaiian tholeiites than to Hawaiian alkalic basalts. In contrast, Nb and Zr show closer affinities to alkalic basalts, whereas P abundances are intermediate between the two Hawaiian lava types. Cr, Cu, and Ni values are lower than those for either Hawaiian type, which may in part be explained as a result of the lack of olivine in most Hole 315A basalts. The minor-element concentrations of basalts from Hole 317A and those of other oceanic ridge tholeiites are generally lower than those of Hawaiian rocks, except for Nb and Zr, which occur in about the same abundance, and Sc and Y, which are more abundant (Table 16b). The basalts of Hole 317A fall within reported ranges of composition of minor elements in oceanic ridge basalts for all of the 13 reported elements.

Major Elements

Major-element compositions, pyroxene analyses, and minor-element concentrations collectively indicate that the Hole 315A basalts are Hawaiian in type, but ambiguous as to whether they resemble Hawaiian tholeiites or alkalic basalts. Since the Hole 315A basalts do plot above Macdonald's (1968) total-alkali silica diagram, we have compared them with a suite of alkalic basalts of the Hawaiian pre-erosional types. Comparison of Table 17 with Table 13 shows that the dry reduced analyses of both sets of basalts are similar. SiO_2, Al_2O_3, and Na_2O are higher in the Hole 315A basalts, whereas CaO and K_2O are lower, on the average. A principal difference is that the Hole 315A basalts contain 4.43% to 16.65% normative hypersthene, whereas the Hualalai basalts contain none. Figure 15 shows Hole 315A basalts plotted on MgO variation diagrams along with the alkalic basalt analyses of Table 17 and Bass et al.'s (1973) analyses (also dry reduced in Table 17). Bass et al.'s (1973) analyses fall in a grouping considerably more alkalic than those of Hualalai basalts, being much richer in Na_2O, K_2O, TiO_2, and P_2O_5 and lower in SiO_2, Al_2O_3, and CaO when compared with the other two groups of rocks, and resemble the basanites and nephelinites of the post-erosional Honolulu Volcanic Series (Jackson and Wright, 1970). The analyses from Hole 315A, on the other hand, where they do not overlap values of the Hualalai basalts tend to diverge in a direction toward Hawaiian tholeiites (Wright, 1971). Total alkali-silica plots of the three sets of rocks (Figure 16) show that the basalts of Hole 315A tend to have higher SiO_2 values than Hualalai basalts, but fall on the alkalic side of Macdonald's (1968) line. The same three groups of basalts are plotted on normative Di, Ol, Hy, weight percent FeO-total alkalis-MgO (AFM), and normative An-Ab-Or triangular diagrams in Figure 17. In the Di, Ol, Hy diagram, the Hualalai alkalic basalts and Bass et al.'s (1973) basanites and nephelinites have normative values such that plots fall of the Di, Ol edge of the diagram; the Hole 315A basalts plot in the lower central part of the diagram. In the AFM diagram, the basalts appear to follow a normal differentiation curve. In the An-Ab-Or diagram, the Hualalai alkalic basalts again plot in a field intermediate between the Hole 315A samples and those of Bass et al. (1973).

It seems clear that the basalts of Hole 315A are compositionally similar to oceanic island basalts of the Hawaiian type. It is possible that they once were tholeiites that lost SiO_2 and CaO and gained Na_2O and MgO during alteration; it seems also possible, but less likely, that these rocks were once alkalic basalts that lost CaO, K_2O, and Al_2O_3 and gained SiO_2 during alteration. However, in view of the pyroxene compositions of these rocks and the intermediate distribution pattern of the "stable" minor elements, it seems most likely that the basalts sampled in Hole 315A were originally truly transitional between oceanic island tholeiites and alkalic basalts.

The basalts of Hole 317A, on the other hand, are less altered than those of Hole 315A, and their major- and minor-element chemical composition and mineralogy all place them in the field of oceanic ridge tholeiites. It has been suggested (Andrews, Packham, et al., in press; Winterer et al., 1974) that the Manihiki and Ontong-Java plateaus were once connected; general similarities between the two areas are given in Part I of this volume. It is therefore of some interest to compare the oceanic ridge basalts of Hole 317A with those recovered from Hole 289 (Stoeser, in press; see Table 17). The Ontong-Java basalts are slightly richer in K_2O, FeO, and TiO_2 and slightly poorer in MgO and, in one analysis, poorer in SiO_2 than the Manihiki basalts (Compare Tables 14 and 17). Figure 18 displays these relations on a MgO variation diagram that is more interesting for its similarities than its differences. Both the Ontong-Java and Manihiki basalts lie in the tholeiite field on a total alkali-silica diagram (Figure 19). An-Ab-Or, AFM, and Di-Ol-Hy triangular diagrams (Figure 20) again show nearly identical plots of basalts from the two sites. There is certainly no chemical reason for the basalts of the two areas to have developed in a different setting.

BASALTS OF HOLES 316 AND 318

Hole 316

In Cores 19, 28, and 29 of Hole 316 several breccia beds contained small (1 mm-1 cm) clasts of scoriaceous basalt, for the most part altered to brown and green clay minerals. In the core catcher of Core 28, an almost completely altered fragment of basalt of the some type was found that is about 1 cm × 1 cm × 4 cm in size (sample 316-28, CC).

In thin section, this sample proved to be an aphyric, scoriaceous basalt. Spherical vesicles ranging from 0.2 to 1.3 mm in diameter, and averaging 0.5 mm, make up 45% of the rock. The former glassy groundmass of the basalt contains about 5% each of virtually unaltered microlites of plagioclase (0.01 × 0.05 mm in size) and augite (0.02 mm in size), although the former glass that contained the microlites is now altered to brown montmorillonite, which makes up about 45% of the rock. The vesicles are lined with brown montmorillonite, and about 40% of them are filled with calcite, analcime, and gmelinite. Calcite also appears to replace some groundmass montmorillonite.

All basalt clasts seen in Hole 316 appear to be nearly identical except in terms of degree of alteration. Nothing short of complete major- and minor-element chemical analyses of these rocks would yield their parentage, and even then, it might well be obscured by alteration. The presence of only one high-calcium pyroxene is these rocks is weak evidence for an alkalic parentage.

Hole 318

In Core 10 of Hole 318, a breccia bed approximately 40 cm in thickness was encountered which was composed of nearly 50% of volcaniclastic debris. Some of the clasts of volcanic rocks are as much as 1 cm in diameter. These rocks are of a wide volcanic materials. Some are intersertal basalts with microphenocrysts of augite, groundmass plagioclase of composition An_{40-45}, and altered groundmass glass. Some are quartz syenites, containing quartz, orthoclase, minor plagioclase, and aegerine augite. Some are mugearites and sanidine-rich trachytes. Two basaltic fragments were collected for closer inspection. One of these (318-10-1, 138-140 cm) proved to be an intersertal basalt containing about 20% phenocrysts of plagioclase (An_{58}) and augite (Ca_{42} Mg_{44} Fe_{14}). Vesicles are small (0.05-0.3 mm), averaging about 0.2 mm, make up about 5% of the rock, and are almost completely filled with calcite. A second generation of plagioclase microphenocrysts up to 0.6 mm in size appear to be present in the rock, and together with finer groundmass plagioclase, make up about 20% of the basalt. Groundmass augite (Ca_{40} Mg_{43} Fe_{17}) makes up about 25% of the rock. Both plagioclase and pyroxene are locally replaced by brown montmorillonite, and plagioclase by calcite. The remainder of the groundmass consists of former glass altered to brown mont-

TABLE 6
Chemical Analyses of Basalts from Hole 317A

Flow Unit	1	2	3	4	5A	5B					
Lab. No.	M121831W[a]	M121832W[a]	M121833W[a]	M121834W[a]	M121835W[a]	M121836W[a]	M121837W[a]	M121851W[a]	D103735[b]	M121838W[a]	M121839W[a]
Sample (Interval in cm)	31-1, 144-146	31-2, 37-39	31-3, 27-29	31-3, 101-103	31-4, 80-82	32-1, 84-86	32-2, 75-77	32-3, 100-111.5	32-3, 100-111.5	32-3, 106-108	32-4, 76-78
SiO_2	46.98	46.79	48.06	48.33	49.29	48.80	50.37	49.83	49.78	49.90	49.58
Al_2O_3	13.58	13.43	14.85	14.60	15.17	14.95	15.14	14.77	15.00	14.50	14.63
Fe_2O_3	5.56	5.39	4.46	4.59	3.69	4.48	3.91	4.51	4.17	4.47	3.75
FeO[c]	5.00	5.14	4.80	4.86	5.72	5.72	6.75	6.64	7.00	6.90	7.07
MgO	9.60	9.71	8.85	8.84	8.18	7.64	7.27	6.87	6.93	7.04	7.33
CaO	9.19	8.97	10.91	11.08	11.07	11.08	10.87	11.18	11.07	10.79	10.88
Na_2O[c]	2.11	2.23	2.06	2.06	2.09	1.97	2.10	1.98	2.05	2.13	2.22
K_2O	0.04	0.04	0.05	0.02	0.09	0.02	0.12	0.09	0.12	0.11	0.06
H_2O^+[d]	1.94	2.14	1.80	1.53	1.80	1.54	1.55	1.13	0.72	1.48	1.52
H_2O^-[c]	5.06	4.60	2.99	2.59	2.66	2.26	1.89	1.64	1.91	1.56	1.87
TiO_2	0.99	0.91	0.89	0.85	0.94	0.92	1.01	0.99	0.98	1.01	1.01
P_2O_5	0.12	0.13	0.12	0.13	0.12	0.12	0.14	0.10	0.08	0.13	0.12
MnO	0.25	0.23	0.32	0.24	0.27	0.23	0.24	0.18	0.18	0.17	0.24
CO_2[c]	<0.05	<0.05	<0.05	<0.05	<0.05	<0.05	0.05	<0.05	0.05	<0.05	<0.05
Cl	0.045	0.05	0.035	0.04	0.035	0.02	0.02	0.025	n.d.	0.03	0.04
BaO	<0.0025	<0.0025	<0.0025	<0.0025	<0.0025	<0.0025	<0.0025	<0.0025	n.d.	<0.0025	<0.0025
SrO	0.0129	0.0130	0.0117	0.0118	0.0125	0.0118	0.0122	0.0109	n.d.	0.0125	0.0122
S	0.015	0.011	0.011	0.013	0.013	0.010	0.009	0.009	0.00	0.009	0.009
Rb_2O	<0.0013	<0.0013	<0.0013	<0.0013	<0.0013	<0.0013	<0.0013	<0.0013	n.d.	<0.0013	<0.0013
SO_3	n.d.	n.d.	n.d.	n.d.	n.d.	n.d.	n.d.	n.d.	0.00	n.d.	n.d.
Cr_2O_3[e]	n.d.	n.d.	n.d.	n.d.	n.d.	n.d.	n.d.	n.d.	<0.03	n.d.	n.d.
NiO[f]	n.d.	n.d.	n.d.	n.d.	n.d.	n.d.	n.d.	n.d.	0.010	n.d.	n.d.
Subtotal	–	–	–	–	–	–	–	–	100.08	–	–
Less Zero	–	–	–	–	–	–	–	–	.00	–	–
Total	100.49	99.78	100.22	99.78	101.15	99.77	101.45	99.95	100.08	100.24	100.34

Flow Unit	6A			6B			7A	7B	9	10	
Lab. No.	M121840W[a]	M121841W[a]	M121842W[a]	M121843W[a]	M121844W[a]	M121845W[a]	M121846W[a]	M121847W[a]	M121848W[a]	M121849W[a]	M121850W[a]
Sample (Interval in cm)	32-4, 126-128	32-5, 95-97	32-6, 113-115	33-1, 138-140	33-2, 82-84	33-3, 94-96	33-4, 103-105	34-1, 40-41	34-2, 91-93	34-3, 118-120	34-4, 65-67
SiO_2	48.22	48.47	48.30	49.26	48.84	47.88	49.38	49.22	50.05	50.42	49.92
Al_2O_3	13.84	13.23	12.88	13.18	13.92	14.62	14.76	14.59	14.71	14.19	15.07
Fe_2O_3	4.12	0.85	4.20	4.08	3.67	4.66	4.09	3.36	3.81	4.92	3.76
FeO[c]	5.86	8.31	5.89	6.26	6.64	5.35	5.46	6.29	5.52	5.92	6.29
MgO	9.03	9.66	9.63	9.15	8.56	8.41	8.14	7.93	7.48	7.46	7.29
CaO	11.87	11.85	11.71	12.18	11.97	10.85	10.56	11.22	11.07	10.70	11.47
Na_2O[c]	1.83	1.73	1.69	1.82	1.86	2.13	2.30	2.19	2.25	2.37	2.19
K_2O	0.04	0.04	0.02	0.07	0.04	0.12	0.25	0.06	0.24	0.15	0.10
H_2O^+[d]	1.77	2.09	1.97	1.45	1.52	2.02	1.47	1.26	1.05	1.30	0.88
H_2O^-[c]	2.32	2.49	2.53	1.68	1.54	2.91	2.77	2.19	1.80	1.67	1.81
TiO_2	0.81	0.81	0.80	0.82	0.88	0.89	1.08	1.01	1.07	1.15	1.06

P_2O_5	0.11	0.12	0.12	0.12	0.11	0.12	0.17	0.16	0.16	0.16	0.13
MnO	0.19	0.25	0.25	0.14	0.17	0.13	0.26	0.26	0.23	0.14	0.18
CO_2[c]	0.07	<0.05	0.05	<0.05	<0.05	<0.05	<0.05	0.07	<0.05	<0.05	<0.05
Cl	0.015	0.015	0.015	0.01	0.005	0.025	0.045	0.040	0.095	0.11	0.065
BaO	<0.0025	<0.0025	<0.0025	<0.0025	<0.0025	<0.0025	<0.0025	<0.0025	<0.0025	<0.0025	<0.0025
SrO	0.0109	0.0096	0.0096	0.0105	0.0099	0.0123	0.0124	0.0125	0.0129	0.0115	0.0139
S	0.013	0.013	0.014	0.006	0.008	0.008	0.014	0.011	0.009	0.010	0.009
Rb_2O	<0.0013	<0.0013	<0.0013	<0.0013	<0.0013	<0.0013	<0.0013	<0.0013	<0.0013	<0.0013	<0.0013
SO_3	n.d.	n.d.	n.d.	n.d.	n.d.	n.d.	n.d.	n.d.	n.d.	n.d.	n.d.
Cr_2O_3[e]	n.d.	n.d.	n.d.	n.d.	n.d.	n.d.	n.d.	n.d.	n.d.	n.d.	n.d.
NiO[f]	n.d.	n.d.	n.d.	n.d.	n.d.	n.d.	n.d.	n.d.	n.d.	n.d.	n.d.
Subtotal	–	–	–	–	–	–	–	–	–	–	–
Less Zero	–	–	–	–	–	–	–	–	–	–	–
Total	100.12	100.13	100.07	100.24	99.74	100.14	100.31	99.87	99.56	100.68	100.22

[a]X-ray fluorescence: A.N. Elsheimer and L. Espos, Analysts; B.P. Fabbi, Project Leader.
[b]Conventional rock analysis: Elain L. Brandt, Analyst; D.R. Norton, Project Leader.
[c]Lois B. Schlocker, Analyst; F.O. Simon, Project Leader.
[d]Marcelyn Cremer, Analyst; F.O. Simon, Project Leader.
[e]Colorimetric determination, G.D. Shipley, Analyst; Claude Huffman Jr., Project Leader.
[f]Atomic absorption, G.D. Shipley, Analyst; Claude Huffman Jr., Project Leader.
[g]n.d. not determined in X-ray fluorescence analyses.

TABLE 7
Comparative Na_2O Values (in percent) Between X-Ray Fluorescence (XRF) and Flame Photometer Values

Sample (Interval in cm)	XRF Low Resolution	XRF High Resolution	Flame Photometer
317A-31-1, 144-146	1.83	2.21	2.11
317A-31-2, 37-39	1.86	2.06	2.23
317A-31-3, 27-29	1.78	2.10	2.06
317A-31-3, 101-103	1.76	2.05	2.06
317A-31-4, 80-82	1.76	2.13	2.09
317A-32-1, 84-86	1.77	2.03	1.97
317A-32-2, 75-77	1.81	1.94	2.10
317A-32-3, 106-108	1.86	1.90	2.13
317A-32-4, 76-78	1.92	2.16	2.22
317A-32-4, 126-128	1.66	2.14	1.83
317A-32-5, 95-97	1.48	2.01	1.73
317A-32-6, 113-115	1.58	1.99	1.69
317A-33-1, 138-140	1.70	1.82	1.82
317A-33-2, 82-84	1.73	1.97	1.86
317A-33-3, 94-96	1.86	1.98	2.13
317A-33-4, 103-105	2.04	2.17	2.30
317A-34-1, 40-41	1.97	2.05	2.19
317A-34-2, 91-93	2.02	2.21	2.25
317A-34-3, 118-120	2.24	2.42	2.37
317A-34-4, 65-67	2.09	2.33	2.19
317A-32-3, 100-111.5	1.88	2.06	1.98
315A-31-1, 115.5-117.5	2.56	3.19	3.15
315A-32-1, 141.5-143.5	2.69	3.06	3.33
315A-32-2, 82.5-83.5	2.83	3.11	3.40
315A-32-3, 9.5-11.5	2.66	3.05	3.24
315A-32-3, 87.5-89.5	2.31	2.96	3.07
315A-32-4, 59-61	2.18	2.71	2.84
315A-33-1, 116.5-118.5	2.39	3.06	3.27
315A-34-1, 73.5-75.5	2.63	3.18	3.23
315A-32-2, 96-105	2.76	3.12	3.35

morillonite. The sample resembles those of Flow Unit 6 in Hole 315A but displays more abundant phenocrysts.

The other fragment studied (318-10-1, 139-141 cm) proved to be an aphyric, vesicular, vitrophyric basalt. Vesicles have irregular to rounded shapes, range in size from 0.05 to 5.0 mm, averaging 2.0 mm, and make up nearly 30% of the rock. The groundmass consists of about 25% of very tiny plagioclase laths (An_{60}), augite prisms (Ca_{42} Mg_{45} Fe_{13}) that make up about 15% of the rock, and feathery ilmenite needles, all set in a matrix of former glass, now altered to brown montmorillonite that makes up the remaining 30% of the rock. The vesicles are lined with thin rims of brown montmorillonite and are partially filled with green montmorillonite and calcite. Plagioclase and augite are little altered. The rock resembles the upper chilled margin of Flow Unit 5A in Hole 315A but contains a considerably greater volume of vesicles.

Both these rocks appear to be tholeiites of the oceanic island type. Their association with mugearites and trachytes suggests that debris shed from the nearby Tuamotu edifices was of the oceanic island type.

CONCLUSIONS

Hole 317A was drilled in the north-central part of Winterer et al.'s (1974) "high plateau" province of the Manihiki Plateau. Mudline was reached 2598 meters below sea level, and the drill bit entered the uppermost flow unit of basalt 3508 meters below sea level. Ten flow

TABLE 8
Quantitative Spectrographic Analyses for Selected Minor Elements of Basalts from Hole 315A[a]

Lab. No.	Sample (Interval in cm)	Cr (ppm)	Nb (ppm)	Ni (ppm)	Zr (ppm)	Y (ppm)	V (ppm)
M121852W	31-1, 115.5-117.5	140	33	69	170	41	180
M121853W	32-1, 141.5-143.5	105	39	62	205	47	170
M121854W	32-2, 82.5-83.5	110	40	43	200	60	280
M121860W	32-2, 96-105	61	34	38	165	48	280
M121855W	32-3, 9.5-11.5	92	44	54	230	56	225
M121856W	32-3, 87.5-89.5	145	32	92	170	39	200
M121857W	32-4, 59-61	140	35	90	180	51	225
M121858W	33-1, 116.5-118.5	105	41	86	190	51	275
M121859W	34-1, 73.5-75.5	73	41	57	220	56	280

[a]Chris Heropoulos, Analyst; Brent Fabbi, Project Leader (Acting). Results reported to two significant figures with an overall accuracy of ±15% (accuracy decreases near the limits of detection where only one digit is intended).

TABLE 9
Quantitative Spectrographic Analyses for Selected Minor Elements of Basalts From Hole 317A[a]

Lab. No.	Sample (Interval in cm)	Cr (ppm)	Nb (ppm)	Ni (ppm)	Zr (ppm)	Y (ppm)	V (ppm)
M121831W	31-1, 144-146	160	N15[b]	60	45	22	230
M121832W	31-2, 37-39	280	N15	92	60	21	215
M121833W	31-3, 27-29	400	N15	110	57	20	190
M121834W	31-3, 101-103	450	N15	94	69	16	170
M121835W	31-4, 80-82	220	N15	81	70	25	220
M121836W	32-1, 84-86	230	N15	73	75	24	215
M121837W	32-2, 75-77	170	N15	66	84	27	225
M121838W	32-3, 106-108	145	N15	65	86	21	230
M121851W	32-3, 100-111.5	135	N15	62	70	34	235
M121839W	32-4, 76-78	130	N15	62	75	25	235
M121840W	32-4, 126-128	610	N15	110	72	25	200
M121841W	32-5, 95-97	920	N15	120	76	21	200
M121842W	32-6, 113-115	580	N15	96	64	24	210
M121843W	33-1, 138-140	550	N15	75	58	25	240
M121844W	33-2, 82-84	430	N15	75	64	20	160
M121845W	33-3, 94-96	325	N15	67	66	19	170
M121846W	33-4, 103-105	325	N15	75	84	27	180
M121847W	34-1, 40-41	420	N15	88	68	30	180
M121848W	34-2, 91-93	370	N15	83	84	26	190
M121849W	34-3, 118-120	370	N15	91	92	14	125
M121850W	34-4, 65-67	350	N15	87	83	30	200

[a]Chris Heropoulos, Analyst; Brent Fabbi, Project Leader (Acting). Results reported to two significant figures with an overall accuracy of ±15% (accuracy decreases near the limits of detection where only one digit is intended).

[b]N = not detected at value shown.

units of basalt are present; four are separated by three moderately thin beds of volcaniclastic siltstone. Although the textures of the basalts of the flow units. vary considerably, their major and minor chemical composition, their mineralogy, and their mineral compositions show only minor variations. These flow units are unquestionably oceanic ridge tholeiites of a type and composition found at or very near present-day spreading ridges. They undoubtedly formed at such a ridge, presumably the Pacific-Phoenix ridge (Larson and Chase, 1972), and spread northward into the Pacific plate some time prior to 110-120 m.y. B.P. Alternatively, they may have initially formed near a triple junction, spread to the southeast or southwest and have been incorporated into the Pacific plate by a southward ridge jump that occurred about 100 m.y. B.P. (Winterer et al., 1974). In either case, the chemical and mineralogic character of the basalts clearly refutes the idea that the high Manihiki Plateau is a subsided microcontinent (Heezen and Hollister, 1971), although refraction profiles in this area suggest rather thick oceanic crust (Sutton et al., 1970). Winterer et al. (1974) suggest that much of the high plateau might have been above sea level in the early part of its history, citing the presence of the coral atolls on its margins as the most direct evidence for its subsidence. The high volumetric proportion and the very large average sizes of vesicles in the basalts beneath the plateau support Winterer et al.'s (1974) contention; we suggest that the Manihiki flows were erupted at water depths of less than 400 meters, and, in the absence of any chemical data that these basalts contained unusually large amounts of volatile constituents, it is possible that

TABLE 10
Minor-element Contents of Basalts From Hole 315A[a]

Lab. No. Sample (Interval in cm)	W-183470 31-1, 115.5-117.5	W-183471 32-1, 141.5-143.5	W-183472 32-2, 82.5-83.5	W-183478 32-2, 96-105	W-183473 32-3, 9.5-11.5	W-183474 32-3, 87.5-89.5	W-183475 32-4, 59-61	W-183476 33-1, 116.5-118.5	W-183477 34-1, 73.5-75.5
Ce (ppm)	31.8	34.3	36.5	37.2	35.1	29.4	32.8	34.1	38.1
Co (ppm)	48.0	46.3	54.3	46.7	43.5	51.8	50.0	55.9	47.5
Cr (ppm)	164	101	86	87	93	167	174	144	75
Cs (ppm)	<1	<1	<1	<1	<1	<1	<1	<1	<1
Eu (ppm)	1.94	2.15	2.26	2.14	2.09	1.86	1.90	2.15	2.29
Fe (%)	8.43	8.94	9.20	9.37	9.05	8.80	9.05	9.41	9.26
Gd (ppm)	3.6	5.5	4.6	7.0	6.3	4.5	4.9	5.8	8.2
Hf (ppm)	4.0	4.8	4.7	4.8	4.9	3.9	3.7	4.5	4.7
Sc (ppm)	27.6	29.2	34.4	32.8	33.3	26.3	25.9	30.1	29.3
Ta (ppm)	1.2	1.3	1.4	1.4	1.4	1.2	1.2	1.3	1.5
Tb (ppm)	1.0	1.1	1.2	1.2	1.1	1.1	1.0	1.0	1.2
Th (ppm)	<1.4	2.0	2.0	1.5	<1.5	1.2	<1.4	<1.4	1.4
U (ppm)[b]	0.1	0.4	0.3	0.1	0.4	<0.1	0.4	0.1	0.3
Yb (ppm)	3.2	3.4	3.7	3.6	3.9	2.9	3.5	3.0	3.6
Zn (ppm)	100	110	130	130	140	110	110	110	120
Zr (ppm)	<200	<200	<200	175	<200	<200	120	<200	<200

[a]Radioactivation and radiochemistry determinations: L.J. Schwartz, Analyst; J.J. Rowe, Project Leader.

[b]Fluorometric determination: Joseph Budinisky and Leuny Mei, Analysts; Frank Cuttitta, Supervisor.

they were subaerial. Thus, it would appear that the high Manihiki Plateau has subsided between 3000 and 3500 meters during the last 110-120 m.y., assuming sea level at that time was near present levels (Hays and Pitman, 1973). It has further been suggested (Andrews and Packham, in press) that the Manihiki and Ontong-Java plateaus were once connected. Nothing in the comparative chemistry of the basalts in Hole 317A and in those of Hole 289 (Stoeser, in press) precludes this possibility.

Hole 315A was drilled 93 km from Fanning Island and is believed to have entered basalts related to that edifice. These basalts are more altered than those penetrated in Hole 317A, but their textures, major- and minor-element compositions, and mineralogy indicate that they are of the oceanic island type. They resemble Hawaiian tholeiites in that they contain hypersthene in their norms, and in that several minor elements are more closely related to such tholeiites than to alkalic basalts. On the other hand, they fall on the alkalic side of Macdonald's (1968) line separating alkalic basalts and tholeiites based on total alkali-silica plots; their pyroxenes proved to be salites, which are diagnostic of Hawaiian alkalic basalts; and several "stable" minor elements show alkalic rather than tholeiitic affinities. We conclude, overall, that the Hole 315A basalts are truly transitional between Hawaiian tholeiites and alkalic basalts, but that their oceanic island affinities are clear-cut. At Site 165, in the northern Line Islands, Bass et al. (1973) drilled into potassic basanites and nephelinites, which, in Hawaii, are similar to post-erosional basalts erupted 2-4 m.y. after construction of the edifices upon which they rest. Jackson (1974) considers that these types of basalts could have formed at almost any time after pre-erosional oceanic island type rocks, if epirogenic processes affected the chain. The composition of the basalts at Hole 316, drilled in the southern Line Islands is unknown, but volcanogenic debris in that hole contains basalts that may be of oceanic island aspect. It would appear, from the nature of the basalts, that the Line Islands are formed of materials not unlike those of the Hawaiian Islands, although the Site 165 material is of the post-erosional type and we cannot say from the three existing sites whether or not the southern Line Islands are a progressive chain. The age of the sea floor along the entire Line Islands chain is poorly known, but if Larson and Chase's (1972) or Pitman et al.'s (1974) magnetic anomalies could be extended into the area, Site 165 would be older than anomaly M 10, Site 315 would lie on an extension of magnetic anomaly M 4, and Hole 316 would lie in the interval between anomalies 33 and M 1. Alternatively, if Winterer's (this volume) model is correct, then the Line Islands could fall on an extension of the Hawaiian lineations, and nearly parallel to them. Although there are differences in opinion about the ages of these anomalies (Baldwin et al., 1974) and particularly over the interval between anomalies 33 and M 1, which might range in age from 80 to 120 m.y. B.P., extension of the anomalies across the chain would result in a crust that becomes younger southward along the Line Islands chain. On the other hand, if Winterer's (this volume) model is correct the oceanic crust beneath the Line Islands would be nearly coeval at about 100 m.y. B.P. In contrast, the age of basalt at Site 165 is given as 79-83 m.y. B.P. (Winterer et al., 1974), at Site 315, 91.2 ±2.7 m.y. B.P. (Lanphere and Dalrymple, this volume) and at Site 316 81-93 m.y. B.P. (Part I, this volume). These data would suggest that although we cannot say whether or not the Line Islands are a progressive chain, they do cut across older oceanic crust, as does the Hawaiian chain (Jackson et al., 1972). It might be suggested that the Line Islands themselves are an abandoned mid-oceanic ridge. The chemistry of the basalts at Sites 165 and 315 is clearly inconsistent with this model, unless the special case of an Iceland-type edifice, which does consist of basalts of the oceanic

TABLE 11
Minor-element Contents of Basalts From Hole 317A[a]

Lab. No.	W-183449	W-183450	W-183451	W-183452	W-183453	W-183454	W-183455
Sample (Interval in cm)	31-1, 144-146	31-2, 37-39	31-3, 27-29	31-3, 101-103	31-4, 80-82	32-1, 84-86	32-2, 75-77
Ce (ppm)	<5	<5	<6	<6	<6	<6	7.5
Co (ppm)	51.3	50.0	50.0	50.4	46.7	48.0	46
Cr (ppm)	328	358	437	442	293	225	155
Cs (ppm)	<1	<1	<1	<1	<1	<1	<1
Eu (ppm)	0.74	0.88	0.78	0.80	0.80	0.87	0.88
Fe (%)	7.64	7.19	6.60	6.77	6.70	7.62	7.53
Gd (ppm)	<6	<6	<6	<6	<6	<6	<6
Hf (ppm)	1.2	1.2	1.2	1.3	1.3	1.3	1.3
Sc (ppm)	41.1	40.4	44.2	43.5	44.7	44.5	43.5
Ta (ppm)	0.3	0.2	0.3	0.3	0.3	0.3	0.2
Tb (ppm)	0.4	0.4	0.4	0.4	0.5	0.4	0.4
Th (ppm)	<1.5	<1.6	<1.6	<1.6	<1.6	<1.6	<1.6
U (ppm)[b]	0.1	<0.1	<0.1	<0.1	<0.1	<0.1	<0.1
Yb (ppm)	2.0	2.1	1.7	1.8	2.1	2.3	2.5
Zn (ppm)	<20	<20	<20	<20	<20	<20	<20
Zr (ppm)	<200	<200	<200	<200	<200	<200	<200

Lab. No.	W-183469	W-183456	W-183457	W-183458	W-183459	W-183460	W-183461
Sample (Interval in cm)	32-3, 100-111.5	32-3, 106-108	32-4, 76-78	32-4, 126-128	32-5, 95-97	32-6, 113-115	33-1, 138-140
Ce (ppm)	<5	8.4	9.5	6.9	7.2	<6	<6
Co (ppm)	47.0	48.3	48.2	41.1	49.8	49.9	50.2
Cr (ppm)	130	125	134	486	683	639	637
Cs (ppm)	<1	<1	<1	<1	<1	<1	<1
Eu (ppm)	0.91	0.89	0.89	0.88	0.73	0.70	0.74
Fe (%)	7.89	8.55	8.21	7.69	6.77	7.39	7.71
Gd (ppm)	<6	<6	<6	<6	<6	<6	<6
Hf (ppm)	1.6	1.6	1.5	1.2	0.9	0.9	1.1
Sc (ppm)	43.0	44.2	43.9	46.5	48.4	46.1	47.2
Ta (ppm)	0.3	0.2	0.2	0.3	0.4	0.3	0.2
Tb (ppm)	0.5	0.6	0.5	0.4	0.4	0.4	0.5
Th (ppm)	<1.6	<1.6	<1.6	<1.7	<1.7	<1.6	<1.7
U (ppm)[b]	0.1	<0.1	0.1	0.1	<0.1	<0.1	<0.1
Yb (ppm)	2.5	2.5	2.3	2.0	2.1	2.0	2.1
Zn (ppm)	<16	<20	<20	<20	<20	<20	<20
Zr (ppm)	<200	<200	<200	<200	<200	<200	<200

Lab. No.	W-183462	W-183463	W-183464	W-183465	W-183466	W-183467	W-183468
Sample (Interval in cm)	33-2, 82-84	33-3, 94-96	33-4, 103-105	34-1, 40-41	34-2, 91-93	34-3, 118-120	34-4, 65-67
Ce (ppm)	<6	6.0	11.8	10.2	11.9	<6	11.2
Co (ppm)	48.1	50.5	44.5	44.2	41.8	45.9	44.0
Cr (ppm)	441	377	408	420	425	357	346
Cs (ppm)	<1	<1	<1	<1	<1	<1	<1
Eu (ppm)	0.75	0.79	0.95	0.87	0.97	1.03	0.91
Fe (%)	7.33	6.91	6.77	7.02	6.56	8.09	7.66
Gd (ppm)	<6	<6	<6	<6	<6	<6	<6
Hf (ppm)	1.3	1.1	1.6	1.7	1.7	1.7	1.6
Sc (ppm)	44.2	44.3	43.3	42.1	43.5	45.3	42.4
Ta (ppm)	0.3	0.3	0.3	0.3	0.3	0.3	0.3
Tb (ppm)	0.4	0.4	0.5	0.5	0.5	0.6	0.5
Th (ppm)	<1.6	<1.5	<1.6	<1.6	<1.6	<1.6	<1.6
U (ppm)[b]	0.1	0.1	0.1	0.1	<0.1	<0.1	<0.1
Yb (ppm)	2.0	2.0	2.3	2.2	2.2	2.6	2.1
Zn (ppm)	<20	<20	<20	<20	<20	<20	<20
Zr (ppm)	<200	<200	<200	<200	<200	<200	<200

[a]Radioactivation and radiochemistry determinations; L.J. Schwartz, Analyst; J.J. Rowe, Project Leader.
[b]Fluorometric determination: Joseph Budinisky and Leung Mei, Analysts; Frank Cuttitta, Supervisor.

TABLE 12
Mineral Analyses of Plagioclases (pc) and Pyroxenes (px) From the Basalts of Holes 315A and 317A[a]

	Hole 315A						Hole 317A			
Sample (Interval in cm)	32-2, 79.5-80		32-4, 53-55		34-1, 99-101		31-2, 37-39			
Flow Unit	2		4		6		2			
Mineral	pc	px	pc	px	pc	px	pc	px	px	px
Texture[b]	m	m	g	g	m	m	g	m	g	m
SiO_2[c]	50.87	46.8	52.18	49.9	51.08	47.9	49.89	54.1	53.2	53.4
Al_2O_3	28.81	6.30	28.76	3.33	29.10	5.37	29.49	2.04	2.20	2.61
FeO	–	9.6	–	11.1	–	10.3	–	5.3	5.2	5.7
MgO	–	9.8	–	11.0	–	9.9	–	19.1	18.7	17.9
CaO	12.78	20.9	12.30	19.6	12.84	20.9	14.14	18.8	19.2	19.6
Na_2O	4.31	0.51	4.53	0.43	4.35	0.46	3.39	0.17	0.18	0.19
K_2O	0.18	–	0.31	–	0.30	–	0.26	–	–	–
TiO_2	–	3.60	–	1.83	–	2.85	–	0.27	0.28	0.34
MnO	–	1.0	–	1.2	–	1.1	–	0.7	0.6	0.7
Total	96.95	98.51	98.08	98.39	97.67	98.78	97.17	100.48	99.56	100.44
	Numbers of Ions on the Basis of 32 Oxygens for Plagioclase and 6 Oxygens for Pyroxene[d]									
Si	9.539 } 15.91	1.794 } 2.00	9.653 } 15.92	1.913 } 2.00	9.516 } 15.91	1.834 } 2.00	9.363 } 15.89	1.955 } 2.00	1.944 } 2.00	1.940 } 2.00
Al (IV)	6.367	0.206	6.271	0.088	6.389	0.166	0.523	0.045	0.056	0.060
Al	–	0.079	–	0.063	–	0.076	–	0.042	0.039	0.052
Ti	–	0.104	–	0.053	–	0.082	–	0.007	0.008	0.009
Mg	–	0.560	–	0.638	–	0.565	–	1.029	1.019	0.969
Fe^{2+}	–	0.308 } 1.98	–	0.356 } 1.98	–	0.330 } 1.98	–	0.160 } 2.00	0.159 } 2.01	0.173 } 2.00
Mn	–	0.033	–	0.039	–	0.036	–	0.021	0.019	0.022
Ca	2.568	0.758	2.433	0.805	2.563	0.857	2.843	0.728	0.752	0.763
Na	1.567 } 4.18	0.098	1.625 } 4.14	0.032	1.571 } 4.21	0.034	1.234 } 4.14	0.012	0.013	0.013
K	0.043	–	0.073	–	0.071	–	0.062	–	–	–
Σ	20.08	3.98	20.06	3.98	20.11	3.98	20.03	4.00	4.01	4.00
K	1.0		1.8		1.7		1.5			
Na	37.5		39.3		37.4		29.8			
Ca	61.5		58.9		60.9		68.7			
Mg		32.4		35.1		32.2		53.7	52.8	50.9
Fe		17.8		19.9		18.8		8.4	8.2	9.1
Ca		49.7		45.0		48.9		38.0	39.0	40.0

[a]M. H. Beeson, analyst.

[b]g = groundmass and m = microphenocryst.

[c]Oxides as received.

[d]Derived from computer program of Jackson et al. (1967), modified by Wright (1970).

TABLE 12 – *Continued*

Hole 317A

Sample (Interval in cm)	31-2, 37-39			32-5, 111.5-112			34-1, 40-41				
Flow Unit	2			5B			7B				
Mineral	px	px	px	pc	px	px	px	pc	px	px	px
Texture[b]	m	g	g	g	m	m	g	g	g	g	g
SiO_2[c]	52.8	53.2	50.8	52.69	49.3	48.8	52.7	51.38	52.5	52.6	53.8
Al_2O_3	2.89	2.97	3.95	28.18	1.21	1.11	1.84	29.16	2.15	1.97	1.88
FeO	5.9	5.9	8.2	–	20.1	20.8	8.7	–	8.3	12.3	6.4
MgO	17.3	17.5	16.7	–	8.0	6.3	15.8	–	15.3	18.2	18.2
CaO	19.7	18.6	14.3	11.86	13.7	13.9	17.8	13.20	18.0	11.7	18.1
Na_2O	0.19	0.18	0.28	4.58	0.17	0.19	0.21	4.06	0.20	0.16	0.16
K_2O	–	–	–	0.24	–	–	–	0.19	–	–	–
TiO_2	0.48	0.47	0.51	–	0.73	0.68	0.43	–	0.61	0.58	0.39
MnO	0.8	0.5	0.6	–	1.8	1.7	0.7	–	0.9	0.9	0.7
Total	100.06	99.32	95.34	97.55	95.01	93.48	98.18	97.99	97.96	98.41	99.63

Numbers of Ions on the Basis of 32 Oxygens for Plagioclase and 6 Oxygens for Pyroxene[d]

Si	1.930 } 2.00	1.948 } 2.00	1.939 } 2.00	9.774 } 15.94	2.013 } 2.01	2.035 } 2.03	1.976 } 2.00	9.531 } 15.91	1.972 } 2.00	1.967 } 2.00	1.967 } 2.00
Al (IV)	0.070	0.053	0.061	6.161	0.0	0.0	0.024	6.375	0.028	0.033	0.033
Al	0.055	0.076	0.117	–	0.058	0.055	0.058	–	0.068	0.054	0.048
Ti	0.013	0.013	0.015	–	0.022	0.021	0.012	–	0.017	0.016	0.011
Mg	0.943	0.955	0.950	–	0.487	0.342	0.883	–	0.857	1.015	0.992
Fe^{2+}	0.180 } 2.00	0.181 } 1.98	0.260 } 1.97	–	0.686 } 1.94	0.725 } 1.89	0.273 } 1.98	–	0.261 } 1.97	0.385 } 1.98	0.196 } 1.99
Mn	0.025	0.016	0.019	–	0.062	0.060	0.022	–	0.029	0.029	0.022
Ca	0.772	0.730	0.585	2.357	0.599	0.621	0.715	2.623	0.725	0.469	0.709
Na	0.014	0.013	0.021	1.647 } 4.06	0.014	0.015	0.015	1.460 } 4.13	0.015	0.012	0.011
K	–	–	–	0.057	–	–	–	0.045	–	–	–
Σ	4.00	3.98	3.98	20.00	3.94	3.92	3.98	20.03	3.97	3.98	3.99
K				1.4				1.1			
Na				40.6				35.4			
Ca				58.0				63.5			
Mg	49.8	51.2	52.9		27.5	22.5	47.2		46.5	54.3	52.3
Fe	9.5	9.7	14.6		38.7	41.7	14.6		14.2	20.6	10.3
Ca	40.7	39.1	32.5		33.8	35.7	38.2		39.3	25.1	37.4

[b]g = groundmass and m = microphenocryst.

[c]Oxides as received.

[d]Derived from computer program of Jackson et al. (1967), modified by Wright (1970).

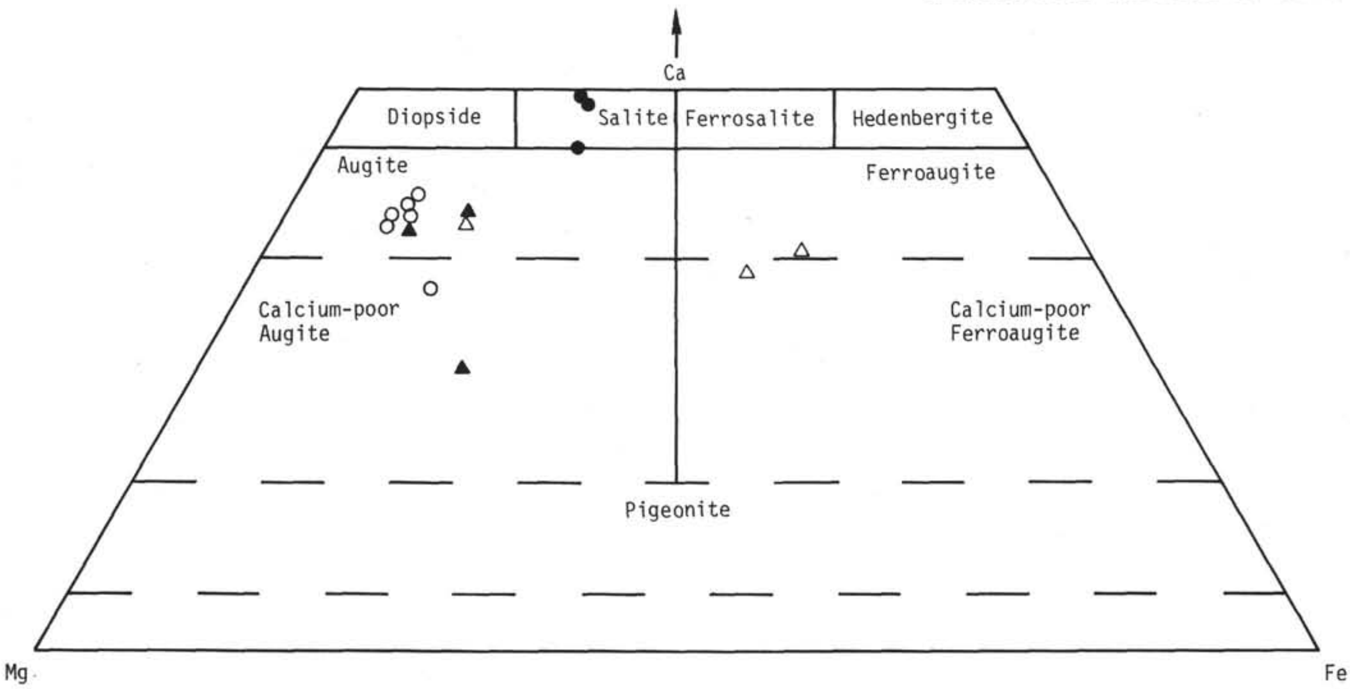

Figure 5. *Ca-Mg-Fe ternary diagram (fields modified from Hess, 1941) for pyroxenes from basalts of Holes 315A and 317A. (Solid circles from Hole 315A; open circles from 317A-31-2, 37-39 cm; closed triangles from 317A-34-1, 40-41 cm; and open triangles from 317A-32-3, 111.5-113 cm).*

TABLE 13
Dry Reduced Chemical Analyses and Norms of Basalts from Hole 315A[a]

Flow Unit	1B	2				3		4	5A	6
Sample (Interval in cm)	31-1, 115.5-117.5	32-1, 141.5-143.5	32-2, 82.5-83.5	32-2, 96-105	32-2, 96-105	32-3, 9.5-11.5	32-3, 87.5-89.5	32-4, 59-61	33-1, 116.5-118.5	34-1, 73.5-75.5
Plotting Symbol[b]	A	B	C	D	E	F	G	H	I	J
SiO_2	48.71	49.56	48.89	48.01	48.01	48.84	48.56	28.63	48.39	48.72
Al_2O_3	16.59	15.81	15.63	15.39	15.57	15.51	16.82	16.06	15.99	15.78
"FeO"[c]	12.12	13.08	13.01	13.64	13.24	13.06	12.24	12.85	13.44	13.51
MgO	7.75	7.52	7.05	7.26	7.66	7.61	7.90	8.07	8.19	7.75
CaO	7.58	6.48	7.32	7.55	7.16	7.10	7.56	7.95	6.47	6.20
Na_2O	3.43	3.59	3.68	3.61	3.67	3.48	3.32	3.03	3.54	3.54
K_2O	0.34	0.43	0.52	0.45	0.49	0.48	0.38	0.28	0.50	0.55
TiO_2	2.50	2.75	3.15	3.15	3.15	2.97	2.40	2.42	2.74	3.13
P_2O_5	0.33	0.33	0.35	0.32	0.35	0.33	0.27	0.32	0.32	0.35
MnO	0.50	0.37	0.36	0.43	0.43	0.42	0.36	0.26	0.27	0.39
S	0.12	0.06	0.04	0.17	0.21	0.18	0.15	0.11	0.13	0.06
Cr_2O_3	0.02	0.02	0.02	0.01	0.03	0.01	0.02	0.02	0.02	0.01
NiO	0.01	0.01	0.01	0.01	0.01	0.01	0.01	0.01	0.01	0.01
Total	100.00	100.01	100.03	100.00	99.98	100.00	99.99	100.01	100.01	100.00
Q										
Or	2.009	2.541	3.072	2.659	2.896	2.836	2.246	1.654	2.954	3.250
Ab	29.024	30.375	31.130	30.547	31.061	29.447	28.096	25.636	29.952	29.954
An	28.867	25.752	24.586	24.459	24.568	25.282	29.873	29.390	26.261	25.542
Ne										
Ns										
Wo	2.748	1.769	3.938	4.553	3.621	3.251	2.452	3.322	1.563	1.223
En	6.732	8.886	5.808	4.208	4.069	7.588	6.644	9.506	5.667	7.380
Fs	6.561	9.510	6.376	4.726	4.153	7.806	6.374	9.392	5.665	7.743
Fo	8.808	6.896	8.230	9.722	10.520	7.964	9.133	7.422	10.321	8.354
Fa	9.461	8.133	9.958	12.031	11.832	9.029	9.656	8.081	11.370	9.659
Cs										
Cm	0.029	0.029	0.029	0.015	0.044	0.015	0.029	0.029	0.029	0.015
Il	4.748	5.222	5.981	5.983	5.984	5.641	4.559	4.596	5.203	5.945
Ap	0.782	0.782	0.829	0.758	0.829	0.782	0.640	0.758	0.758	0.829
Pr	0.225	0.112	0.075	0.318	0.393	0.337	0.281	0.206	0.243	0.112
Total	99.993	100.006	100.012	99.979	99.971	99.977	99.981	99.992	99.987	100.008

[a]Calculated from Tables 5 and 8.

[b]See Figures 15–17.

[c]"FeO" is FeO + 0.9 Fe_2O_3 after summing to 100% dry weight.

TABLE 14
Dry Reduced Chemical Analyses and Norms of Basalts From Hole 317A[a]

Flow Unit	1	2	3	4	5A	5B					
Sample (Interval in cm)	31-1, 144-146	31-2, 37-39	31-3, 27-29	31-3, 100-103	31-4, 80-82	32-1, 84-86	32-2, 75-77	32-3, 100-111.5	32-3, 100-111.3	32-3, 106-108	32-4, 76-78
Plotting Symbol[b]	A	B	C	D	E	F	G	H	I	J	K
SiO_2	50.57	50.59	50.59	50.75	51.18	51.08	51.62	51.33	51.51	51.58	51.35
Al_2O_3	14.62	14.52	15.63	15.33	15.78	15.65	15.52	15.47	15.27	14.99	15.15
"FeO"[c]	10.76	10.80	9.27	9.44	9.39	10.21	10.53	11.08	11.08	11.29	10.81
MgO	10.33	10.50	9.32	9.28	8.49	8.00	7.45	7.15	7.10	7.28	7.59
CaO	9.89	9.70	11.48	11.64	11.49	11.60	11.14	11.41	11.56	11.15	11.27
Na_2O	2.27	2.41	2.17	2.16	2.17	2.06	2.15	2.11	2.05	2.20	2.30
K_2O	0.04	0.04	0.05	0.02	0.09	0.02	0.12	0.12	0.09	0.11	0.06
TiO_2	1.07	0.98	0.94	0.89	0.98	0.96	1.04	1.01	1.02	1.04	1.06
P_2O_5	0.13	0.14	0.13	0.14	0.13	0.13	0.14	0.08	0.10	0.13	0.12
MnO	0.27	0.25	0.34	0.25	0.28	0.24	0.25	0.19	0.19	0.18	0.25
S	0.02	0.01	0.01	0.01	0.01	0.01	0.01		0.01	0.01	0.01
Cr_2O_3	0.03	0.04	0.06	0.07	0.03	0.04	0.03	0.03	0.02	0.02	0.02
NiO	0.01	0.01	0.02	0.01	0.01	0.01	0.01	0.01	0.01	0.01	0.01
Total	100.01	99.99	100.01	99.99	100.03	100.01	100.01	99.99	99.99	99.99	99.99
Q							0.605	0.170	0.827	0.315	
Or	0.236	0.236	0.295	0.118	0.532	0.118	0.709	0.709	0.532	0.650	0.355
Ab	19.206	20.395	18.360	18.279	18.356	17.429	18.191	17.856	17.348	18.618	19.464
An	29.581	28.686	32.756	32.078	33.041	33.393	32.339	32.389	32.201	30.704	30.840
Ne											
Ns											
Wo	7.778	7.735	9.746	10.338	9.643	9.729	9.189	9.895	10.230	9.924	10.143
En	18.404	17.245	17.468	18.040	18.927	19.195	18.552	17.809	17.684	18.133	17.777
Fs	13.194	12.293	12.090	12.697	14.426	16.929	18.053	19.025	18.960	19.331	17.456
Fo	5.130	6.242	4.023	3.556	1.550	0.509					0.790
Fa	4.053	4.904	3.069	2.758	1.302	0.495					0.855
Cs											
Cm	0.044	0.059	0.088	0.103	0.044	0.059	0.044	0.044	0.029	0.029	0.029
Il	2.032	1.861	1.785	1.690	1.861	1.823	1.975	1.918	1.937	1.975	1.994
Ap	0.308	0.332	0.308	0.332	0.308	0.308	0.332	0.190	0.237	0.308	0.284
Pr	0.037	0.019	0.019	0.019	0.019	0.019	0.019		0.019	0.019	0.019
Total	100.005	100.007	100.008	100.007	100.007	100.007	100.007	100.006	100.005	100.006	100.006

Flow Unit	6A			6B			7A	7B	9	10	
Sample (Interval in cm)	32-4, 126-128	32-5, 95-97	32-6, 113-115	33-1, 138-140	33-2, 82-84	33-3, 94-96	33-4, 103-105	34-1, 40-41	34-2, 91-93	34-3, 118-120	34-4, 65-67
Plotting Symbol[b]	L	M	N	O	P	Q	R	S	T	U	V
SiO_2	50.42	50.81	50.74	50.91	50.68	50.53	51.38	51.25	51.98	51.89	51.38
Al_2O_3	14.47	13.87	13.53	13.62	14.44	15.43	15.36	15.19	15.28	14.60	15.51
"FeO"[c]	10.01	9.51	10.16	10.26	10.31	10.07	9.51	9.69	9.30	10.65	9.95
MgO	9.44	10.13	10.12	9.46	8.88	8.88	8.47	8.28	7.77	7.68	7.50
CaO	12.41	12.42	12.30	12.59	12.42	11.45	10.99	11.68	11.50	11.01	11.81
Na_2O	1.91	1.81	1.78	1.88	1.93	2.25	2.39	2.28	2.34	2.44	2.25
K_2O	0.04	0.04	0.02	0.07	0.04	0.13	0.26	0.06	0.25	0.15	0.10
TiO_2	0.85	0.85	0.84	0.85	0.91	0.94	1.12	1.05	1.11	1.18	1.09
P_2O_5	0.12	0.13	0.13	0.12	0.11	0.13	0.18	0.17	0.17	0.16	0.13
MnO	0.20	0.26	0.26	0.14	0.18	0.14	0.27	0.27	0.24	0.14	0.19
S	0.01	0.01	0.02	0.01	0.01	0.01	0.02	0.01	0.01	0.01	0.01
Cr_2O_3	0.09	0.14	0.09	0.08	0.07	0.05	0.05	0.06	0.06	0.06	0.05
NiO	0.02	0.02	0.01	0.01	0.01	0.01	0.01	0.01	0.01	0.01	0.01
Total	99.99	100.00	100.00	100.00	99.99	100.02	100.01	99.98	100.02	99.98	99.98
Q									0.052		
Or	0.236	0.236	0.118	0.414	0.236	0.768	1.536	0.355	1.477	0.887	0.591
Ab	16.163	15.316	15.062	15.908	16.333	19.035	20.221	19.297	19.796	20.651	19.043
An	30.794	29.603	28.869	28.518	30.622	31.612	30.412	31.042	30.445	28.447	31.932
Ne											
Ns											
Wo	12.524	13.012	13.070	13.845	12.643	10.159	9.573	10.774	10.641	10.496	10.781
En	18.020	20.822	20.750	19.516	18.460	15.775	17.833	18.401	19.347	18.838	18.136
Fs	13.250	13.565	14.532	14.599	14.775	12.235	13.568	14.765	15.633	17.544	16.291
Fo	3.849	3.088	3.121	2.834	2.563	4.440	2.284	1.524		0.205	0.383
Fa	3.119	2.217	2.409	2.336	2.261	3.795	1.915	1.348		0.211	0.379
Cs											
Cm	0.133	0.206	0.133	0.118	0.103	0.074	0.074	0.088	0.088	0.088	0.074
Il	1.614	1.614	1.595	1.614	1.728	1.785	2.127	1.995	2.108	2.242	2.071
Ap	0.284	0.308	0.308	0.284	0.261	0.308	0.426	0.403	0.403	0.379	0.308
Pr	0.019	0.019	0.037	0.019	0.019	0.019	0.037	0.019	0.019	0.019	0.019
Total	100.005	100.007	100.004	100.005	100.005	100.005	100.007	100.009	100.009	100.007	100.006

[a]Calculated from Tables 6 and 9.

[b]See Figures 18-20.

[c]"FeO" is FeO plus 0.9 Fe_2O_3 after summing to 100% dry weight.

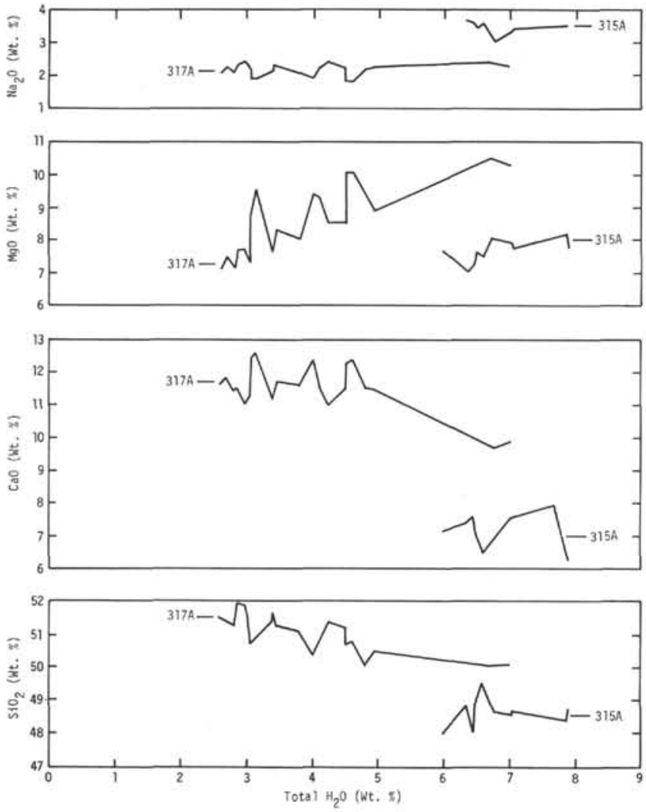

Figure 6. *Variation of SiO_2, CaO, MgO, and Na_2O, with total H_2O content of basalts from Holes 315A and 317A. (Oxides are dry, reduced, normalized.)*

island type, capped the ridge. Schilling (1973) and Moore and Schilling (1973) have carefully examined a suite of basalts from the Reykjanes Ridge, over a distance equivalent to 5° in latitude and onto Iceland proper. The basalts gradually change in minor-element content, vesicle size, and vesicle abundance from purely oceanic ridge values at the south end of the ridge to oceanic island type materials on subaerial Iceland. K_2O, TiO_2, P_2O_5, and rare-earth behavior patterns of these basalts do not compare with Hawaiian patterns until subaerial rocks are analyzed. Even at the margins of Iceland itself, Schilling (1973) gives P_2O_5 values of 0.18%-0.26%, K_2O values of 0.16%-0.26%, and TiO_2 values of 1.4%-2.1%. The range of these constituents in Hole 315A basalts is 0.27%-0.35%, 0.28%-0.55%, and 2.4%-3.15%, respectively. By an Iceland analogy, the entire Line Islands between at least Sites 165 and 316 would be expected to have been subaerial some 80-90 m.y. B.P. Moore and Schilling (1973) show that vesicle volumes exceed 40% at water depths as shallow as 100 meters. The vesicles in basalts at Site 165A (Bass et al., 1973) range from absent to 3.0%, average 1.0%, and are small. The vesicles in the Hole 315A basalts range from 1.5% to 9.5%, average 5.0%, and are small. These vesicles suggest that the Hole 315A basalts crystallized at depths of 1000-3000 meters beneath sea level, although Hays and Pitman (1973) reported water depths were up to 500 meters deeper 80-90 m.y. B.P. than at present, so that the area could have subsided somewhat

TABLE 15
Range and Average Abundance of Oxides and Elements in Basalts from Holes 315A and 317A

	Hole 315A		Hole 317A	
	Range	Average	Range	Average
Oxide (%)				
SiO_2	44.41-45.95	45.03[a]	46.79-50.42	48.99[b]
Al_2O_3	14.27-15.57	14.74[a]	12.88-15.17	14.35[b]
Fe_2O_3	5.88-8.56	6.96[a]	0.85-5.56	4.11[b]
FeO	4.17-7.03	5.79[a]	4.80-8.31	6.06[b]
MgO	6.52-7.57	7.11[a]	6.87-9.71	8.23[b]
CaO	5.61-7.46	6.60[a]	8.97-12.18	11.02[b]
Na_2O	2.84-3.41	3.24[a]	1.69-2.37	2.06[b]
K_2O	0.26-0.50	0.41[a]	0.02-0.25	0.09[b]
H_2O^+	1.36-3.56	2.57[a]	0.72-2.14	1.54[b]
H_2O^-	3.20-5.26	4.27[a]	1.54-5.06	2.40[b]
TiO_2	2.22-2.93	2.62[a]	0.80-1.15	0.95[b]
P_2O_3	0.25-0.33	0.30[a]	0.08-0.17	0.13[b]
MnO	0.24-0.46	0.35[a]	0.13-0.32	0.22[b]
Element (ppm)				
Ba	92-144	117[a]	<22-<22	<22[b]
C	100-1200	400[a]	<0.01-0.02	0.01[b]
Ce	29.4-38.1	34.4[e]	<5-11.9	7[f]
Cl	50-600	120[a]	50-1100	371[b]
Co	43.5-55.9	49.3[e]	41.1-51.3	47.4[f]
Cr	205-205	205[a]	<205-<205	<205[b]
Cr	61-145	108[c]	130-920	360[d]
Cr	75-174	121[e]	125-683	373[f]
Cs	<1-<1	<1[e]	<1-<1	<1[f]
Eu	1.90-2.29	2.09[e]	0.70-1.03	0.85[f]
Gd	3.6-8.2	5.6[e]	<6-<6	<6[f]
Hf	3.7-4.9	4.4[e]	0.9-1.7	1.3[f]
Nb	32-44	38[c]	N15[g]-N15	N15[d]
Ni	38-92	66[c]	60-120	82[d]
Ni	63-63	63[a]	79-79	79[b]
Rb	<12-<12	<12[a]	<12-<12	<12[b]
S	320-2000	1100[a]	0-150	102[b]
Sc	25.9-34.4	29.9[e]	40.4-48.4	44.1[f]
Sr	237-275	249[a]	81-118	100[b]
Ta	1.2-1.5	1.3[e]	0.2-0.3	0.3[f]
Tb	1.0-1.2	1.1[e]	0.4-0.6	0.5[f]
Th	1.2-2.0	1.5[e]	<1.5-<1.7	<1.6[f]
U	<0.1-0.4	0.2[e]	<0.1-0.1	<0.1[f]
V	170-280	235[c]	125-240	201[d]
Y	39-60	50[c]	14-34	24[d]
Yb	2.9-3.9	3.4[e]	1.7-2.6	2.2[f]
Zn	100-140	118[e]	<16-<20	<20[f]
Zr	165-230	192[c]	45-92	72[d]
Zr	120-<200	188[e]	<200-<200	<200[f]

[a]From Table 3, this report.
[b]From Table 4, this report.
[c]From Table 6, this report.
[d]From Table 7, this report.
[e]From Table 8, this report.
[f]From Table 9, this report.
[g]N Not detected at value shown.

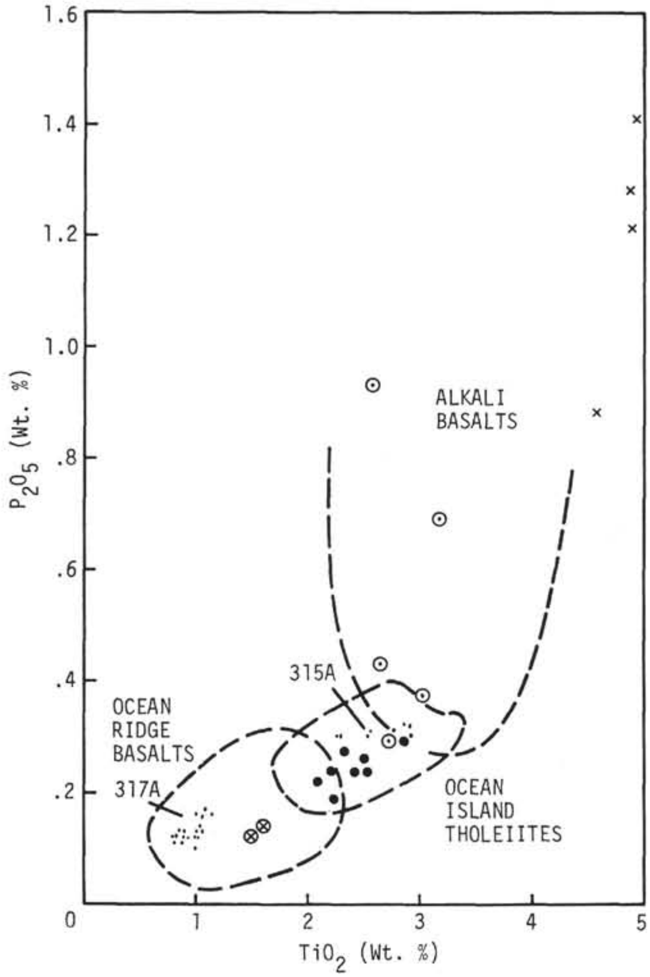

Figure 7. *TiO_2 versus P_2O_5 diagram comparing Leg 33 basalts with basalts from DSDP Legs 17 (Hole 165A) and 30 (Hole 289), and average Hawaiian tholeiites and alkalic basalts. (Crosses, as well as basalt fields are from Bass et al., 1973; average Hawaiian tholeiites solid circles and alkalic basalts open circles from Macdonald and Katsura, 1964, Tables 9 and 10; Circled crosses from Stoeser, in press; and small dots, Leg 33, Holes 315A and 317A from Tables 5 and 6, this report.)*

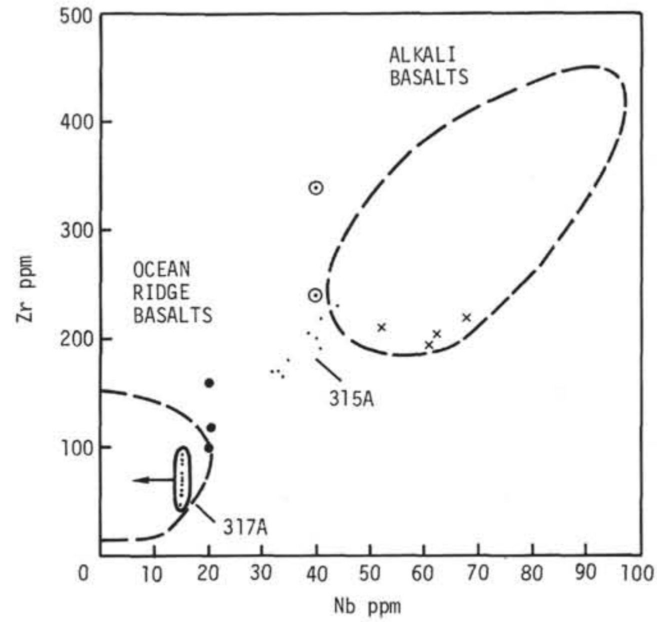

Figure 8. *Zr: Nb diagram comparing Leg 33 basalts with basalts from DSDP Leg 17 (Hole 165A) and the Hawaiian Islands. (Crosses and field boundaries are from Bass et al., 1973; Hawaiian tholeiites, solid circles, and alkalic basalts, open circles, from Hubbard, 1967; and, dots, Leg 33, Holes 315A and 317A from Tables 8 and 9, this report.)*

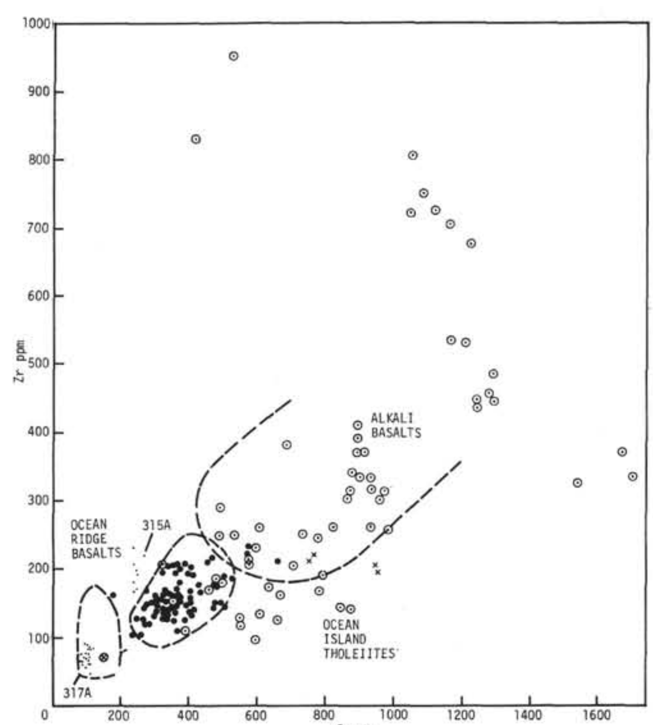

Figure 9. *Zr: Sr diagram comparing Leg 33 basalts with basalts from DSDP Legs 17 (Hole 165A) and 30 (289), and the Hawaiian Islands. (Crosses and field boundaries are from Bass et al., 1973; circled cross, from Stoeser, in press; Hawaiian tholeiites, solid circles and alkalic basalts, open circles, from Hubbard, 1967; and dots, Leg 33, Holes 315A and 317A are from Tables 5, 6, 8, and 9, this report.)*

since the crystallization of the basalts. In addition, the present bathymetry of the Line Islands bears little resemblance to a sunken Iceland.

The variety of oceanic island rock types in the breccia beds of Hole 318 suggest that these were derived from local Tuamotu edifices, and that the basaltic character of these islands is of the oceanic island basalt type. Age data further southeast along the Tuamotus are so scanty it is presently impossible to say whether or not these islands are edifices of a propagating chain.

REFERENCES

Andrews, J.E., Packham, G., et al., in press. Initial Reports of the Deep Sea Drilling Project, Volume 30: Washington (U.S. Government Printing Office).

Aumento, F., 1968. The mid-Atlantic ridge near 45° N. II. Basalts from the area of Confederation peak: Canadian J. Earth Sci., v. 5, p. 1-21.

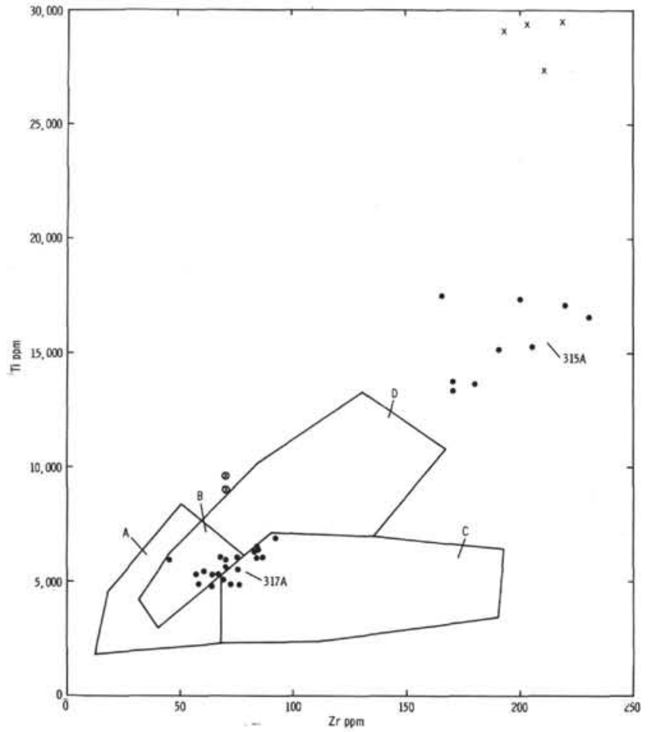

Figure 10. *Ti: Zr diagram comparing Leg 33 basalts with basalts from DSDP Legs 17 (Hole 165A) and 30 (Hole 289). (Crosses from Bass et al., 1973; circled crosses, from Stoeser, in press; fields are from Pearce and Cann, 1973; and dots, Leg 33, Holes 315A and 317A are from Tables 8 and 9 and calculated from Tables 5 and 7, this report.) According to Pearce and Cann (1973) "ocean floor basalts" plot in fields D and B; "low potassium tholeiites" in fields A and B, and "calc-alkali basalts" in fields C and B.*

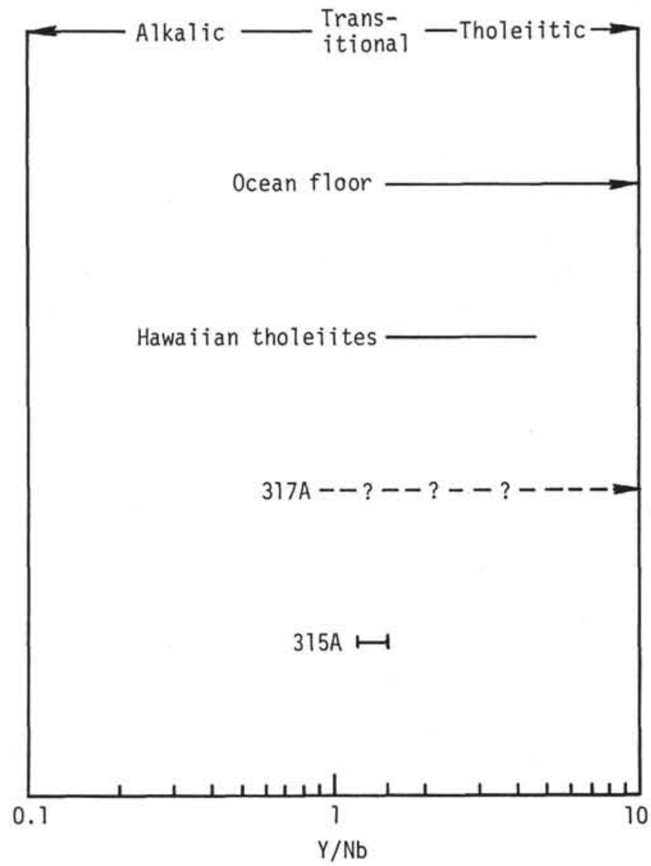

Figure 11. *Y/Nb petrographic character diagrams comparing ocean floor basalts, Hawaiian tholeiites and basalts from Leg 33, Holes 315A and 317A. (Ocean floor basalts, Hawaiian tholeiites and fields are from Pearce and Cann, 1973; 315A and 317A are from Tables 8 and 9, this report.)*

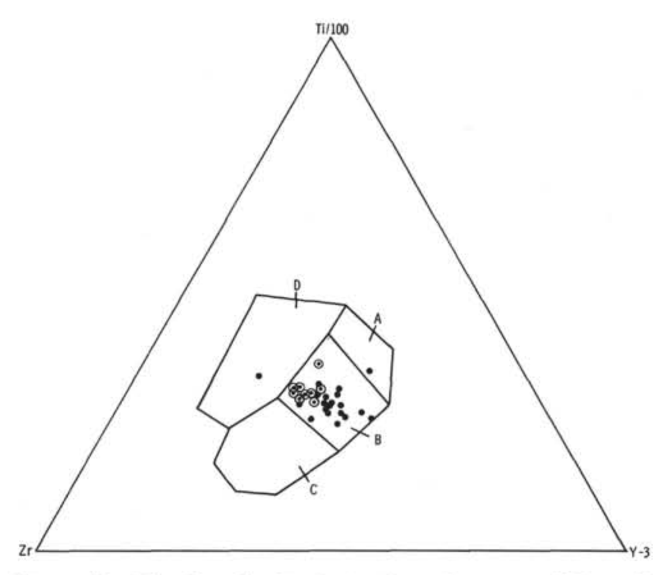

Figure 12. *Ti: Zr: Y discrimination diagram of Leg 33 basalts. (After Pearce and Cann, 1973, open circles 315A and solid circles 317A data from Tables 5, 6, 8, and 9, this report.) "Within plate basalts" plot in field D "Ocean floor basalts" in field B.*

________, 1971. Vesicularity of mid-oceanic pillow lavas: Canadian J. Earth Sci., v. 8, p. 1314-1319.

Baldwin, B., Coney, P.J., and Dickinson, W.R., 1974. Dilemna of a Cretaceous time scale and rates of sea-floor spreading: Geology, v. 2, p. 267-270.

Bass, M.N., Moberly, R., Rhodes, M.J., and Shih, C., 1973. Volcanic rocks cored in the central Pacific, Leg 17, Deep Sea Drilling Project. *In* Winterer, E.L., Ewing, J.I., et al., Initial Reports of the Deep Sea Drilling Project, Volume 17: Washington (U.S. Government Printing Office), p. 429-503.

Bastron, H., Barnett, P.R., and Murata, K.J., 1960. Method for the quantitative spectrochemical analysis of rocks, minerals, ores, and other materials by a powder D-C arc technique: U.S. Geol. Surv. Bull. 1084-G, p. 165-182.

Beeson, M.H., 1973. Petrology, mineralogy, and geochemistry of the lavas of east Molokai volcano, Hawaii: Unpublished Ph.D. thesis, University of California at Santa Cruz, p. 151.

Bradley, W.F., 1945. Diagnostic criteria for clay minerals: Am. Mineral., v. 30, p. 704-713.

Dalrymple, G.B., Lanphere, M.A., and Jackson, E.D., 1974. Contributions to the petrography and geochronology of volcanic rocks from the leeward Hawaiian Islands: Geol. Soc. Am. Bull., v. 85, p. 727-738.

Engel, A.E.J., Engel, C.G., and Havens, R.G., 1967. Chemical characteristics of oceanic basalts and the upper mantle: Geol. Soc. Am. Bull., v. 76, p. 719-734.

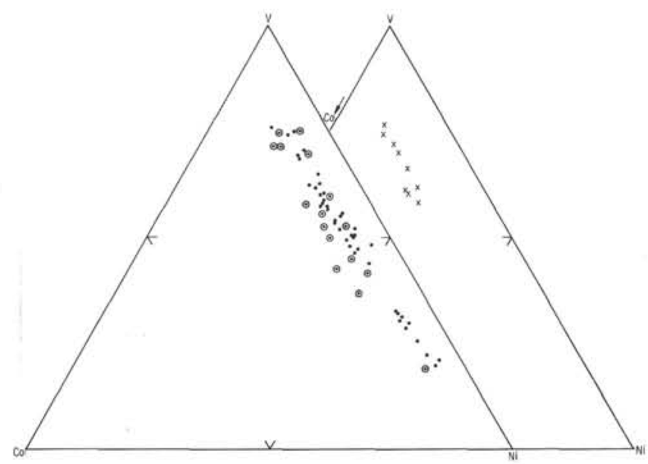

Figure 13a. *V-Co-Ni ternary diagram (after Ishikawa, 1968) comparing Hole 315A basalts with tholeiitic and alkalic basalts from Hawaii. (Crosses, Hole 315A, this report; dots, Hawaiian tholeiites from Hubbard, 1967; open circles, Hawaiian alkalic basalts from Hubbard, 1967 and unpublished analyses of E. D. Jackson and T. L. Wright.*

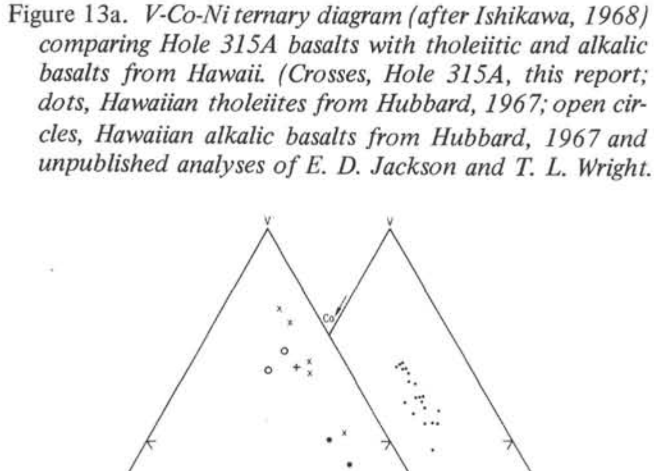

Figure 13b. *V-Co-Ni ternary diagram (after Ishikawa, 1968) comparing Hole 317A basalts with other oceanic basalts. (Dots 317A, this report; solid circles, Stoeser, in press; open circles, Marshall, in press; crosses, Engel et al., 1965; and pluses, Stewart et al., 1973.*

Fabbi, B.P., 1971. X-ray fluorescence determination of barium and strontium in geologic samples: Appl. Spectroscopy, v. 25, p. 316-318.

_______, 1972. A refined fusion X-ray fluorescence technique, and determination of major and minor elements in silicate standards: Am. Mineral., v. 57, p. 237-245.

_______, 1973. X-ray fluorescence determination of sodium in silicate standards using direct dilution and dilution fusion preparation techniques: X-ray Spectrom., v. 2, p. 15-17.

Fabbi, B.P. and Espos, L.F., 1972a. X-ray fluorescence determination of Cl in standard silicate rocks: Appl. Spectroscopy, v. 26, p. 293-295.

_______, 1972b. X-ray fluorescence determination of As, Sb, Ni, Rb, Sc, V, and An in rock standards and other rock samples: in Geological Survey Research 1972: U.S. Geol. Surv. Prof. Paper 800-B, p. B147-B152.

Fabbi, B.P. and Moore, W.J., 1970. Rapid X-ray fluorescence determination of sulfur in mineralized rocks from the Bingham Mining District, Utah: Appl. Spectroscopy, v. 24, p. 426-428.

Flanagan, F.J., Wright, T.L., Taylor, S.R., Annell, C.S., Christian, R.C., and Dinnin, J.E., in press. Basalt, BHVO-1 from Kilauea crater, Hawaii: U.S. Geol. Surv. Prof. Paper 850.

Fodor, R.V., Keil, K., and Bunch, T.E., 1975. Contributions to the mineral chemistry of Hawaiian rocks, V. Pyroxenes in rocks from Haleakala and West Maui volcanoes: Contrib. Mineral. Petrol., v. 50, p. 173-195.

Green-Kelly, R., 1953. The identification of montmorillonoids in clays: J. Soil Sci., v. 4, p. 233-237.

Grim, R.E., 1968. Clay mineralogy: New York (McGraw-Hill Book Co.).

Hart, S.R., 1971. K, Rb, Cs, Sr, and Ba contents and Sr isotope ratios of ocean floor basalts: Roy. Soc. London Phil. Trans. Sci. A., v. 268, p. 573-587.

Hart, S.R. and Nalwalk, A.J., 1970. K, Rb, Cs, and Sr relations in submarine basalts from the Puerto Rico Trench: Geochim. et Cosmochim. Acta, v. 34, p. 145-156.

Haskin, L.A., Haskin, M.A., Frey, F.A., and Wildeman, T.R., 1968. Relative and absolute terrestrial abundances of the rare earths. *In* Ahrens, L.H., (Ed.), Proc. Symp., IAGC, Paris, 1967: New York (Pergamon Press), p. 889-912.

Hays, J.D. and Pitman, W.C., III, 1973. Lithospheric plate motion, sea level changes and climatic and ecological consequences: Nature, v. 246, p. 18-22.

Heezen, B.E. and Hollister, C.D., 1971. The face of the deep: Oxford, England (Oxford University Press).

Hess, H.H., 1941. Pyroxenes of common mafic magmas: Am. Mineral., v. 26, p. 515-535.

_______, 1959. Notes on operation of Frantz Isodynamic Magnetic Separator: Pamphlet published by S.G. Frantz Co., Inc., 6p.

Hubbard, N.J., 1967. Some trace elements in Hawaiian lavas: Unpublished Ph.D Thesis, University of Hawaii. 128 p.

Irvine, T.N. and Baragar, W.R.A., 1971. A guide to the chemical classification of common volcanic rocks: Canadian J. Earth Sci., v. 8, p. 523-548.

Ishikawa, H., 1968. Some aspects of geochemical trends and fields in the ratios of vanadium, nickel, and cobalt: Geochim. Cosmochim. Acta, v. 32, p. 913-917.

Jackson, E.D., 1961. X-ray determination curve for some natural plagioclase of composition An 60-85: U.S. Geol. Surv. Prof. Paper 424C, p. C286-C288.

_______, 1974. Linear island chains in the Pacific basin (abstract): Program with Abstracts, International Woollard Symposium, Hawaii Inst. Geophysics, p. 30.

Jackson, E.D. and Wright, T.L., 1970. Xenoliths in the Honolulu Volcanic Series, Hawaii: J. Petrol., v. 11, p. 405-430.

Jackson, E.D., Silver, E.A., and Dalrymple, G.B., 1972. Hawaiian-Emperor chain and its relation to Cenozoic circumpacific tectonics: Geol. Soc. Am. Bull., v. 83, p. 601-618.

Jackson, E.D., Stevens, T.E., and Bowen, R.W., 1967. A computer-based procedure for deriving mineral formulas from mineral analyses: U.S. Geol. Surv. Prof. Paper, 565-C, p. C23-C31.

Kay, R., Hubbard, N.J., and Gast, P.W., 1970. Chemical characteristics and origin of oceanic ridge volcanic rocks: J. Geophys. Res., v. 75, p. 1585-1613.

Keil, K., Fodor, R.V., and Bunch, T.E., 1972. Contributions to the mineral chemistry of Hawaiian rocks, II. Feldspars and interstitial material in rocks from Haleakala and West Maui volcanoes, Maui, Hawaii: Contrib. Mineral. Petrol., v. 37, p. 253-276.

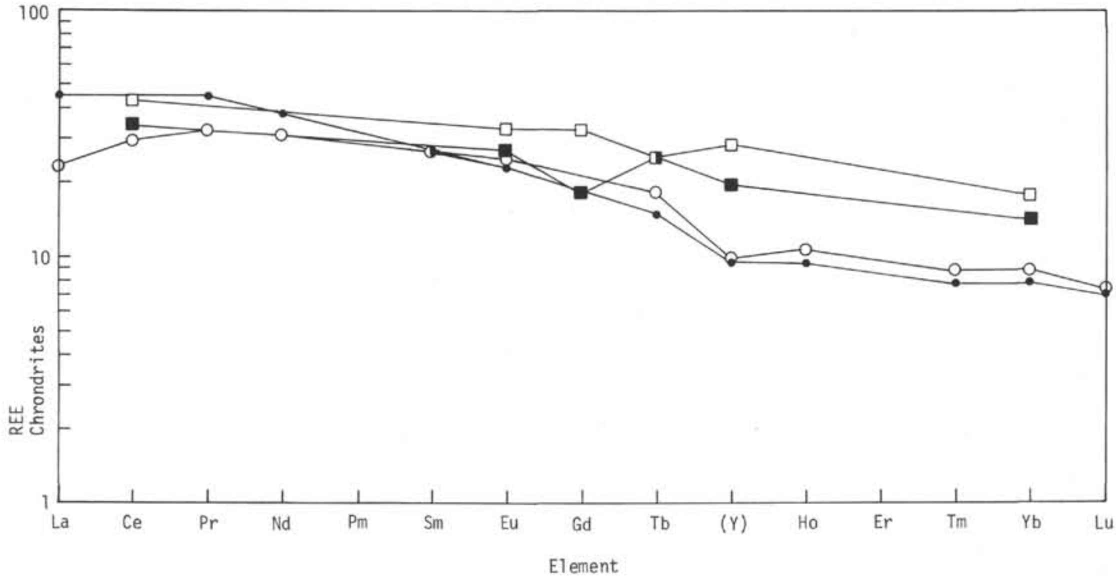

Figure 14a. *Chrondrite-normalized trends of rare earth elements for basalts from the Hawaiian Islands compared with those of basalts from Leg 33, Hole 315A. (Solid circles are average Hawaiian alkalic basalts and open circles are average Hawaiian tholeiites from Schilling, 1966; open squares, Sample 315A-34-1, 73.5-75.5 cm, selected for highest Eu value, and solid squares, Sample 315A-32-3, 87.5-89.5 cm, selected for lowest Eu value, from Tables 8 and 10, this report.) (Half solid symbols values coincide.) Our values are chrondrite normalized using data from Haskin et al., 1968.*

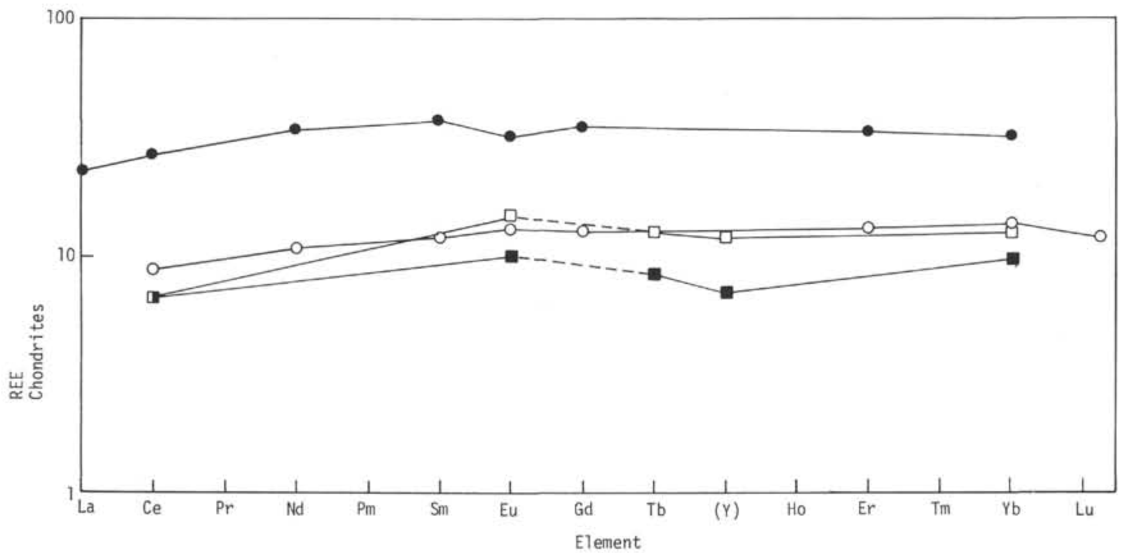

Figure 14b. *Chrondrite-normalized trends of rare-earth elements of oceanic ridge basalts compared with those of basalts from Leg 33, Hole 317A. (Solid circles are basalts from the Juan de Fuca ridge from Kay et al., 1970; open circles are basalts from Leg 6, Site 54 from Ridley et al., 1974; open squares, Sample 317A-34-3, 118-120 cm, selected for highest Eu value; closed squares, Sample 317A-32-6, 113-115 cm, from Tables 9 and 11, this report.) (Half solid symbols values coincide.) Our values are chrondrite normalized using data from Haskin et al., 1968.*

TABLE 16a
Range and Average Abundance of Selected Minor Elements in Basalts of Hole 315A Compared With Those of Hawaiian Tholeiites and Alkalic Olivine Basalts

Element	Hole 315A Range	Hole 315A Average	Hawaiian Tholeiites Range	Hawaiian Tholeiites Average	Hawaiian Alkalic Olivine Basalts Range	Hawaiian Alkalic Olivine Basalts Average	Source
Ba	92-144	117[a]	50-300	120	200-1000	420	e, f, g, h, i, j
Sr	237-275	249[a]	100-1000	383	262-1000	607	e, f, g, h, i, j, k
Co	43.5-55.9	49.3[b]	20-71	48	30-100	66	e, f, g, h, i, j
Cr	75-174 61-145	121[b] 108[c]	150-1500	567	20-1000	433	e, f, g, h, i, j
Cu	70-100	87[d]	50-200	139	30-300	105	e, f, g, h, i, j
Nb	32-44	38[c]	>10	>10	10-40	20	e, f, g, h, i, j
Ni	38-92	66[c]	50-1240	235	15-972	219	e, f, g, h, i, j
P	1091-1397	1314[a]	524-2095	1135	873-3317	1615	l, m
Sc	25.9-34.4	29.9[b]	20-70	32	20-50	30	e, f, g, h, i, j
Ti	13309-17505	15527[a]	10971-22122	14988	11091-24100	18045	l, m
V	170-280	235	150-500	289	30-500	323	e, f, g, h, i, j
Y	39-60	50[c]	15-50	26	19-50	27	e, f, g, h, i, j, k
Zr	165-230	192[c]	70-247	131	70-348	149	e, f, g, h, i, j

[a]X-ray fluorescence analyses.
[b]Radioactivation and radiochemistry analyses.
[c]Quantitative spectrographic analyses.
[d]Semiquantitative spectrographic analyses.
[e]Unpublished semiquantitative spectrographic analyses of E.D. Jackson.
[f]Unpublished semiquantitative spectrographic analyses of R.L. Christiansen.
[g]Unpublished semiquantitative spectrographic analyses of D.A. Swanson.
[h]Unpublished semiquantitative spectrographic analyses of R.I. Tilling.
[i]Unpublished semiquantitative spectrographic analyses of T.L. Wright.
[j]Hubbard (1967).
[k]Schilling (1966).
[l]Macdonald and Katsrua (1964).
[m]Macdonald (1968).

TABLE 16b
Range and Average Abundance of Selected Minor Elements in Basalts of Hole 317A Compared With Those of Other Oceanic Ridge Basalts

Element	Hole 317A Range	Hole 317A Average	Oceanic Ridge Basalts Range	Oceanic Ridge Basalts Average	Source
Ba	<22	<22[a]	2-180	25	e, f, g, h
Sr	81-118	100[a]	70-440	199	e, f, g, h, i, j
Co	41.1-51.3	47.4[b]	6-75	42	e, f, g, h, j
Cr	130-920 125-683	360[c] 373[b]	70-700	320	e, f, g, h
Cu	50-200	112[d]	10-700	148	e, f, g, h, j
Nb	<15	<15[c]	1.9-88	14	i, j
Ni	60-120	82[c]	15-500	149	e, f, g, h, i
P	436-742	563[a]	131-2226	865	e, f, g, h, i, j
Sc	40.4-48.4	44.1[b]	30-70	51	e, f, g, h, j
Ti	4796-6894	5681[a]	3537-17086	9452	e, f, g, h, i, j
V	125-240	201[c]	150-440	246	e, f, g, h
Y	14-34	24[c]	15-100	37	e, f, g, h, i, j
Zr	45-92	72[c]	15-950	137	e, f, g, h, i, j

[a]X-ray fluorescence analyses.
[b]Radioactivation and radiochemistry analyses.
[c]Quantitative spectrographic analyses.
[d]Semiquantitative spectrographic analyses.
[e]Stoeser (in press).
[f]Marshall (in press).
[g]Engel et al. (1965).
[h]Stewart et al. (1973).
[i]Bass et al. (1973).
[j]MacLeod and Pratt (1973).

Laniz, R.V., Stevens, R.E., and Norman, M.B., 1964. Staining of plagioclase feldspar and other minerals with F.D. and C red no. 2: U.S. Geol. Surv. Prof. Paper 501B, p. B152-B153.

Larson, R.L. and Chase, C.G., 1972. Late Mesozoic evolution of the western Pacific ocean: Geol. Soc. Am. Bull., v. 83, p. 3627-3644.

Macdonald, G.A., 1968. Composition and origin of Hawaiian lavas. *In* Coats, R.R., Hay, R.L., and Anderson, C.A. (Eds.), Studies in volcanology: Geol. Soc. Am. Mem. 116, p. 477-522.

Macdonald, G.A. and Katsura, T., 1964. Chemical composition of Hawaiian lavas: J. Petrol., v. 5, p. 82-133.

Macleod, N.S. and Pratt, R.M., 1973. Petrology of volcanic rocks recovered on Leg 18, Deep Sea Drilling Project. *In* Kulm, L.D., von Huene, R., et al., Initial Reports of the Deep Sea Drilling Project, Volume 18: Washington (U.S. Government Printing Office), p. 935-945.

Marshall, M., 1975. Petrology and chemical composition of basaltic rocks recovered on Leg 32, Deep Sea Drilling Project. *In* Larson, R.L., Moberly, R., Jr., et al., Initial Reports of the Deep Sea Drilling Project, Volume 32: Washington (U.S. Government Printing Office). p. 563-570.

Matthews, D.H., 1971. Altered basalts from Swallow Bank, an abyssal hill in the NE Atlantic, and from a nearby seamount: Roy. Soc. London Phil. Trans. Sci. A, v. 268, p. 551-571.

Moberly, R., Jr., and Heath, G.R., 1971. Volcanic rocks from the western and central Pacific: Leg 7, Deep Sea Drilling Project. *In* Winterer, E.L., Riedel, W.R., et al., 1971, Initial Reports of the Deep Sea Drilling Project, Volume 7: Washington (U.S. Government Printing Office), p. 1011-1026.

Moore, J.G., 1965. Petrology of deep-sea basalt near Hawaii: Am. J. Sci., v. 263, p. 40-52.

Moore, J.G. and Schilling, J.G., 1973. Vesicles, water, and sulfur in Reykjanes ridge basalts: Contrib. Mineral. Petrol., v. 41, p. 105-118.

Mumpton, F.A., 1960. Clinoptilolite redefined: Am. Mineral., v. 45, p. 351-369.

Murata, K.J. and Whitely, K.R., 1973. Zeolites in the Miocene Briones sandstone and related formations of the central Coast Ranges, California: U.S. Geol. Surv. J. Res., v. 1, p. 255-265.

Myers, A.T., Havens, R.G., and Dunton, P.J., 1960. A spectrochemical method for the semiquantitative analysis of rocks, minerals, and ores: U.S. Geol. Surv. Bull. 1084-I, p. 207-229.

Pearce, J.A. and Cann, J.R., 1973. Tectonic setting of basic volcanic rocks determined using trace element analyses: Earth and Planet. Sci. Lett., v. 19, p. 290-300.

Peck, L.C., 1964. Systematic analysis of silicates: U.S. Geol. Surv. Bull. 1170.

Pitman, W.C., III, Larson, R.L., and Herron, E.M., 1974. Ages of the ocean basins determined from magnetic anomaly lineations: Magnetic lineations of the oceans, Geol. Soc. Am. Special Map.

Ridley, I., Rhodes, J.M., Reid, A.M., Jakes, P., Shih, C., and Bass, M.N., 1974. Basalts from Leg 6 of the Deep Sea Drilling Project: J. Petrol., v. 15, p. 140-159.

Schilling, J.G., 1966. Rare earth fractionation in Hawaiian volcanic rocks: Unpublished Ph.D Thesis, Massachusetts Institute Technology, 390 p.

———, 1971. Sea-floor evolution: rare earth evidence: Roy, Soc. London Phil. Trans. Ser. A., v. 268, p. 663-706.

———, 1973. Iceland mantle plume: Geochemical study of Reykjanes ridge: Nature, v. 242, p. 565-571.

Schoen, R. and Lee, D.E., 1964. Successful separation of silt-size minerals in heavy liquids: U.S. Geol. Surv. Prof. Paper 501-B, p. B154-157.

Shand, S.J., 1939. On the staining of feldspathoids, and on zonal structure in nepheline: Am. Mineral., v. 24, p. 508-513.

Shih, C., 1974. Rare earth goechemistry of basaltic rocks from Leg 17 of the Deep Sea Drilling Project (abstract): Abstracts with Programs, v. 6, (Boulder, Colo.), p. 952-953.

Stewart, R.J., Natland, J.H., and Glassby, W.R., 1973. Petrology of volcanic rocks from the North Pacific Ocean and the Bering Sea. *In* Creager, J.S., Scholl, D.W., et al., Initial Reports of the Deep Sea Drilling Project, Volume 19: Washington (U.S. Government Printing Office), p. 615-628.

Stoeser, D.B., in press. Igneous rocks from Leg 30 of the Deep Sea Drilling Project. *In* Andrews, J.E., Packham, G., et al. Initial Reports of the Deep Sea Drilling Project, Volume 30: Washington (U.S. Government Printing Office).

Sutton, G.H., Meynard, G.L., and Hussong, D.M., 1970. Widespread occurrences of a high velocity layer in the capitol Pacific crust, found with repetitive sources and sonabuoys. *In* Heacock, J.G. (Ed.), Structural and physical properties of the earth's crust: Geophys. Mono., v. 14, p. 193-209.

Winterer, E.L., Lonsdale, P.F., Matthews, J.L., and Rosendahl, B.R., 1974. Structure and acoustic stratigraphy of the Manihiki Plateau: Deep-Sea Res., v. 21, p. 793-814.

Wright, T.L., 1970 Mineral norms—Mod I: U.S. Geol. Surv. Computer Contrib. C-463.

———, 1971. Chemistry of Kilauea and Mauna Loa Lava in space and time: U.S. Geol. Surv. Prof Paper 735, 40 p.

TABLE 17
Dry Reduced Chemical Analyses and Norms of Basalts From Hualalai Volcano, Hawaii, DSDP Leg 17 (Hole 165A) and DSDP Leg 30 (Hole 289)

Sample	65AAM1[a]	65FAR1[a]	65FAR2[a]	65HON1[a]	65HU2[a]	65HU8[a]	65HU9[a]	65HU10[a]	65HUE2[a]	65JAC1[a]	65JAC2[a]	65JAC4[a]
Plotting Symbol[b]	1	1	1	1	1	1	1	1	1	1	1	1
SiO_2	46.74	46.68	46.81	47.04	46.76	47.86	47.37	46.83	46.30	46.68	46.83	46.36
Al_2O_3	14.78	14.63	14.87	15.67	14.76	15.73	14.47	14.79	13.95	14.79	14.80	14.94
"FeO"[c]	12.56	12.44	12.43	12.78	12.48	12.40	12.28	12.57	12.46	12.48	12.47	12.21
MgO	8.95	9.48	8.98	7.74	9.14	5.59	8.93	9.14	11.22	9.01	9.00	9.73
CaO	9.89	10.41	10.41	9.56	10.20	10.55	10.64	10.09	10.55	10.19	10.12	11.03
Na_2O	3.15	2.75	2.83	3.33	2.85	3.37	2.71	2.83	2.43	3.04	2.96	2.40
K_2O	0.96	0.86	0.90	1.00	0.91	1.15	0.86	0.91	0.72	0.91	0.93	0.74
TiO_2	2.48	2.27	2.29	2.37	2.41	2.69	2.30	2.38	1.95	2.41	2.40	2.07
P_2O_5	0.30	0.27	0.29	0.32	0.29	0.46	0.25	0.27	0.23	0.28	0.29	0.34
MnO	0.19	0.19	0.19	0.19	0.19	0.20	0.18	0.19	0.19	0.19	0.19	0.18
S												
Cr_2O_3												
NiO												
Total	100.00	99.98	100.00	100.00	99.99	100.00	99.99	100.00	100.00	99.98	99.99	100.00
Q												
C												
Or	5.673	5.083	5.318	5.909	5.378	6.796	5.082	5.377	4.255	5.379	5.496	4.373
Ab	17.691	16.808	17.305	19.822	17.657	21.569	18.717	18.039	14.713	17.062	17.791	15.733
An	23.354	25.040	25.213	24.856	24.796	24.397	24.781	24.965	25.030	24.027	24.352	27.807
Lc												
Ne	4.856	3.503	3.598	4.526	3.500	3.763	2.284	3.200	3.168	4.695	3.932	2.478
Wo	9.917	10.376	10.245	8.551	9.986	10.412	11.013	9.740	10.775	10.316	10.006	10.310
En	5.164	5.512	5.335	4.138	5.247	4.450	5.758	5.095	6.027	5.390	5.226	5.544
Fs	4.477	4.541	4.626	4.274	4.447	5.977	4.941	4.366	4.317	4.633	4.497	4.424
Fo	12.001	12.686	11.935	10.608	12.276	6.638	11.552	12.381	15.358	11.951	12.047	13.096
Fa	11.465	11.516	11.407	12.074	11.466	9.826	10.926	11.692	12.122	11.323	11.425	11.518
Cs												
Cm												
Il	4.710	4.312	4.349	4.501	4.578	5.109	4.369	4.520	3.703	4.578	4.559	3.931
Tn												
Ru												
Ap	0.711	0.640	0.687	0.758	0.687	1.090	0.592	0.640	0.545	0.663	0.687	0.805
Pr												
Total	100.018	100.016	100.017	100.019	100.017	100.026	100.015	100.016	100.014	100.017	100.017	100.020

Sample	65JAC5[a]	65KAI2[a]	65KAP11[a]	65KAP15[a]	65KAP20[a]	65KEA1[a]	65KEA2[a]	65KEU1[a]	65KIH3[a]	65MAL3[a]	67-101[d]	67-101B[d]
Plotting Symbol[b]	1	1	1	1	1	1	1	1	1	1	1	1
SiO_2	46.63	46.47	46.88	46.12	46.84	46.27	46.36	46.68	46.63	46.77	46.98	45.59
Al_2O_3	16.10	12.90	14.76	14.35	14.79	13.08	13.39	14.40	14.73	14.73	14.68	15.35
"FeO"[c]	13.59	12.10	12.55	12.82	12.57	11.94	11.82	12.55	12.59	12.47	12.32	14.66
MgO	5.82	11.81	8.88	9.69	9.03	12.29	11:54	10.04	9.09	9.09	9.25	5.94
CaO	10.88	11.02	10.18	10.59	9.91	11.30	11.63	10.36	10.20	10.14	10.73	9.13
Na_2O	2.91	2.31	2.90	2.66	2.97	2.25	2.30	2.69	2.98	2.95	2.72	3.30
K_2O	0.87	0.85	0.92	0.86	0.95	0.66	0.66	0.82	0.90	0.93	0.81	0.98
TiO_2	2.71	2.10	2.44	2.43	2.44	1.81	1.86	2.01	2.42	2.44	2.07	4.03
P_2O_5	0.28	0.26	0.29	0.28	0.29	0.21	0.24	0.26	0.27	0.28	0.25	0.82
MnO	0.20	0.18	0.19	0.19	0.19	0.18	0.18	0.19	0.19	0.19	0.18	0.20
S												
Cr_2O_3												
NiO												
Total	99.99	100.00	99.99	99.99	99.98	99.99	99.98	100.00	100.00	99.99	99.99	100.00
Q												
C												
Or	5.142	5.023	5.437	5.082	5.615	3.901	3.901	4.846	5.318	5.496	4.787	5.791
Ab	18.820	13.137	18.138	14.907	18.266	12.145	12.336	16.354	16.952	17.507	17.021	23.494
An	28.301	22.319	24.542	24.678	24.223	23.643	24.267	24.795	24.158	24.206	25.457	24.177
Lc												
Ne	3.145	3.472	3.469	4.119	3.722	3.736	3.862	3.472	4.477	4.040	3.249	2.400
Wo	9.958	12.799	10.051	10.871	9.626	12.964	13.308	10.398	10.305	10.135	10.917	6.580
En	4.109	7.405	5.212	5.775	5.022	7.575	7.656	5.578	5.383	5.321	5.734	2.759
Fs	5.911	4.805	4.565	4.758	4.334	4.769	5.053	4.479	4.631	4.518	4.864	3.848
Fo	7.279	15.422	11.847	12.867	12.244	16.143	14.779	13.614	12.092	12.137	12.127	8.434
Fa	11.541	11.029	11.435	11.682	11.644	11.201	10.750	12.048	11.465	11.358	11.336	12.966
Cs												
Cm												
Il	5.147	3.988	4.635	4.616	4.635	3.438	3.533	3.817	4.596	4.635	3.932	7.654
Tn												
Ru												
Ap	0.663	0.616	0.687	0.663	0.687	0.497	0.569	0.616	0.640	0.663	0.592	1.942
Pr												
Total	100.017	100.016	100.017	100.017	100.017	100.013	100.015	100.016	100.016	100.017	100.015	100.045

[a]Previously unpublished analyses of E.D. Jackson; Hualalai volcano, Hawaii.

[b]For 1, W, X, Y, and Z, see Figures 15-17; for 3 and 4, see Figures 18-20.

[c]"FeO" is FeO plus 0.9 Fe_2O_3 after summing to 100% dry weight.

[d]Previously unpublished analyses of T.L. Wright; Hualalai volcano, Hawaii.

TABLE 17 – *Continued*

Sample Plotting Symbol[b]	67-102[d] 1	67-103[d] 1	67-105[d] 1	67-106[d] 1	67-107B[d] 1	67-109[d] 1	67-113A[d] 1	67-114[d] 1	67-118[d] 1	C-218[e] 1	C-219[e] 1	C-220[e] 1
SiO_2	47.24	46.86	48.33	46.97	47.40	46.74	46.61	46.90	46.27	47.14	45.81	46.50
Al_2O_3	15.15	15.03	16.44	14.09	15.20	14.04	14.12	14.73	13.80	14.49	13.92	15.33
"FeO"[c]	12.37	12.64	11.84	12.57	12.15	12.20	12.11	12.46	11.98	12.31	13.15	13.08
MgO	8.70	9.01	5.94	10.22	8.42	10.51	10.98	8.99	12.28	8.60	10.05	8.05
CaO	10.93	10.52	8.67	9.99	10.66	11.03	10.44	10.47	10.41	11.60	10.43	9.64
Na_2O	2.33	2.61	4.01	2.75	2.54	2.44	2.49	2.80	2.31	2.46	2.72	3.22
K_2O	0.78	0.79	1.49	0.88	0.90	0.69	0.74	0.91	0.66	0.86	1.00	1.09
TiO_2	2.06	2.10	2.57	2.06	2.28	1.92	2.05	2.29	1.90	2.15	2.42	2.57
P_2O_5	0.25	0.26	0.52	0.27	0.26	0.23	0.27	0.26	0.21	0.24	0.31	0.35
MnO	0.18	0.18	0.19	0.19	0.18	0.19	0.18	0.19	0.18	0.16	0.18	0.17
S												
Cr_2O_3												
NiO												
Total	99.99	100.00	100.00	99.99	99.99	99.99	99.99	100.00	100.00	100.01	99.99	100.00
Q												
C												
Or	4.610	4.668	8.805	5.201	5.319	4.078	4.373	5.377	3.900	5.081	5.910	6.441
Ab	18.892	17.940	24.228	17.612	19.454	15.499	16.310	17.217	14.665	15.984	13.059	17.786
An	28.578	26.962	22.458	23.505	27.418	25.321	25.168	24.936	25.336	25.952	22.821	24.156
Lc												
Ne	0.447	2.246	5.257	3.066	1.106	2.790	2.580	3.508	2.644	2.616	5.395	5.125
Wo	10.028	9.824	7.164	10.145	9.926	11.650	10.383	10.567	10.412	12.535	11.232	8.928
En	5.128	5.051	3.228	5.483	5.091	6.416	5.850	5.498	6.090	6.420	5.982	4.377
Fs	4.650	4.520	3.895	4.316	4.584	4.800	4.105	4.776	3.822	5.800	4.896	4.387
Fo	11.592	12.185	8.105	13.996	11.129	13.849	15.065	11.837	17.164	10.509	13.350	10.982
Fa	11.584	12.015	10.779	12.140	11.043	11.420	11.650	11.334	11.873	10.464	12.042	12.128
Cs												
Cm												
Il	3.913	3.988	4.881	3.913	4.331	3.647	3.894	4.349	3.609	4.083	4.597	4.881
Tn												
Ru												
Ap	0.592	0.616	1.232	0.640	0.616	0.545	0.640	0.616	0.497	0.568	0.734	0.829
Pr												
Total	100.015	100.016	100.029	100.016	100.016	100.014	100.016	100.016	100.013	100.014	100.018	100.020

Sample Plotting Symbol[b]	C-221[e] 1	C-222[e] 1	C-223[e] 1	30-289-132-3, 50[f] 3	30-289-132-4, 27[f] 4	17-165A-24-1, 117-121[g] W	17-165A-24-1, 117-121[g] X	17-165A-26-2, 80-84[g] Y	17-165A-27-2, 60-65[g] Z
SiO_2	46.99	46.68	46.29	49.30	50.80	46.16	45.91	44.29	43.49
Al_2O_3	15.45	13.99	14.18	15.00	15.30	14.15	13.64	14.15	14.27
"FeO"[c]	12.78	12.85	12.87	12.30	11.50	10.76	11.10	12.97	13.03
MgO	7.17	9.43	9.37	7.00	6.80	5.63	5.92	6.71	6.28
CaO	11.03	10.77	10.81	11.80	10.90	9.68	11.27	8.46	9.44
Na_2O	2.85	2.70	2.69	2.20	2.40	3.91	3.98	3.75	4.68
K_2O	0.93	0.87	0.97	0.46	0.35	2.68	2.00	2.56	1.87
TiO_2	2.34	2.26	2.36	1.50	1.60	5.12	4.77	5.11	5.10
P_2O_5	0.31	0.29	0.29	0.12	0.14	1.26	0.92	1.46	1.34
MnO	0.16	0.16	0.17	0.19	0.14	0.33	0.38	0.26	0.23
S						0.36	0.06	0.30	0.27
Cr_2O_3									
NiO									
Total	100.01	100.00	100.00	99.87	99.93	100.04	99.95	100.02	100.00
Q									
C									
Or	5.495	5.141	5.732	2.722	2.070	15.831	11.824	15.125	11.050
Ab	17.641	15.855	14.159	18.640	20.322	15.863	12.072	14.636	11.789
An	26.614	23.484	23.752	29.734	29.962	13.138	13.453	14.213	12.407
Lc									
Ne	3.507	3.788	4.660			9.323	11.713	9.258	15.066
Wo	10.887	11.713	11.684	11.732	9.702	11.122	15.229	7.604	10.718
En	5.091	6.123	6.105	10.569	14.923	5.983	7.855	3.879	5.299
Fs	5.674	5.256	5.246	12.406	16.510	4.769	6.974	3.539	5.210
Fo	8.944	12.167	12.075	4.826	1.418	5.629	4.833	8.990	7.247
Fa	10.986	11.512	11.435	6.243	1.729	4.945	4.729	9.038	7.853
Cs									
Cm									
Il	4.444	4.292	4.482	2.853	3.041	9.720	9.064	9.703	9.686
Tn									
Ru									
Ap	0.734	0.687	0.687	0.285	0.332	2.983	2.180	3.457	3.174
Pr						0.673	0.112	0.561	0.505
Total	100.018	100.017	100.017	100.008	100.009	99.979	100.037	100.004	100.005

[e]Analyses from Macdonald (1968); Hualalai volcano, Hawaii.

[f]Analyses from Stoeser (in press).

[g]Analyses from Bass et al. (1973).

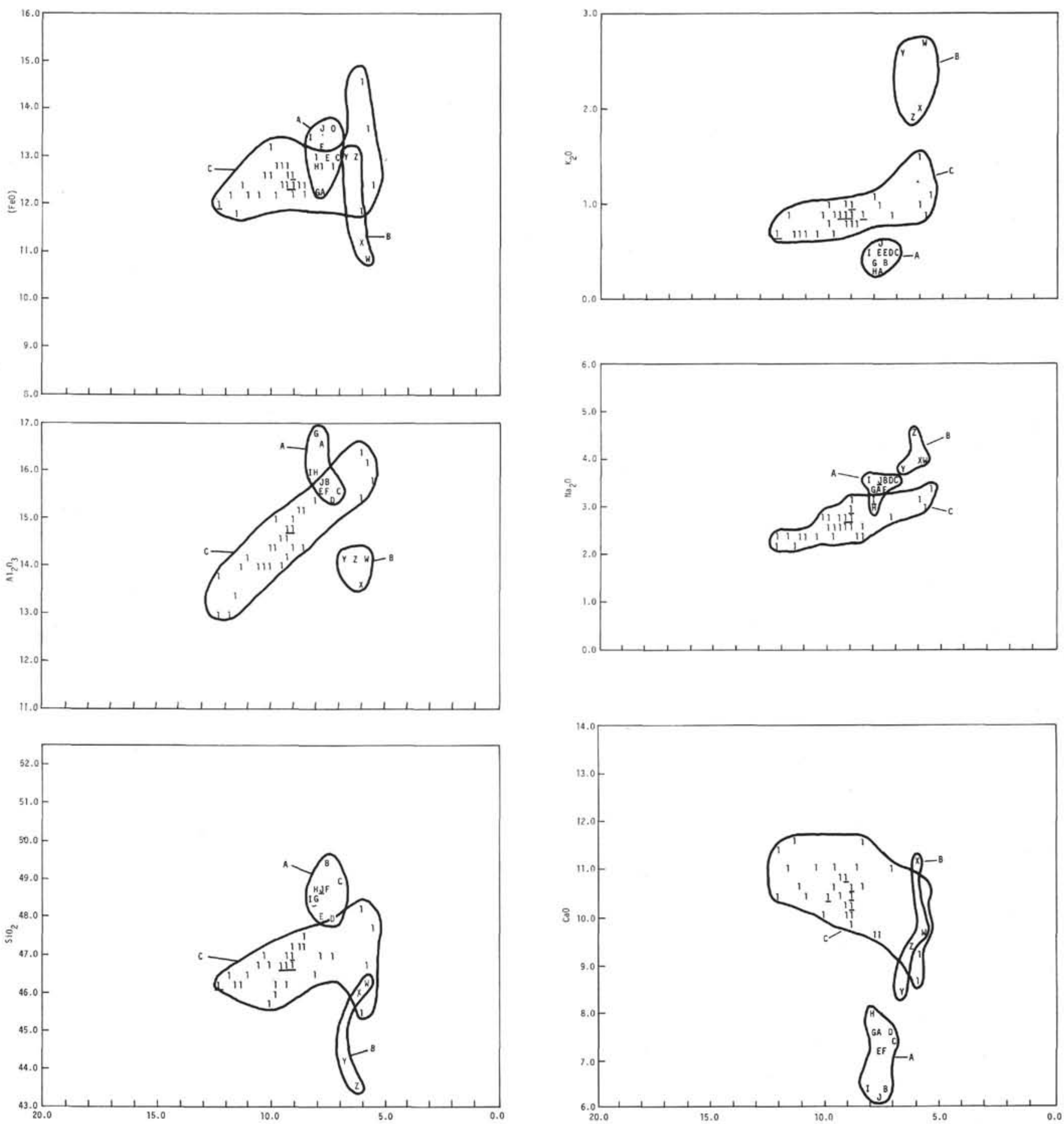

Figure 15. *MgO variation diagrams for dry, reduced oxides of basalts from Leg 33 (Hole 315A) compared with basalts from Leg 17 (Hole 165A) and the Hualalai volcanic series from Hawaii. (A 315A from Table 13, this report; B (Hole 165A) calculated from Bass et al., 1973 Table 17, this report; and C (Hualalai basalts) calculated from Macdonald, 1968 (GAM), and unpublished analyses of E. D. Jackson (EDJ) and T. L. Wright (TLW) from Table 17, this report.) Underlined symbols indicate more than one sample plotted at that point.*

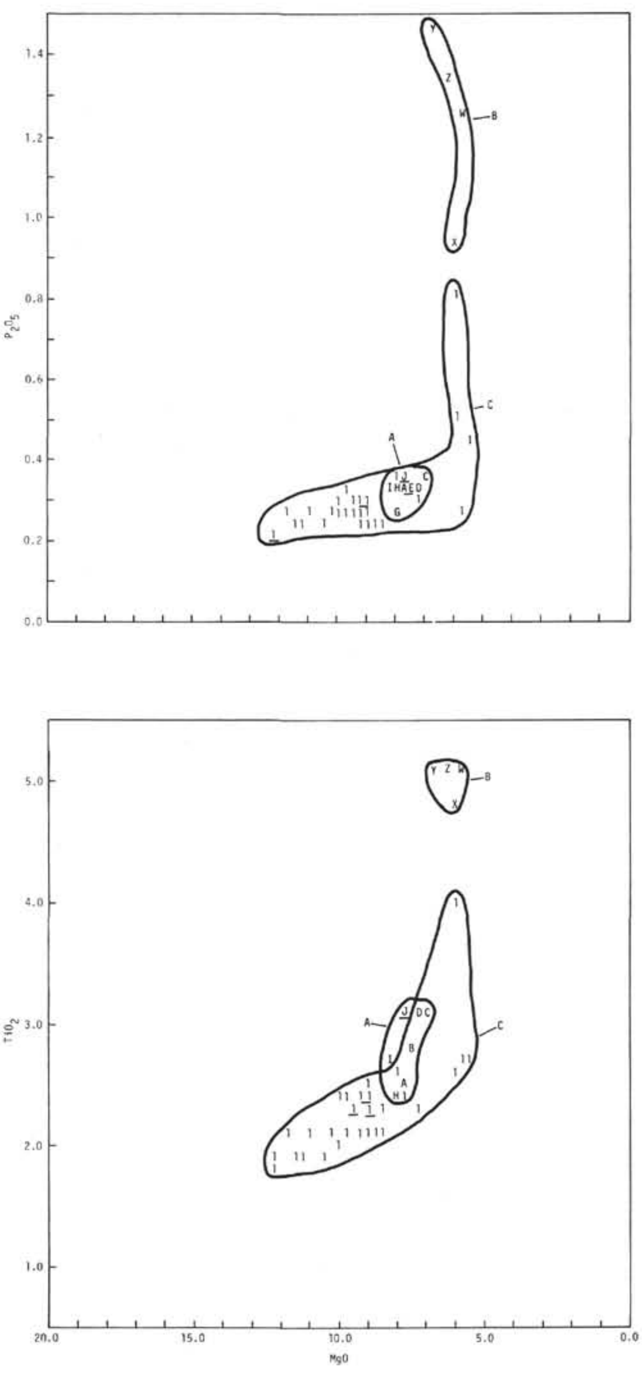

Figure 15. *(Continued)*

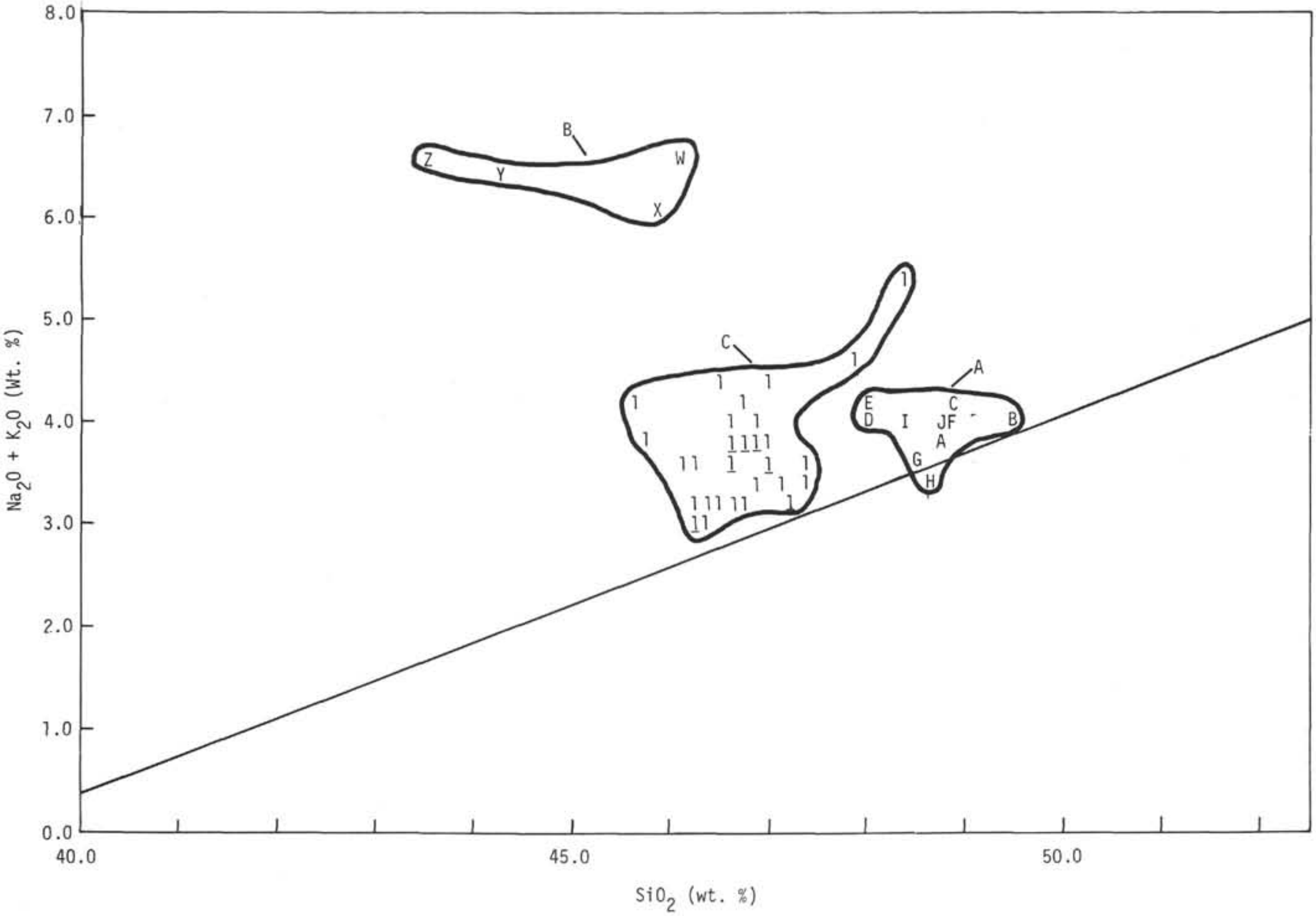

Figure 16. *Alkali:silica diagram (after Macdonald and Katsura, 1964) comparing Leg 33 (Hole 315A) basalts with basalts from Leg 17 (Hole 165A) and Hualalai volcano, Hawaii. (Underlined symbols and references same as in Figure 15.)*

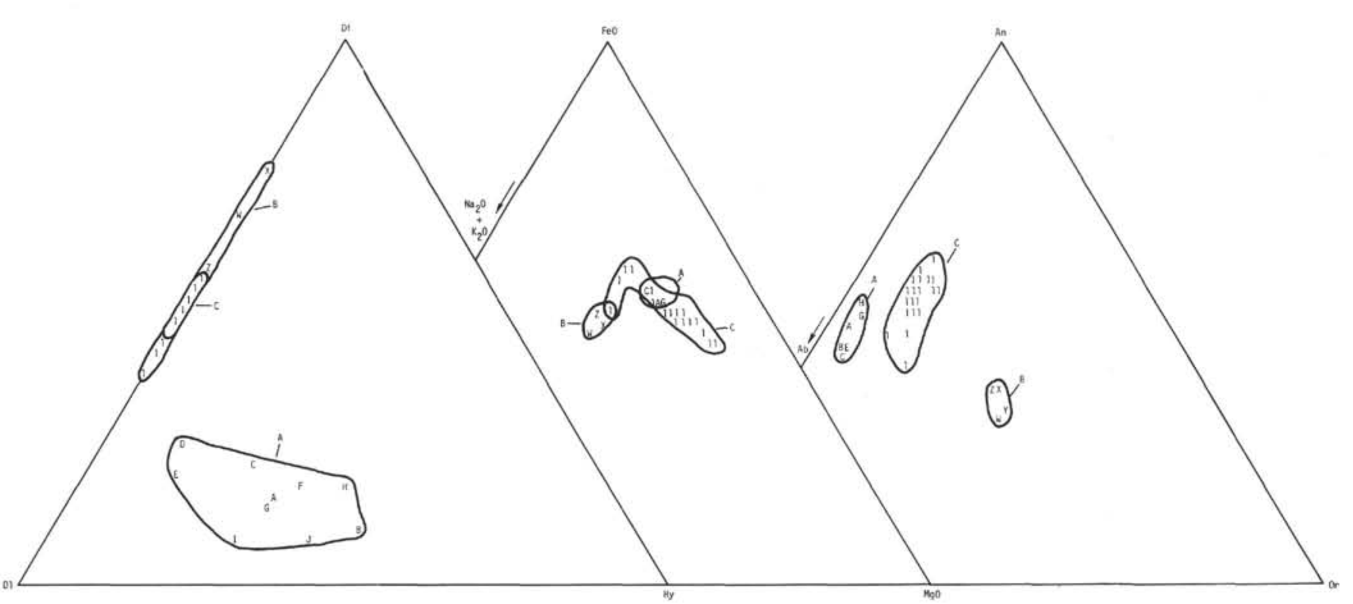

Figure 17. *A-F-M, DI-OL-HY, and An-Ab-Or ternary diagrams (after Irvine and Baragar, 1971) comparing Leg 33 (Hole 315A) basalts from Leg 17 (Hole 165A) and the Hualalai volcanic series. (Underlined symbols and references same as in Figure 15.)*

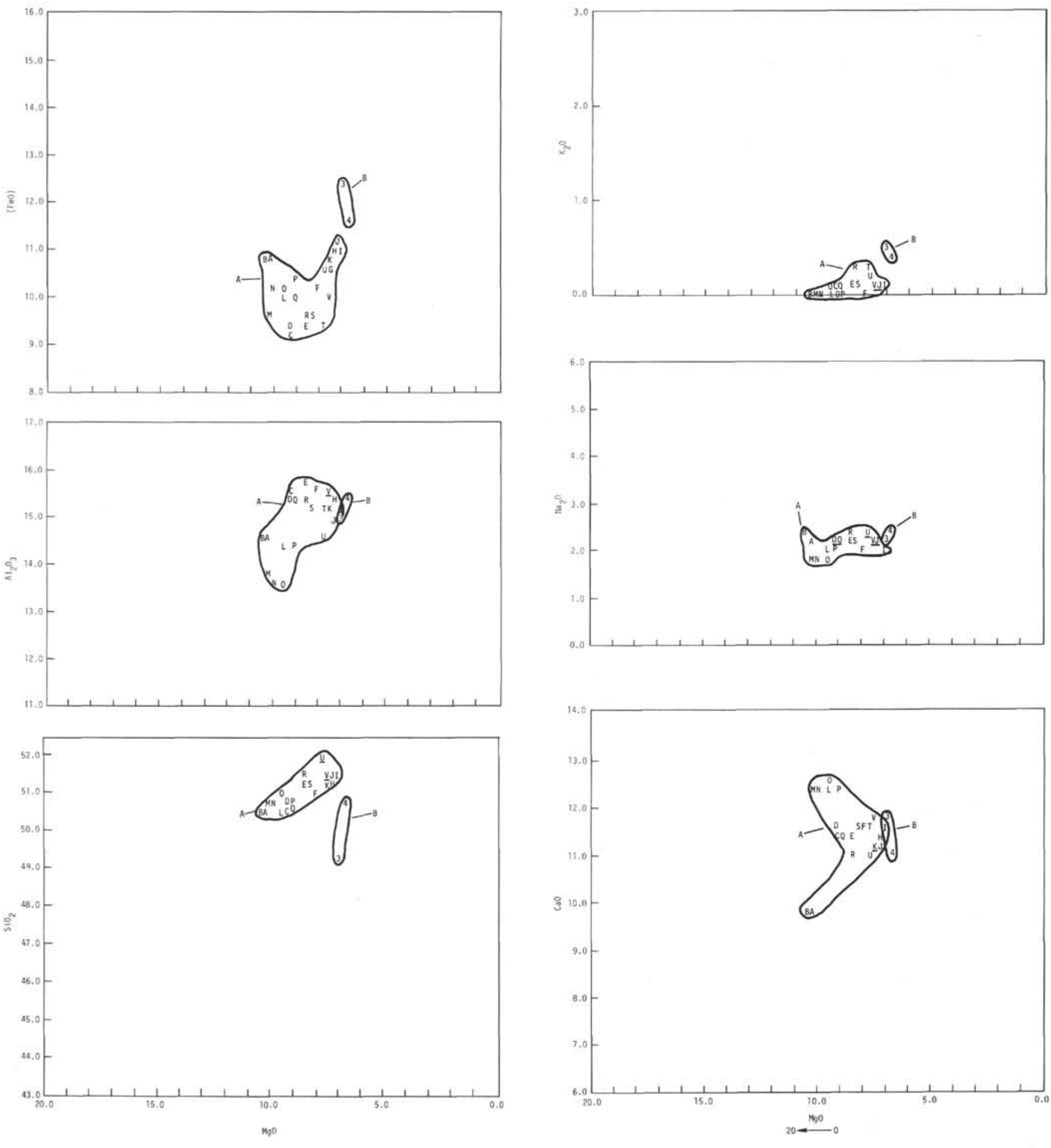

Figure 18. *MgO variation diagrams for dry, reduced oxides of basalts from Leg 33 (Hole 317A) compared with Leg 30 (Hole 289) basalts. (A 317A from Table 14, this report; B calculated from Stoeser (in press) for Table 17, this report.) Note that point E which represents Flow Unit 5A is nearly identical in all elements with analyses F-K of Flow Unit 5B. Similarly points L-N which represent Flow Unit 6A group with points O-Q of Flow Unit 6B. Again points R of Flow Unit 7A and S of Flow Unit 7B fall together. This suggests the petrographic grouping of these flow units is supported by bulk chemical data. Underlined symbols indicate that more than one sample plotted at that point.*

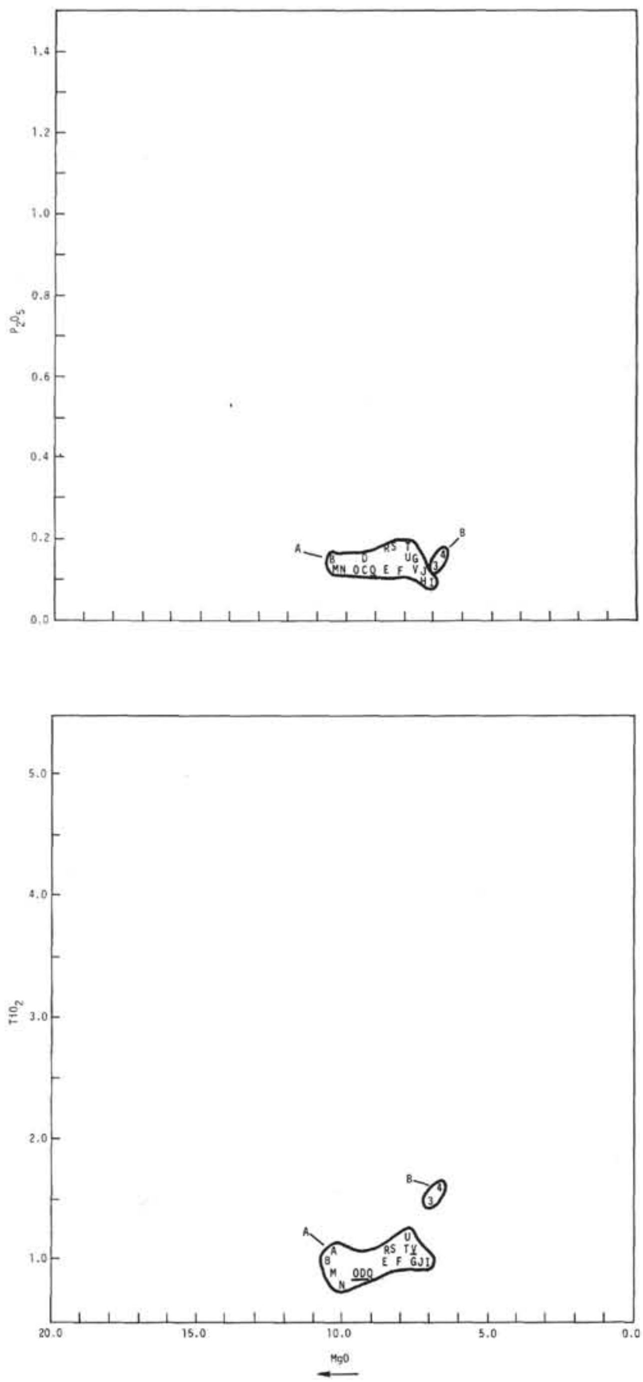

Figure 18. *(Continued)*

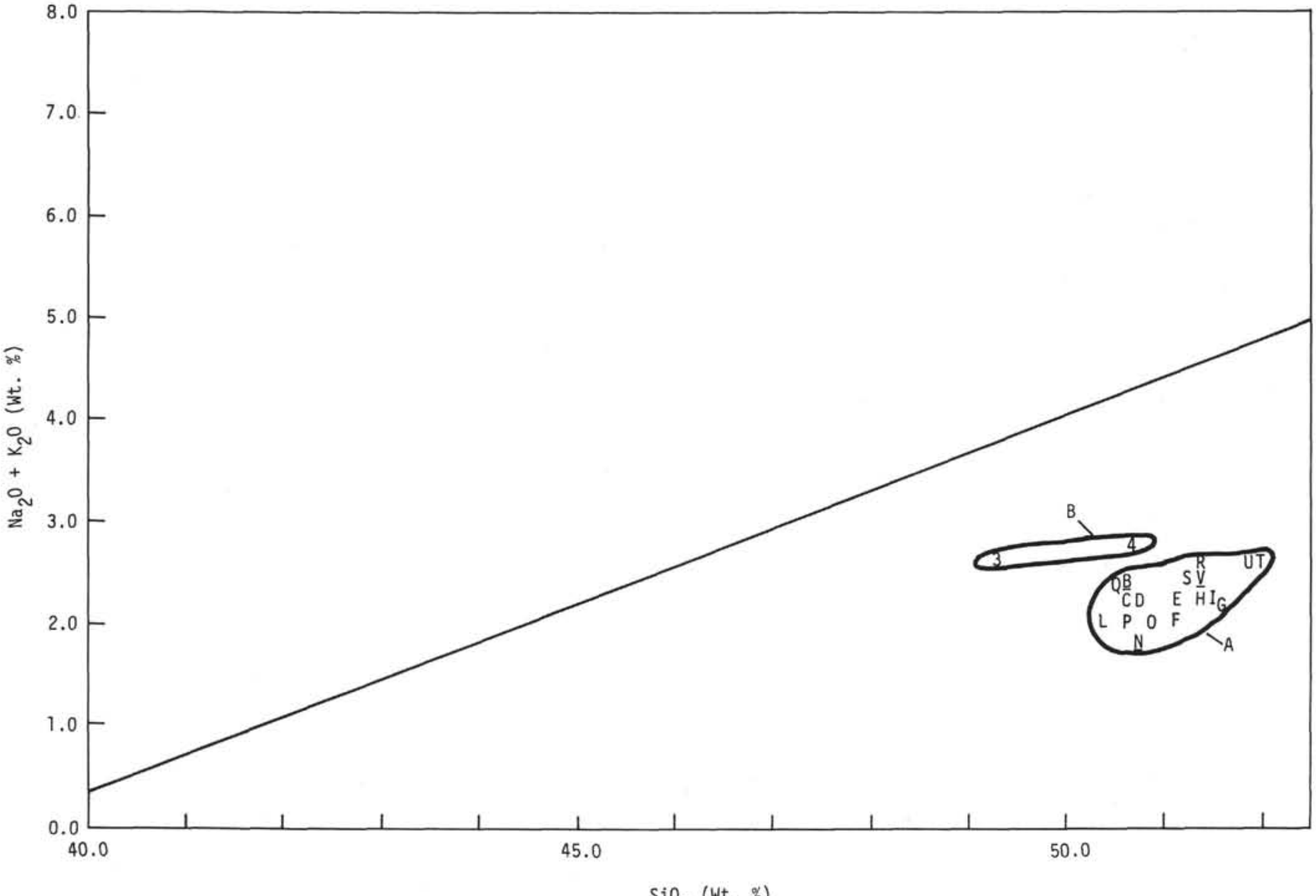

Figure 19. *Alkali:silica diagram (after Macdonald and Katsura, 1964) comparing Leg 33 (Hole 317A) basalts with basalts from Leg 30 (Hole 389). (Underlined symbols and references same as in Figure 18.)*

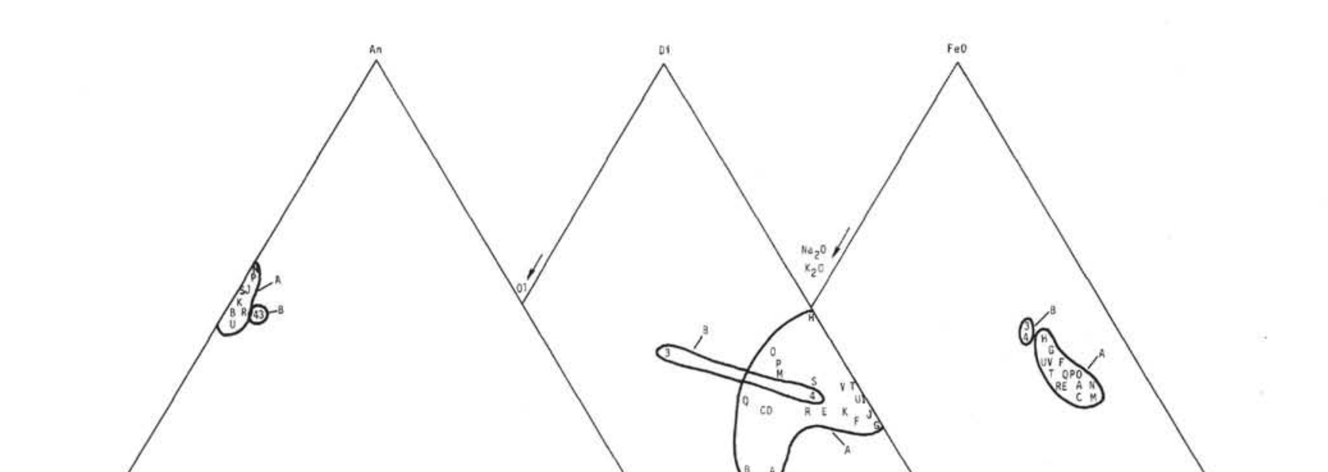

Figure 20. *A-F-M, DI-OL-HY, and An-Ab-Or ternary diagrams (after Irvine and Baragar, 1971) comparing Leg 33 (Hole 317A) basalts with basalts from Leg 30 (Hole 389). (Underlined symbols and references same as in Figure 18.)*

PLATE 1

Photomicrographs of Sample 315A-32-2, 105-106 cm, a finer grained variant of Flow Unit 2.

Figure 1 — Notch in section is up core, and section is cut in the vertical plane of the core. Crossed nicols. Vertical dimension is 11 mm. White laths are plagioclase, rounded, darker gray areas are vesicles filled with green montmorillonite. Lighter gray areas between plagioclase are augite. Slight alinement of plagioclases perpendicular to core axis is evident, but must less well developed than in other samples. Texture diabasic.

Figure 2 — Section cut in horizontal plane of core. Vertical dimension is 8.3 mm, plane light. Darkest areas are filled vesicles. Centers of plagioclase grains are altered to brown montmorillonite.

Figure 3 — Same as 2; crossed nicols.

PLATE 1

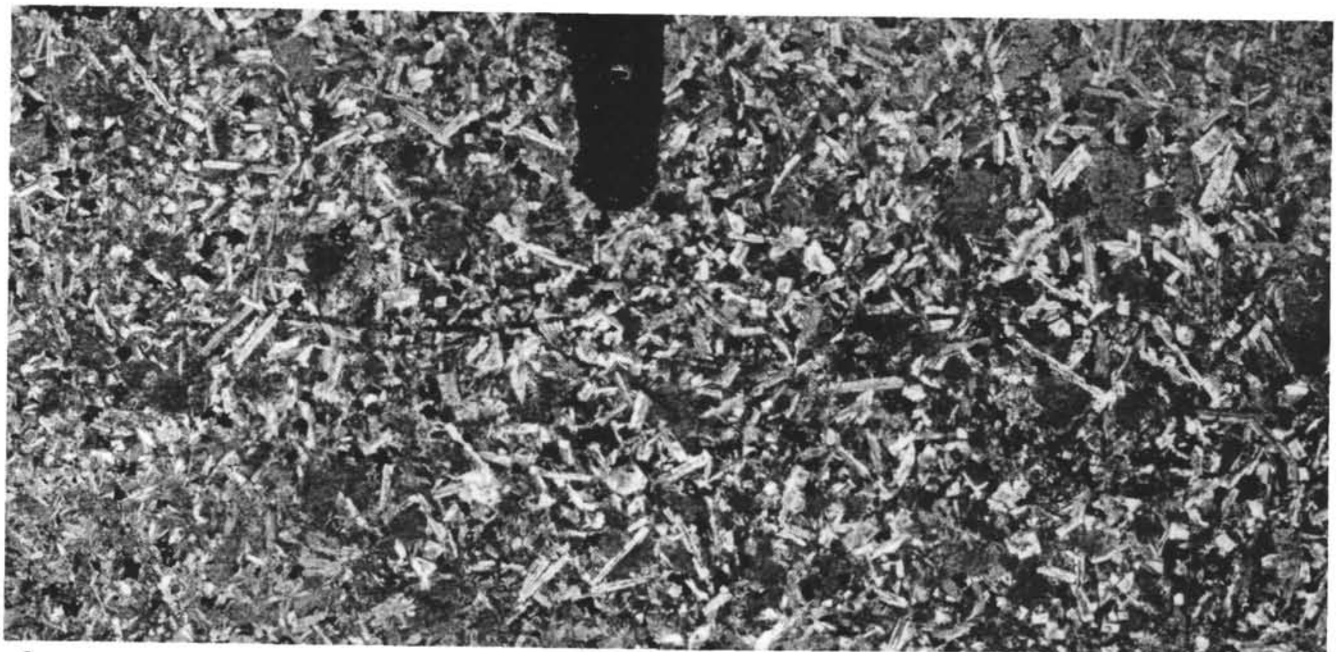

1

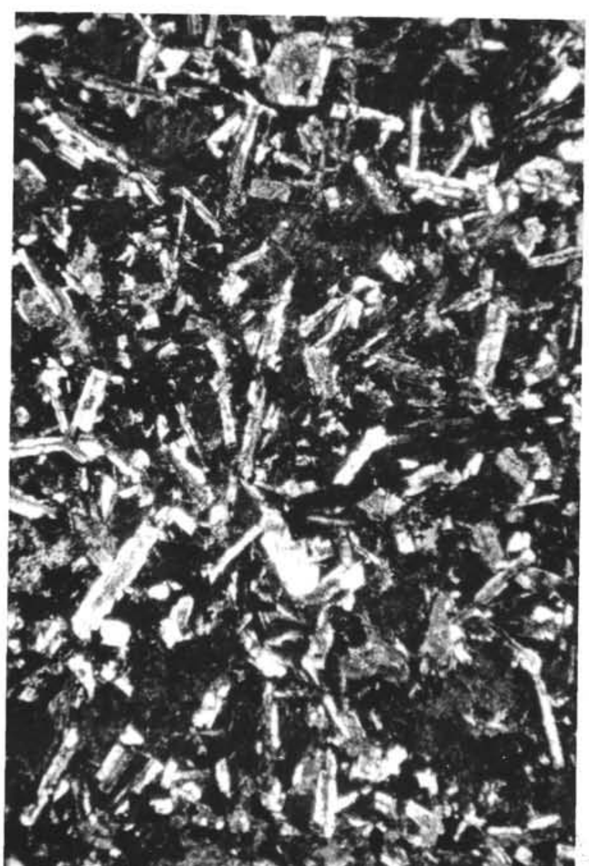

2

3

PLATE 2

Photomicrographs of samples from Hole 317A

Figure 1	Sample 317A-32-3, 96-97.8 cm. Area of slide 15 × 15 mm. Plane light. Section cut in the vertical plane of the core. Three vesicles are present, one at lower-right edge, filled with green montmorillonite. One in center and one in upper-right rimmed by brown montmorillonite. Intermediate gray areas are microphenocrysts of augite and pigeonite. Texture is diabasic to intersertal. Flow Unit 5B.
Figure 2	Same as 1, crossed nicols.
Figure 3	Same sample as 1 and 2. Area of slide is 2.3 × 2.3 mm. Plane light. Former groundmass glass in wedge-shaped interstices is altered to brown montmorillonite.
Figure 4	Same as 3, crossed nicols.
Figure 5	Sample 317A-34-4, 62-64 cm. Area of slide is 5.6 × 5.6 mm. Plane light. Glomeroporphyritic clots of pyroxene and plagioclase in a vitrophyric groundmass. Flow Unit 10.
Figure 6	Same as 5, crossed nicols.

PLATE 2

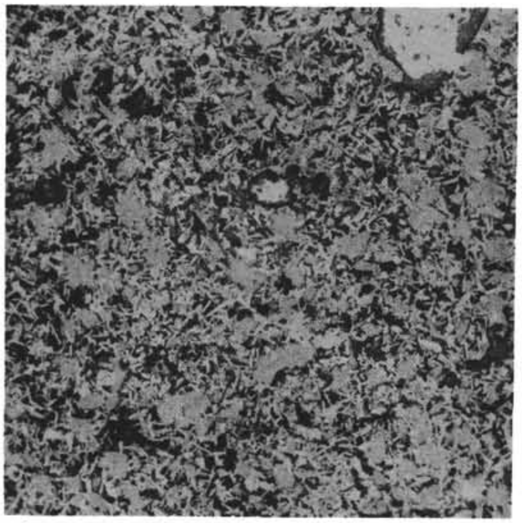

1

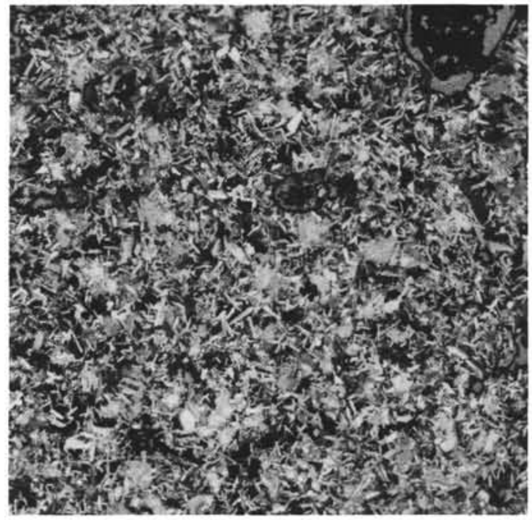

2

3

4

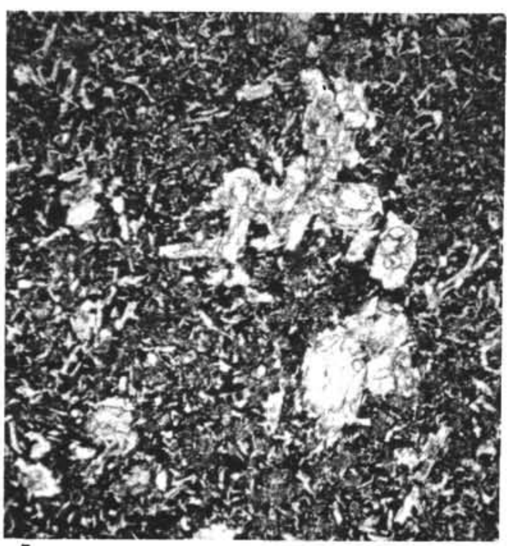

5

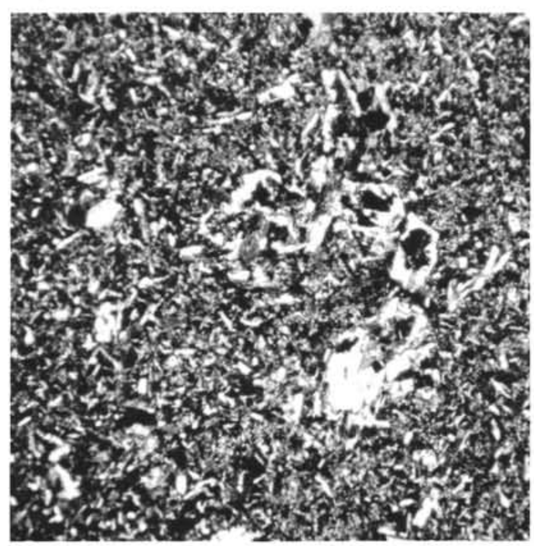

6

PLATE 3

Photographs and photomicrographs of rocks from Hole 317A.

Figure 1	Photograph of vesicles in Sample 317A-34-3, 75-79 cm. Scale is 1 cm. Vesicles range in size up to 20 mm, although they average 5-6 mm. They also form up to 30% of the rock. Vesicles in this sample are filled with heulandite. Flow Unit 10.
Figure 2	Another view of the same sample.
Figure 3	Photomicrograph of Sample 317A-34-3, 115-117 cm. Horizontal dimension of slide is 20 mm. Section cut in vertical plane of the core; notch marks up. Plane light. vesicles largely open, some have thin rims of green montmorillonite.
Figure 4	Same as 3; crossed nicols.

PLATE 3

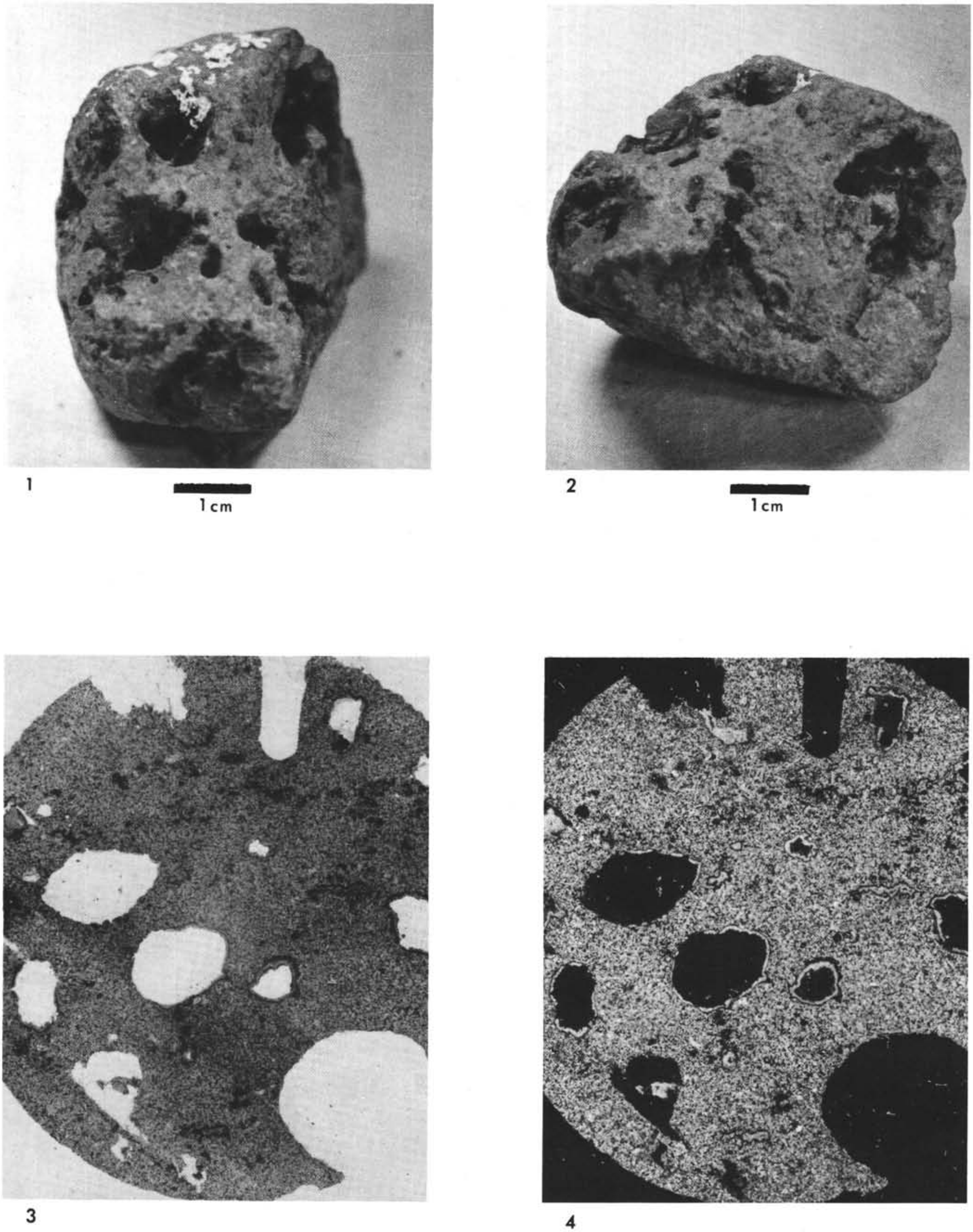

TABLE 3
Petrographic Data for Sampled Basalts of Hole 315A

Sample (Interval in cm)	Phenocrysts and Microphenocrysts[a]			Vesicles[a]			Groundmass[a]			Alteration	Other Work[b]	Remarks
	Mineral	Percent	Average Size (mm)	Percent	Size Range	Average Size (mm)	Percent	Average Size (mm)	Dominant Texture			
30-2, 141.5-143.5 (Flow Unit 1A)	Plagioclase Augite Olivine	27.5 10.0 <1	0.4 × 1.5 0.5 0.5	1.5	0.1-1.0	0.5	61.0	<0.2	Variolitic	Heavily altered variolitic basalt; plagioclase 15-20% altered to montmorillonite; augite (probably once ~ 30% of rock) almost entirely altered to green montmorillonite; <1% 0.5mm grains of iddingsite suggest the former presence of very minor amounts of olivine; groundmass appears to have been glass, now entirely altered to brown montmorillonite; vesicles partly to wholly filled; these have green montmorillonite rims and calcite interiors; stained sections and X-ray data show no nepheline or K-feldspar	Sts (N) Sts (K) X (w.r.) X (v.f.)	Abundant (2-3%) tiny (0.05 mm) euhedral magnetite grains present as inclusions in plagioclase microphenocrysts and along their boundaries
31-1, 113-115 (Flow Unit 1B)	Plagioclase Augite Olivine	34.0 12.5 <1	1.0 × 3.0 1.0	2.5	0.1-1.0	0.5	61.0	<0.2	Variolitic	A coarser and slightly fresher variant of 30-2, 141.5-143.5 augite, and shapes are better preserved; distribution of ilmenite microlites suggests rock consisted of ~ 10% glass now completely altered; X-ray shows minor amounts of pyrite and anatase	Sts (N) Sts (K) X (w.r.)	Same magnetite distribution as above, but magnetites are coarser – up to 0.25mm
31-1, 115.5-117.5 (Flow Unit 1B)	Identical to 31-1, 113-115								Variolitic		C.A. X (w.r.) X (v.f.) pts	Polished section shows no chromite; euhedral and skeletal magnetite without ilmenite intergrowths occurs; elongate skeletal ilmenite partly altered to anatase, a very small amount of chalcopyrite scattered through the rock
31, CC (Flow Unit 1B)	Plagioclase Augite Olivine	27.0 10.0 <1	0.4 × 1.5 0.5	2.0	0.1-0.5	0.4	61.0	<0.2	Variolitic	Same as 30-2, 141.5-143.5 but lacks altered olivine in available sections	Sts (N) Sts (K) X (w.r.) X (v.f.)	Appears identical to 30-2, 141.5-143.5; considerably finer grained than 1, 113-115 and 115.5-117.5
32-1, 139-141 (Flow Unit 2)	Aphyric	–	–	3.5	1.0-2.0	1.5	96.5	<0.05	Vitrophyric	Moderately altered vitrophyric basalt, plagioclase in small random laths somewhat altered to montmorillonite; augite is stellate; also somewhat altered to montmorillonite; formerly very fine grained and glassy areas completely altered to brown and green montmorillonite which also partially fills vesicles; magnetite euhedra and ilmenite skeletal laths abundant; no calcite present; stained sections and X-ray data show no nepheline or K-feldspar	Sts (N) Sts (K) X (w.r.) X (v.f.)	
32-1, 141.5-143.5 (Flow Unit 2)	Same as 32-1, 139-141									Somewhat fresher than 32-1, 139-141	C.A. X (w.r.) X (v.f.) pts	In reflected light "magnetite" skeletal crystals and euhedra are magnetite-ilmenite intergrowths; ilmenite skeletal laths are also present
32-2, 79.5-80 (Flow Unit 2)	Included in description of 32-2, 80-82										pts	In reflected light "magnetites" are complex magnetite-ilmenite intergrowths; bladed homogeneous ilmenite also occurs; scattered rounded grains of chalcopyrite and veins of pyrite occur throughout the rock

32-2, 80-81 (Flow Unit 2)	Included in description of 32-2, 80-82										K/A (w.r.)	
32-2, 80-82 (Flow Unit 2)	Plagioclase Augite	38.5 8.5	0.4 × 1.0 0.5 × 2.0	5.5	0.5-2.5	1.5	47.5	<0.5	Diabasic-trachytic	Moderately altered diabasic basalt; plagioclase in stubby laths that tend to be oriented parallel to core; centers of some laths show montmorillonite alteration; a few augites occur as microphenocrysts, remainder diabasically enclose plagioclase; groundmass pyroxene moderately altered; very fine patches of groundmass pyroxene moderately altered; very fine patches of groundmass marked by feldspar and ilmenite microlites completely altered to brown montmorillonite; some vesicles filled by green montmorillonite; others filled with calcite	Sts (N) Sts (K) X (w.r.) X (v.f.)	Magnetite scattered quite evenly through rock
32-2, 82.5-83.5 (Flow Unit 2)	Plagioclase Augite	20.5 7.0	0.4 × 1.0 0.5 × 2.0	5.0	0.5-3.0	1.5	67.5	<0.5	Diabasic-trachytic	Identical to 32-2, 80-82. Calcite detected in X-ray; not seen in thin sections	C.A. pts Sts(N) Sts (K) X (w.r.) X (v.f.)	In reflected light, same as 32-2, 79.5-80 except magnetite is pinker and shows less tendency to exolve ilmenite
32-2, 83.5-91 (Flow Unit 2)										X-ray identical to 33-2, 82.5-83.5	K/A (pc) X (w.r.) X (v.f.)	
32-2, 95-96 (Flow Unit 2)	Same as 32-2, 82.5-83.5									Same as 32-2, 82.5-83.5 except that pyrite grains as large as 1 mm occur as vesicle fillings inside montmorillonite rims	Sts (N) Sts (K) X (w.r.) X (v.f.)	
32-2, 96-105 (Flow Unit 2)										X-ray identical to 33-2, 80-82 and 95-96	C.A. X (w.r.) X (v.f.)	
32-2, 105-106 (near base of Flow Unit 2)	Aphyric			5.5	0.5-3.0	1.5	74.5	<0.5	Diabasic-trachytic	Identical in mineral proportions, texture, and alteration to 32-1, 139-141; finer grained but otherwise identical to section from 32-2, 79.5-82, 82.5-83.5, and 95-96	pts	In reflected light similar to 32-1, 141.5-143.5 except that pyrite is more abundant, especially as vesicle fillings
32-3, 7-9 (Flow Unit 3)	Aphyric			8.5	1.0-4.0	2.0	91.5	<0.5	Diabasic	Moderately to heavily altered aphyric diabasic basalt; plagioclases stubby, slightly altered to montmorillonite in central parts; interstitial augite about half altered to montmorillonite; rock is even-grained and appears to have contained little glass; magnetite tends to occur in interstices between plagioclase grains; ilmenite is concentrated in pyroxene; vesicles are completely filled with montmorillonite; pyrite is locally abundant, replacing central parts of vesicles; stained sections and X-rays show no nepheline or K-feldspar	Sts (N) Sts (K) X (w.r.) X (v.f.)	
32-3, 9.5-11.5 (Flow Unit 3)	Same as 32-3, 7-9									Same as 32-3, 7-9	C.A. X (w.r.) X (v.f.) pts	"Magnetite" occurs as magnetite-ilmenite intergrowths in euhedral to skeletal cyrstals; ilmenite in laths, mostly in pyroxene; chalcopyrite in tiny rounded grains throughout the rock; pyrite is abundant in grains as large as 1mm in vesicles; in some cases it is rimmed by platelets of hematite

TABLE 3 – *Continued*

Sample (Interval in cm)	Pehnocrysts and Microphenocrysts[a]			Vesicles[a]			Groundmass[a]			Alteration	Other Work[b]	Remarks
	Mineral	Percent	Average Size (mm)	Percent	Size Range	Average Size (mm)	Percent	Average Size (mm)	Dominant Texture			
32-3, 85-87 (Flow Unit 3)	Aphyric			9.5	0.5-3.0	1.0	90.5	<0.5	Diabasic	Appears identical in texture and alteration to 32-3, 7-9 except slightly more vuggy, slightly coarser grained, and calcite appears as a vesicle-filling mineral	Sts (N) Sts (K) X (w.r.) X (v.f.)	Marcasite identified in vesicle filling by X-ray diffraction
32-3, 87.5-89.5 (Flow Unit 3)	Same as 32-3, 85-87									Same as 32-3, 85-87	C.A. X (w.r.) X (v.f.) pts	In reflected light is much like 32-3, 9.5-11.5 except contains much less pyrite as a vug filling material
32-4, 53-55 (Flow Unit 4)	Aphyric			9.0	0.2-2.0	0.8	91.0	<0.5	Diabasic-intersertal	Moderately altered diabasic-intersertal baslat; plagioclases stubby, little altered; augites diabasic, partially altered to montmorillonite; magnetite interstitial to plagioclase laths; ilmenite not abundant, concentrated in patchy areas that appear to have been glassy; all glassy material altered to brown montmorillonite; vesicles completely filled with green and brown montmorillonite; no calcite observed, but some pyrite occurs as vesicle fillings; no nepheline or K-feldspar present	K/A (w.r.) pts X (w.r.) X (v.f.)	In reflected light magnetite is pinkish, and does not exsolve ilmenite, but is intergrown with unusual amounts of ulvospinel; ilmenite occurs as sparse laths, chalcopyrite is present as minor blebs; pyrite is present as sparse veins and occurs in one vesicle
32-4, 56-58 (Flow Unit 4)	Same as 32-4, 53-55									Same as 32-4. 53-55, but somewhat fewer formerly glassy areas and fresher	Sts (N) Sts (K) X (w.r.) X (v.f.)	
32-4, 59-61 (Flow Unit 4)	Same as 32-4, 53-55									Same as 32-4, 56-58, but contains more calcite	C.A. X (w.r.) X (v.f.) pts	In reflected light same as 32-4, 53-55, but contains more chalcopyrite and pyrite
32-4, 149-150 (Flow Unit 4)	Same as 32-4, 56-58									Same as 32-4. 59-61	Sts (N) Sts (K)	
33-1, 116.5-118.5 (Flow Unit 5A)	Same as 33-1, 121-123 below										C.A. X (w.r.) X (v.f.) pts	In reflected light very tiny (0.01) mm octahedra of magnetite exsolving ulvospinel; some tiny laths of ilmenite; very minor amounts of sulfides seen in sections
33-1, 121-123 (Flow Unit 5A)	Aphyric			2.0	0.1-1.0	0.5	98.0	<0.2	Vitrophyric	Heavily altered vitrophyric basalt; plagioclase in tiny (0.05 × 0.5 mm) laths, unaltered; augite present in very small amounts and almost completely altered to montmorillonite; opaque oxides very tiny and scattered throughout the rock; apparently the rock consisted of nearly 40% glass is now completely altered to montmorillonite; no nepheline or K-feldspar present; all vesicles were filled with calcite	Sts (N) Sts (K) X (w.r.) X (v.f.)	
33, CC (Flow Unit 5A)	Same as 33-1, 121-123									Much like 33-1, 121-123, but slightly coarser; plagioclase laths average 0.4 × 0.6 mm and augite is present as 0.4 × 0.8 laths and stubby crystals; pyroxene is less altered than 121-123	Sts (N) Sts (K) X (w.r.) X (v.f.)	

34-1, 71-73 (Flow Unit 6)	Aphyric to microphenocrysts of plagioclase and augite		7.5	0.2-1.0	0.5	92.5	<0.5	Intersertal-diabasic	Moderately altered intersertal-diabasic basalt; plagioclases seriate from 0.05 × 0.5 mm to 0.5 × 3 mm; slightly altered to montmorillonite in centers; augite is mostly diabasically enclosing the plagioclase, partly as stubby 0.3 mm crystals almost completely altered to montmorillonite; perhaps 20% of rock was glassy, intersertal; now is completely altered; opaques are scattered rather evenly through the rock; vesicles completely filled with montmorillonite and calcite; no nepheline or K-feldspar is observed	Sts (N) Sts (K) X (w.r.) X (v.f.)	
34-1, 173.5-75.5 (Flow Unit 6)	Same as 34-1, 71-73									C.A. X (w.r.) X (v.f.) pts	In reflected light magnetite exsolves ulvospinel, ilmenite laths are localized in formerly glassy areas; chalcopyrite is present but not abundant
34-1, 99-101 (Flow Unit 6)	Same as 34-1, 71-73								Same as 31-1, 71-73 and 73.5-75.5 except more calcite is present as veins and pyrite occurs as a vesicle-filling material	K/A (w.r.) pts Sts (N) Sts (K) X (w.r.) X (v.f.)	Same as 34-1, 73.5-75.5 except some anatase present as alteration of ilmenite; X-ray determination of plagioclase: 68.6
34, CC (Flow Unit 6)	Aphyric		7.5	0.2-9.0	0.5	92.5	<0.2	Vitrophyric	Plagioclases are very fine-grained (0.01-0.5 mm) appear unaltered; no pyroxene remains in section; original material appears to have been largely glass, is now completely altered to montmorillonite; vesicles now appear to be completely filled by calcite	Sts (N) Sts (K) X (w.r.)	

[a]Average points counted 300; percentages rounded to nearest 0.5%.

[b]Sts (N) = section stained for nepheline and melilite;
Sts (K) = section stained for potassic feldspar;
X (v.f.) = vesicle filling X-ray diffraction pattern;
X (w.r.) = whole rock X-ray diffraction pattern;
C.A. = chemical analysis;
pts = polished thin section;
K/A(w.r.) = potassium argon whole-rock (minimum) age;
K/A (p.c.) = potassium argon age on separated plagioclase.

TABLE 4
Petrographic Data for Sampled Basalts of Hole 317A

Sample (Interval in cm)	Phenocrysts and Microphenocrysts[a]			Vesicles[a]			Groundmass[a]			Alteration	Other Work[b]	Remarks
	Mineral	Percent	Average Size (mm)	Percent	Size Range	Average Size (mm)	Percent	Average Size (mm)	Dominant Texture			
31-1, 141-143 (Flow Unit 1)	Plagioclase Augite	1.0 1.5	0.4 × 1.0 0.6	24.5	0.5-10.0	2.0	73.0	<0.1	Diabasic-intersertal	Moderately altered basalt; plagioclase microphenocrysts almost entirely altered to montmorillonite, groundmass plagioclase partly altered; augite microphenocrysts fresh, groundmass pyroxene consists of augite and Ca-poor augite slightly altered to montmorillonite; part of the groundmass appears to have been glassy, intersertal, but now is completely altered to brown montmorillonite; vesicles are partially to completely filled with green montmorillonite; no nepheline or K-feldspar observed	Sts (N) Sts (K) X (w.r.) X (v.f.)	
31-1, 144-146 (Flow Unit 1)	Same as 31-1, 141-143										pts C.A. X (w.r.) X (v.f.)	In reflected light tiny skeletal magnetites scattered evenly through rock; some apparently altered by an opaque nonreflective material; ilmenite laths present but not abundant; chalcopyrite present as tiny spheres and veinlets, in some cases intergrown with pyrrhotite
31-2, 34-36 (Flow Unit 2)	Augite	6.5	0.5	29.5	0.5-10.0	2.5	64.0	<0.1	Diabasic	Heavily altered basalt; only the pyroxene microphenocrysts escape rather extensive montmorillonite alteration; no plagioclase microphenocrysts; part of the groundmass plagioclase and most of the groundmass pyroxene is altered; vesicles filled with green montmorillonite; no nepheline or K-feldspar	Sts (N) Sts (K) X (w.r.) X (v.f.)	Very similar to 31-1, 141-143 except for increased microphenocryst content and somewhat greater degree of alteration of rock
31-2, 37-39 (Flow Unit 2)	Augite	6.0	0.5	30.0	0.5-10.0	3.0	64.0	<0.1	Diabasic	Moderately altered basalt; most of the groundmass plagioclase is fresh; pyroxene microphenocrysts are unaltered; groundmass pyroxene consisted of augite and Ca-poor augite and is partially altered to montmorillonite; vesicles as in 31-2, 34-36; contained less glass than 31-1, 141-143	pts C.A. X (w.r.) X (v.f.)	Very similar to 31-1, 141-143 except that the microphenocryst count remains high like 31-2, 34-36, but rock is much fresher; in reflected light is similar to 31-1, 144-146, but several grains of red-brown chromite observed
31-3, 24-26 (Flow Unit 3)	Augite	11.5	0.7	5.0	0.3-1.5	0.5	83.5	<0.3	Intersertal	Somewhat altered basalt; augite microphenocrysts fresh; groundmass pyroxene consists of augite and Ca-poor augite largely unaltered; groundmass plagioclase appears fresh, but all former intersertal glass in groundmass has been altered to brown montmorillonite; vugs less abundant than Flow Units 1 and 2, lined with dark brown montmorillonite, and partially filled with green montmorillonite; a few round vesicles are filled only with calcite; no nepheline or K-feldspar present	Sts (N) Sts (K) X (w.r.) X (v.f.)	
31-3, 27-29 (Flow Unit 3)	Same as 31-3, 24-26										pts C.A. X (w.r.) X (v.f.)	In reflected light magnetite is scattered evenly through the rock some apparently altered by an opaque nonreflective material; ilmenite is sparse and occurs as rare laths; chalcopyrite occurs as tiny blebs and lines some vesicle walls; some is intergrown with pyrrhotite

31-3, 98-100 (Flow Unit 4)	Augite	4.5	1.0	12.0	0.2-1.0	0.3	83.5	<0.2	Diabasic-intersertal	Somewhat altered basalt; augite phenocrysts fresh; groundmass pyroxene consists of augite and Ca-poor augite largely unaltered; groundmass plagioclase are fresh; rock contained less intersertal glass than 31-3, 24-26, but it is altered to brown montmorillonite; vugs are smaller, but more abundant than in the above sample, but partially filled in the same manner by green montmorillonite; calcite partially to completely fills vesicles; no nepheline or K-feldspar present	Sts (N) Sts (K) X (w.r.) X (v.f.)	
31-3, 101-103 (Flow Unit 4)	Same as 31-3, 98-100										pts C.A. X (w.r.) X (v.f.)	In reflected light magnetite is scattered evenly through rocks, apparently altered by an opaque, nonreflective material; ilmenite and chalcopyrite present but very sparse
31-4, 77-79 (Flow Unit 5A)	Aphyric			16.5	1.0-5.0	2.0	83.5	<0.4	Diabasic-intersertal	Somewhat altered basalt; groundmass pyroxene consists of augite and Ca-poor augite and is unaltered; groundmass plagioclase fresh; groundmass glass, where once present, is altered to brown montmorillonite; vugs are lined with brown montmorillonite and generally filled with green montmorillonite; some calcite is in the centers of vesicles; no nepheline or K-feldspar	Sts (N) Sts (K) X (w.r.) X (v.f.)	A small amount of quartz is present intersertally between plagioclase laths
31-4, 80-82 (Flow Unit 5A)											pts C.A. X (w.r.) X (v.f.)	In reflected light much like 31-3, 101-103, but considerably more chalcopyrite is present and a few red-brown chromites occur in the section; quartz identified from vesicle filling by X-ray, but not seen in thin section
31, CC (Flow Unit 5A)	Plagioclase Augite Ca-poor augite	1.5 6.5 2.0	0.6	9.0	0.6-4.0	1.25	81.0	<0.4	Diabasic-intersertal	Moderately altered basalt; pyroxene microphenocrysts unaltered; groundmass pyroxene consists of augite and Ca-poor augite unaltered; plagioclase is very sparsely altered to montmorillonite and groundmass glass is completely altered to brown montmorillonite; vesicles are filled with green montmorillonite and calcite	X (w.r.)	Identical to 31-4, 80-82, except for microphenocrysts
32-1, 81-83 (Flow Unit 5B)	Plagioclase Augite Ca-poor augite	1.5 3.5 1.0	0.5	18.5	1.0-8.0	2.0	75.5	<0.4	Diabasic-intersertal	Somewhat altered basalt; pyroxene phenocrysts fresh; groundmass pyroxene also unaltered; plagioclase laths fresh; groundmass formerly glass is completely altered to brown montmorillonite; vesicles and vugs have rims of brown montmorillonite; partially filled with green montmorillonite and calcite; no nepheline or K-feldspar	pts Sts (N) Sts (K) X (w.r.) X (v.f.) K/A (w.r.)	
32-1, 84-86 (Flow Unit 5B)	Same as 32-1, 81-83										pts C.A. X (w.r.) X (v.f.)	Magnetite is scattered evenly through the rock, and contains a few blebs of exsolved ilmenite, and is partly altered to an opaque, nonreflective material; ilmenite laths and chalcopyrite blebs present, but are not abundant; some chalcopyrite is intergrown with pyrrhotite

TABLE 4 – Continued

Sample (Interval in cm)	Phenocrysts and Microphenocrysts[a]			Vesicles[a]			Groundmass[a]			Alteration	Other Work[b]	Remarks
	Mineral	Percent	Average Size (mm)	Percent	Size Range	Average Size (mm)	Percent	Average Size (mm)	Dominant Texture			
32-2, 72-74 (Flow Unit 5B)	Augite Ca-poor augite	5.5 2.0	0.5	12.5	0.5-3.0	1.0	80.0	<0.4	Diabasic-intersertal	Same as 32-1, 81-83	Sts (N) Sts (K) X (w.r.) X (v.f.)	
32-2, 75-77 (Flow Unit 5B)	Same as 32-2, 72-74 except no calcite noted										pts C.A. X (w.r.) X (v.f.)	Same as 32-1, 84-86 except magnetite does not exsolve ilmenite, is less altered, and more ilmenite is present in the rock
32-3, 83.5-84 (Flow Unit 5B)	Same as 32-2, 72-74										pts	Same as 32-2, 75-77
32-3, 84-85 + 86-88 (Flow Unit 5B)											K/A (p.c.)	
32-3, 85-86 (Flow Unit 5B)											K/A (w.r.)	
32-3, 87-89 (Flow Unit 5B)											X (w.r.) X (v.f.)	X-ray diffraction shows plagioclase, pyroxene, and montmorillonite
32-3, 90-91.5											Sts (N) Sts (K)	
32-3, 91.5-93												
32-3, 93-94.5	This series of sections was cut to assure uniformity of this flow unit between areas of plagioclase K/AR dates and areas of major chemical analysis; the sections are remarkably similar; augite and Ca-poor augite microphenocrysts range from 5-9% with the variability more apparent than real, due to the definition of a microphenocrysts as being greater than 0.5 mm in size; Vesicle content varies between 9 and 15% depending on whether the larger vugs are present in certain sections. The textures remain diabasic to intersertal; the pyroxene/plagioclase ratio is constant and the alteration is as described in 32-1, 81-83 and 32-3, 103-105										Sts (N) Sts (K)	
32-3, 94.5-96												
32-3, 96-97.8											Sts (N) Sts (K)	
32-3, 98.5-99.3												
32-3, 99.3-100 (Flow Unit 5B)											Sts (N) Sts (K)	
32-3, 103-105 (Flow Unit 5B)	Augite Ca-poor augite	5.0 2.0	0.5	9.0	0.5-7.0	1.0	83.5	<0.4	Diabasic-intersertal	Somewhat altered basalt; augite microphenocrysts are unaltered; groundmass pyroxene consists of augite and Ca-poor augite and is unaltered; groundmass plagioclase is fresh; former groundmass glass is altered to brown montmorillonite; vesicles filled with brown montmorillonite rims, green montmorillonite, and calcite cores	Sts (N) Sts (K) X (w.r.) X (v.f.)	
32-3, 106-108 (Flow Unit 5B)	Same as 32-3, 103-105										pts C.A. X (w.r.) X (v.f.)	In reflected light opaque minerals scattered through sections evenly, but now consist of complex magnetite-ilmenite intergrowths; no free ilmenite observed; very minor chalcopyrite blebs present
32-3, 100-111.5 (Flow Unit 5B)											C.A.	
32-3, 111.5-112 (Flow Unit 5B)	Same as 32-3, 103-105										pts	Same as 32-3, 106-108 except very minor amounts of free ilmenite were observed

32-4, 73-75 (Flow Unit 5B)	Aphyric			23.5	1.0-10.0	6.0	76.5	<0.2	Intersertal diabasic	Moderately altered basalt; groundmass pyroxene (augite and Ca-poor augite) and plagioclase are slightly altered to montmorillonite. Former intersertal glass is much more abundant than in previous sections of this flow unit, completely altered to montmorillonite; vugs are very large and altered to montmorillonite and calcite	Sts (N) Sts (K) X (w.r.) X (v.f.)	
32-4, 76-78 (Flow Unit 5B)											pts C.A. X (w.r.) X (v.f.)	In reflected light magnetite is scattered evenly through the rock, very little exsolving ilmenite; magnetite is partly altered to opaque, nonreflective material; ilmenite blades and chalcopyrite blebs are very sparse
32-4, 123-125 (Flow Unit 6A)	Aphyric			6.0	0.5-2.0	1.0	94.0	<0.4	Diabasic-intersertal	Somewhat altered basalt; groundmass pyroxene (augite and Ca-poor augite) feldspar fresh; former intersertal glass is somewhat less abundant than in Flow Unit 5, but completely altered to brown montmorillonite; vesicles are filled with green montmorillonite; no calcite seen in X-ray diffraction or optically; no nepheline or X-Feldspar	Sts (N) Sts (K) X (w.r.) X (v.f.)	
32-4, 126-128 (Flow Unit 6A)	Same as 32-4, 123-125										pts C.A. X (w.r.)	In reflected light complex magnetite-ilmenite intergrowths are scattered evenly throughout the rock; a very few ilmenite laths are seen in formerly glassy areas; very sparse tiny blebs of chalcopyrite; some are intergrown with pyrrhotite
32-5, 92-94 (Flow Unit 6A)	Aphyric			6.0	0.5-2.0	1.0	94.0	<0.4	Diabasic-intersertal	Same as 32-4, 123-125	Sts (N) Sts (K) X (w.r.) X (v.f.)	
32-5, 95-97 (Flow Unit 6A)	Same as 32-5, 92-94										pts C.A. X (w.r.)	Same as 32-4, 126-128
32-5, 103-105 (Flow Unit 6A)											X (w.r.)	X-ray diffraction pattern shows plagioclase pyroxene, magnetite, and montmorillonite
32-6, 110-112 (Flow Unit 6A)	Aphyric			10.5	0.5-2.0	1.0	89.5	<0.4	Diabasic-intersertal	Same as 32-4, 123-125, but slightly more vesicular; in addition, the amount of altered intersertal glass is somewhat less	Sts (N) Sts (K) X (w.r.)	
32-6, 113-115 (Flow Unit 6A)	Same as 32-6, 110-112										pts C.A. X (w.r.) X (v.f.)	Same as 32-4, 126-128
32-6, 115-117 (Flow Unit 6A)	Aphyric			10.5	0.5-2.0	1.0	89.5	<0.4	Diabasic-intersertal	Same as 32-6, 110-112; vesicles are more abundant in this part of the flow unit and the amount of altered intersertal glass is <5%.	pts X (w.r.) X (v.f.) K/A (w.r.)	X-ray determination of plagioclass; average composition is An 73.5
32, CC (Flow Unit 6A)	Aphyric			8.5	0.5-2.0	1.0	91.5	<0.4	Diabasic-intersertal	Same as 32-6, 115-117, but small calcite vein cuts sample; calcite also follows some vesicle walls and occurs as replacement patches locally	X (w.r.)	
33-1, 37-39 (Flow Unit 6B)											X (w.r.)	X-ray diffraction pattern shows plagioclase, pyroxene, and montmorillonite

TABLE 4 – *Continued*

Sample (Interval in cm)	Phenocrysts and Microphenocrysts[a]			Vesicles[a]			Groundmass[a]			Alteration	Other Work[b]	Remarks
	Mineral	Percent	Average Size (mm)	Percent	Size Range	Average Size (mm)	Percent	Average Size (mm)	Dominant Texture			
33-1, 135-137 (Flow Unit 6B)	Aphyric			8.5	0.5-2.0	1.0	91.5	<0.4	Diabasic-intersertal	Somewhat altered basalt; groundmass pyroxene (augite and Ca-poor augite) and feldspar fresh; former groundmass glass (~5%) altered to brown montmorillonite; vesicles are filled with green montmorillonite; no calcite is seen in the section or X-ray diffraction pattern; no nepheline or K-feldspar	Sts (N) Sts (K) X (w.r.)	
33-1, 138-140 (Flow Unit 6B)	Same as 33-1, 135-137										pts C.A. X (w.r.)	In reflected light complex magnetite ilmenite intergrowths are scattered throughout the rock; a very few ilmenite laths are present in formerly glassy areas.
33-2, 79-81 (Flow Unit 6B)	Aphyric			8.5	0.5-2.0	1.0	91.5	<0.4	Diabasic-intersertal	Same as 33-1, 135-137	Sts (N) Sts (K) X (w.r.)	
33-2, 82-84 (Flow Unit 6B)	Same as 33-2, 79-81										pts C.A. X (w.r.) X (v.f.)	Same as 33-1, 138-140 X-ray vesicle filling shows possible celadonite
33-3, 91-93 (Flow Unit 6B)	Aphyric			9.0	0.5-1.5	0.8	91.0	<0.4	Diabasic-intersertal	Moderately altered basalt; groundmass pyroxene (augite and Ca-poor augite) and plagioclase fresh; former groundmass glass is more abundant than 33-1, 135-137 and 33-2, 79-81 and completely altered to brown montmorillonite; vesicles are filled with green montmorillonite; no calcite is seen in the section or X-ray diffraction pattern	Sts (N) Sts (K) X (w.r.) X (v.f.)	
33-3, 94-96 (Flow Unit 6B)	Same as 33-3, 91-93										pts C.A. X (w.r.) X (v.f.)	In reflected light opaques are about equally divided between complex magnetite-ilmenite intergrowths, free ilmenite, and free pinkish magnetite. Very sparse chalcopyrite blebs; some are intergrown with pyrrhotite
33-3, 102-104 (Flow Unit 6B)	Aphyric			5.5	0.5-1.5	0.8	94.5	<0.3	Diabasic-intersertal	Same as 33-3, 91-93, but contains less vesicles, considerably less altered groundmass glass, and is finer grained	pts X (w.r.) X (v.f.) K/A (w.r.)	In reflected light, is similar to 33-3, 94-96 but finer grained
33-3, 110-114 Coherent, partially baked siltstone with incipient hornfels texture											X (w.r.)	X-ray mineralogy (in order of abundance); plagioclase, pyroxene; heulandite; montmorillonite; quartz; celadonite; and pyrite
33-3, 124-128 Coherent, partially baked siltstone											X (w.r.)	X-ray mineralogy (in order of decreasing abundance), plagioclase; pyroxene; celadonite; montmorillonite; quartz; and pyrite.

33-3, 130-132 Coherent siltstone							Bulk		2-20μm	<2μm	X (mode)	
			Quartz				8.1		13.4	3.4		
			K-feldspar				8.7		10.0	5.3		
			Plagioclase				36.1		45.3	18.2		
			Mica (Celadonite?)				10.5		5.6	18.0		
			Montmorillonite				13.4		4.3	39.2		
			Clinoptilolite (Heulandite?)				10.0		10.3	0.8		
			Hematite				13.2		10.6	15.1		
			Pyrite				–		0.4	–		
						from Zemmels and Cook (this volume)						
33-3, 141-145 Claystone											X (w.r.)	X-ray mineralogy (in order of decreasing abundance) montmorillonite; quartz; plagioclase; pyroxene, and pyrite
33-4, 28-30 Claystone											X (w.r.)	In order of decreasing abundance: montmorillonite; calcite; plagioclase; pyroxene; pyrite and magnetite
33-4, 100-102 (Flow Unit 7A)	Aphyric			5.0	0.2-1.5	1.0	95.0	<0.3	Intergranular-intersertal	Heavily altered basalt; groundmass pyroxene (augite and Ca-poor augite) and plagioclase partly altered to montmorillonite; former intersertal glass entirely altered to montmorillonite; vein of same material cuts section; vesicles are filled with green montmorillonite; no calcite, nepheline, or K-feldspar	Sts (N) Sts (K) X (w.r.)	
33-4, 103-105 (Flow Unit 7A)	Same as 33-4, 100-102										pts C.A. X (w.r.) X (v.f.)	In reflected light magnetite is scattered evenly through the rock, partially altered to opaque, non-reflective material; sparse ilmenite blades occur in areas of former intersertal glass
33, CC (Flow Unit 7A)	Aphyric			5.0	0.6-1.8	1.0	95.0	<0.3	Intergranular-intersertal	Same as 33-4, 100-102 except calcite occurs as vesicle fillings and replacement patches	X (w.r.)	
34-1, 34-36 (Flow Unit 7B)	Aphyric			11.0	0.5-1.5	1.0	88.5	<0.3	Intergranular-intersertal	Moderately altered basalt; groundmass pyroxene (augite and Ca-poor augite) and plagioclase are fresh. Former intersertal glass altered to brown montmorillonite; vesicles are parially filled with green montmorillonite; some vesicle centers contain calcite. No nepheline or K-feldspar	Sts (N) Sts (K) X (w.r.) X (v.f.)	
34-1, 40-41 (Flow Unit 7B)	Same as 34-1, 34-36										pts C.A. X (w.r.) X (v.f.)	In reflected light identical to 33-4, 103-105 except that a few scattered chalcopyrite blebs were observed, some intergrown with pyrrhotite
34-2, 84-86 (Flow Unit 9)	Glomero-porphyritic clots of plagioclase and pyroxene	2.0	1.5	19.0	0.5-7.0	2.5	79.0	<0.2	Intersertal-diabasic	Moderately altered basalt; clots fresh; groundmass pyroxene (augite and Ca-poor augite) and plagioclase are fresh; former intersertal glass are all altered to brown montmorillonite; vesicles range to very large sizes; smaller filled with green montmorillonite; larger have only thin rims; pale green celadonite coats some larger vesicle walls; no calcite, nepheline, or K-feldspar observed	Sts (N) Sts (K) X (w.r.) X (v.f.)	

TABLE 4 – *Continued*

Sample (Interval in cm)	Phenocrysts and Microphenocrysts[a]			Vesicles[a]			Groundmass[a]			Alteration	Other Work[b]	Remarks
	Mineral	Percent	Average Size (mm)	Percent	Size Range	Average Size (mm)	Percent	Average Size (mm)	Dominant Texture			
34-2, 91-93 (Flow Unit 9)	Same as 34-2, 84-86										pts C.A. X (w.r.) X (v.f.)	In reflected light, magnetite is scattered evenly throughout the rock, partially replaced by an opaque, nonreflective material; sparse ilmenite occurs as blocky grains and laths
34-3, 115-117 (Flow Unit 10)	Aphyric			26.5	0.5-10.0	5.0	73.5	<0.05	Vitrophyric	Moderately altered rock; microlites of pyroxene (augite and Ca-poor augite) and plagioclase are fresh; former groundmass glass (~50% of non-vesicular part of the rock) is completely altered to brown montmorillonite; huge vesicles are largely open with thin rims of green montmorillonite; some greenish celadonite replacing groundmass; small amounts of calcite is observed in section; no K-feldspar	Sts (K) X (w.r.) X (v.f.)	Heulandite identified in vesicle filling by X-ray diffraction
34-3, 118-120 (Flow Unit 10)	Same as 34-3, 115-117									No nepheline is present	pts C.A. Sts (N) X (w.r.) X (v.f.)	In reflected light tiny crystals of magnetite are scattered evenly through rock, partially altered to an opaque nonreflective substance; a few ilmenite laths and minute chalcopyrite blebs are present
34-4, 62-64 (Flow Unit 10)	Glomero-porphyritic clots of pyroxene and plagioclase	8.0	1.6	18.5	2.0-8.0	5.0	73.5	<0.05	Vitrophyric	Same as 34-3, 115-117 except for presence of unaltered clots and the presence of somewhat more calcite	Sts (K) X (w.r.) X (v.f.)	
34-4, 65-67	Same as 34-4, 62-64										pts C.A. X (w.r.) X (v.f.)	In reflected light, same as 34-3, 118-120
34, CC	Glomero-porphyritic clots of pyroxene and plagioclase	17.0	1.0	7.0	2.0-10.0	5.0	76.0	<0.05	Vitrophyric	Same as 34-4, 62-64 except contains more clots and less vesicles	X (w.r.)	

[a]Average points counted 300; percentages rounded to nearest 0.5%.

[b]Sts (N) = section stained for nepheline and melilite; Sts (K) = section stained for potassic feldspar; X (v.f.) = vesicle filling X-ray diffraction pattern; X (w.r.) = whole rock X-ray diffraction pattern; C.A. = chemical analysis; pts = polished thin section; K/A (w.r.) = potassium argon whole-rock (minimum age); K/A (p.c.) = potassium argon age on separated plagioclase.